FEDERAL UNIVERSITY OF SANTA CATARINA
TECHNOLOGY CENTER
AUTOMATION AND SYSTEMS DEPARTMENT
UNDERGRADUATE COURSE IN CONTROL AND AUTOMATION ENGINEERING

Rhanna Kaenna Auler

Process-parallel spindle speed control during 5-axis milling of a thin-walled turbomachinery component

Aachen
2022

Rhanna Kaenna Auler

Process-parallel spindle speed control during 5-axis milling of a thin-walled turbomachinery component

Final report of the subject DAS5511 (Course Final Project) as a Concluding Dissertation of the Undergraduate Course in Control and Automation Engineering of the Federal University of Santa Catarina.
Academic Supervisor: Prof. Rodolfo César Costa Flesch, Dr.
Company Supervisor: Pascal Kienast, M.Sc.

Aachen
2022

Ficha de identificação da obra elaborada pelo autor,
através do Programa de Geração Automática da Biblioteca Universitária da UFSC.

Auler, Rhanna Kaenna
Process-parallel spindle speed control during 5-axis milling of a thin-walled turbomachinery component / Rhanna Kaenna Auler ; orientador, Rodolfo César Costa Flesch, coorientador, Pascal Kienast, 2022.
101 p.

Trabalho de Conclusão de Curso (graduação) - Universidade Federal de Santa Catarina, , Graduação em , Florianópolis, 2022.

Inclui referências.

1. . 2. Fresamento com máquinas de cinco eixos. 3. Componentes de paredes finas. 4. Controle de vibrações. 5. Aquisição de dados. I. Costa Flesch, Rodolfo César. II. Kienast, Pascal. III. Universidade Federal de Santa Catarina. Graduação em . IV. Título.

Rhanna Kaenna Auler

Process-parallel spindle speed control during 5-axis milling of a thin-walled turbomachinery component

This dissertation was evaluated in the context of the subject DAS5511 (Course Final Project) and approved in its final form by the Undergraduate Course in Control and Automation Engineering

Florianópolis, August 03, 2022.

Prof. Hector Bessa Silveira, Dr.
Course Coordinator

Examining Board:

Prof. Rodolfo César Costa Flesch, Dr.
Advisor
UFSC/CTC/DAS

Pascal Kienast, M.Sc.
Supervisor
Fraunhofer IPT

Prof. Nestor Roqueiro, Dr.
Evaluator
UFSC/CTC/DAS

Prof. Eduardo Camponogara, Dr.
Board President
UFSC/CTC/DAS

ABSTRACT

The aviation industry has defined ambitious economic and environmental objectives aiming to reduce emissions and to increase fuel efficiency. The design of blades combined into disks, known as blade integrated disks (blisks), has been a major trend in recent years to address these objectives and to achieve highly fuel-efficient engines. Due to the desired high-quality and long process that takes to machine a single blisk, a well previously studied process and the guarantee that a good quality part will be machined are necessary. The challenges of blisks design and machining are also increased by the fact that these thin-walled components have a reduced stiffness, resulting in an higher chance of vibrations arising while machining the component, which reflects negatively in the final surface. This thesis aims to develop a data-based application capable of monitoring and controlling vibrations during the 5-axis milling process of thin-walled turbomachinery components. Suitable processing techniques for the process-parallel acquired data were analyzed to detect occurring vibrations by using key performance indicators. An offline application was first developed to perform sensitivity analyses with data from previously milled thin-walled components. The data processing functionalities of the offline tool were then integrated to an existing data acquisition system in LabVIEW. A second way of communication was then added to the system, allowing the integrated application to send data back to the milling machine for spindle speed adaptation. The application is evaluated by milling trials, where a blisk blade is machined. An experimental setup is conducted with suitable sensory and data acquisition hardware. The control performance is measured by comparing the results of a blade machined with and without taking actions over the process to reduce such vibrations. Visual inspection and process data analyses have shown the reduction of chatter marks when the control was applied in the 5-axis milling process.

Keywords: 5-axis milling. Thin-walled components. Vibration control. Data acquisition. Chatter.

RESUMO

A indústria da aviação definiu objetivos econômicos e ambientais ambiciosos com o propósito de reduzir emissões de CO_2 e aumentar a eficiência energética. O design de *blades* (lâminas) combinadas em discos, conhecidos como *blisks* (blade integrated disks), tem sido uma grande tendência nos últimos anos para atender a esses objetivos e alcançar motores altamente eficientes em termos de consumo de combustível. Devido à alta qualidade desejada e o longo processo que leva a usinagem de um único disco, é necessário um estudo do processo e a garantia de que uma peça de boa qualidade será usinada. Os desafios do projeto e usinagem de *blisks* também são aumentados pelo fato de que estes componentes de paredes finas têm uma rigidez reduzida, resultando em uma maior chance de vibrações durante a usinagem do componente, o que se reflete negativamente na superfície final. Este projeto de fim de curso visa desenvolver uma aplicação baseada em dados capaz de monitorar e controlar as vibrações durante o processo de fresagem de componentes de turbomáquinas de paredes finas com máquinas de cinco eixos. Técnicas de processamento adequadas para os dados adquiridos em paralelo ao processo foram analisadas para detectar as vibrações ocorridas usando *KPIs* (indicadores-chave de desempenho). Uma aplicação offline foi inicialmente desenvolvida para realizar análises de sensibilidade com dados de *blisks* previamente fresadas. As funcionalidades de processamento de dados da ferramenta offline foram então integradas a um sistema de aquisição de dados existente no LabVIEW. Uma segunda forma de comunicação foi então adicionada à aplicação, permitindo que o serviço integrado envie dados de volta para a máquina para adaptação da velocidade do *spindle*. O sistema de controle e monitoramento é avaliado através de ensaios de fresagem, onde uma lâmina de *blisk* é usinada. Uma configuração experimental é conduzida com sensores e *hardware* de aquisição de dados adequados. O desempenho do controle é medido pela comparação dos resultados de uma lâmina usinada com e sem tomar ações sobre o processo para reduzir vibrações. A inspeção visual e a análise dos dados do processo mostraram a redução das marcas de vibração quando o controle foi aplicado no processo de fresagem de cinco eixos.

Keywords: Fresamento com máquinas de cinco eixos. Componentes de paredes finas. Controle de vibrações. Aquisição de dados.

LIST OF FIGURES

LIST OF TABLES

LIST OF ABBREVIATIONS AND ACRONYMS

blisks	blade integrated disks
CAD	computer aided design
CAM	computer aided manufacturing
cDAQ	compact data acquisition
CNC	computer numerical control
CPS	cyber-physical systems
cRIO	compact reconfigurable input-output
DAQ	data acquisition
DDE	delay differential equation
DNC	direct numerical control
EMA	experimental modal analysis
FEM	finite element method
FFT	fast fourier transform
FPGA	field-programmable gate array
FRF	frequency response function
HSM	high speed machining
I/O	input/output
IEPE	integrated electronics piezo-electric
IoT	internet of things
IP	Internet Protocol
IPC	industrial personal computer
IPT	institute for production technology
KPI	key performance indicator
MQTT	message queuing telemetry transport
NC	numerical control
NCK	numerical control kernel
NI MAX	National Instruments measurement and automation explorer
OMA	operational modal analysis
PC	personal computer
PIB	power-in-band
PLC	programmable logic controller
RMS	root mean square
RSD	relative standard deviation
SLD	stability lobe diagram
SSV	spindle speed variation
STFT	short-time fourier transform
TDMS	technical data management streaming

WCS	workpiece coordinate system

LIST OF SYMBOLS

v_f	feed rate
n	spindle speed
D_c	cutter diameter
v_c	cutting speed
$v_{c,eff}$	Average Effective Cutting Speed
N_t	cutting tool teeth
f_z	tooth feed
M	mass matrix
D	damping matrix
K	stiffness matrix
x	displacement vector
F_s	cutting force stationary term
K_t	cutting force coefficient
a_p	depth of cut
A	cartesian directional matrix
F_d	process damping force
f_t	tooth passing frequency
f_s	sampling rate
N	frequency bins
n_s	number of samples
t_s	time steps
l	window length
T	time duration
t_r	Time Resolution
d_t	distance between samples
O	overlap
f_r	resonant frequency
f_0	reference frequency
f_i	initial tooth passing frequency
f_d	desired tooth passing frequency

CONTENTS

1 INTRODUCTION AND MOTIVATION

The aviation industry has defined ambitious economic and environmental objectives aimed at reducing emissions and increasing fuel efficiency. The design of blades combined into disks, known as blade integrated disks (blisks), has been a major trend in recent years to address these objectives and to achieve highly fuel-efficient engines [1][2]. As an example of this trend in aviation economy, MTU Aero Engines predicts to be producing 6,000 blisks per year in the coming years in its centre of excellence [3].

Blisks are capable of reducing the weight of turbomachinery components, such as happened with the high-pressure compressor Trent XWB, which had its weight reduced by 15 %, such a reduction directly translates as fuel economy and reduction of CO_2 emissions [1]. A case study developed by Ericsson [4] has shown that improving blisks production by, for example, monitoring process-parallel and acquiring data to refine machining, leads to more efficient blisks. Highly-efficient blisks results in a considerable decrease in the amount of CO_2 emissions: supposing a 2% of improvement, 16 million metric tons of CO_2 emissions could be saved [4]. Moreover, according to Dilba [3], blisks not only reduce component weight, but they also occupy a reduced amount of space and provide better aerodynamics [3]. Furthermore, contrary to traditional disks that have blades mounted, there is no need to individually assembly blade by blade [3].

More sophisticated 3D-designed geometries commonly reflect in increased ambitious manufacturing specifications [5][2]. Due to the desired high-quality and long process that takes to machine a single blisk, the requirements of a well previously studied process and the guarantee that a good quality part will be produced are increased [2]. The challenges of blisks design and machining are also increased by the fact that these thin-walled components have a reduced stiffness, thus resulting in an higher chance of vibrations arising while machining the component, which reflects negatively in the final surface.

The effects of vibrations have been a major subject of investigation in cutting processes, such as milling [6]. The milling is characterized as an interrupted cut with a harmonic excitation that acts on the mechanical system, tool and workpiece, coupled with the clamping situation. Considering the mechanical machining dynamic properties and the desired part geometry and surface, advantageous parameters are determined preliminary such as spindle speed. However, only a discrete state of an entire mechanical system is considered previously, but metal-cutting processes change dynamically along the part production [7]. If a fluctuation of process influences becomes too extensive, this usually results in the increased occurrence of vibrations, particularly in thin-walled components such as blisks.

Hence, the High Performance Cutting department at the Fraunhofer institute for production technology (IPT) is researching novel approaches for the highly efficient

and sustainable production of these thin-walled turbomachinery components, primarily using 5-axis milling machines. Thus, this thesis aims to develop an application capable of monitoring and controlling vibrations occurring during thin-walled components milling. An existing data acquisition system is expanded by the development of data processing and a control module for spindle speed adaptation.

2 STATE OF THE ART

The production of complex-geometry blisks requires a good understanding of the process and well-planned stages to prevent shape deviations in the surface being manufactured. Thin-walled components tend to deflect and are anticipated to generate vibrations, which are a known cause of instabilities that lead to chatter in the system. These phenomena affect the required turbomachinery components quality. Therefore, studies of blisks production are commonly linked to the prevention of such instabilities, aiming to achieve the desired surface and geometry quality necessary in the aerospace industry. Thus, this chapter aims to discuss current studies in the area of 5-axis milling process of a thin-walled turbomachinery component, and to present the necessary literature to develop a process-parallel spindle speed control that reduces chatter.

Along the years, with the ever growing importance of cutting process on component manufacturing, more and more technologies have been developed for milling process. Multiple axis machines are used to produce complex geometry parts with a high quality surface, in an efficient and well-planned process. The technologies of milling processes are discussed in section 2.1

Milling is characterized by an interrupted cut of a tool mounted in a tool holder connected to a rotating spindle, as described in section 2.2. Different phenomena impact milling dynamics, such as vibrations which are commonly related with chatter marks on blisks surfaces. Techniques to detect and prevent vibrations on the milling process have been broadly studied and developed, and commonly require representing the milling system using a mathematical model.

Digitalization has enabled new possibilities for acquiring and studying process data. Therefore, studies of how to monitor and detect vibrations in machining have been developed. Vibration monitoring commonly requires data acquisition and processing, in both time and frequency domains. For the process-parallel prevention of vibrations, a control loop can be implemented to lead the system to a target steady state, aiming to achieve the required component quality. Digitalization, vibration monitoring and control systems are further discussed in section 2.3.

2.1 TECHNOLOGY OF MILLING PROCESS

5-axis milling process of thin-walled turbomachinery components is characterized by an interrupted cut and a harmonic excitation that acts in the milling process. Milling is a commonly applied type of metal cutting processes, which consists primarily of the material removal of a workpiece to achieve a desired surface and geometry [8]. Kinematics of milling processes are further presented in subsection 2.1.2. The three main stages of a milling process are roughing, pre-finishing, and finishing. These steps are automatically run one after the other when a computer numerical control (CNC)

machine with programming capabilities is used, as described in subsection 2.1.1.

2.1.1 Simultaneous 5-axis Milling

After the development of the first numerical control (NC) machine in the 1950s, CNC has become broadly applied in the industry [9]. The development of these programmable controllers has impacted positively machining efficiency and flexibility. The capabilities of CNC machines have expanded considerably with more and more technologies being created to the industry sector [10]. Not only complex geometry and very thin parts can be produced, but also advanced technology can be used to manufacture these parts, involving multi-axes and multi-tools in a single process.

On the other hand, the complexity of CNC machines programming has also increased, thus requiring a well-prepared process planning that links the machining process with the workpiece design. computer aided design (CAD) and computer aided manufacturing (CAM) software have been key tools for planning and programming complex parts for CNC machining. CAD software is usually applied in the first stage of a milling process chain, the workpiece design. Subsequently, the production is commonly planned using CAM. From the planning software, the process tool paths are translated in a machine language as G or M code using each machine post-processor, in order to achieve the piece geometry designed. After tool paths are generated, simulations of the process can be performed to identify its potential critical points. Afterwards, the machine is configured and the material is removed from a raw metal piece to achieve the planned product. [8][10][9]

Modern CNC machines are being required to have ever more high speed, precision and efficiency [11]. high speed machining (HSM) has been widely applied to machining process, resulting in a high-speed rotating milling process which leads to a high material removal rate. According to Dewes and Aspinwall [12], HSM can reduce the manufacturing costs and times. A higher material removal rate impacts positively the milling process efficiency, which is mainly impacted by the spindle speed, depth-of-cut, and feed rate [13].

According to Özel and Altan [14], the cost efficiency of high-speed machining is defined by the relation between process variables and performance measurements, such as tool wear and surface quality. Therefore, modeling the process is a key aspect to predict the process variables and achieve an optimized process [14]. According to Dewes and Aspinwall [12], many aspects should be considered when using high-speed milling, such as the process stability and the tool geometry. Additionally, with multiple axis and multiple speeds being used, more complex programming of the machine and NC programming methods are required [15].

Using simulation and modeling the milling process lead to potential improvements in the process, so ideal conditions can be selected [14]. Such as the simulation

described by Holst et al [16], which apply technological models such as milling engagement simulation with a CAD-CAM system. Therefore, process optimization in the planning phase and prediction of tool wear is possible. Figure 1 shows the manufacturing steps followed since the workpiece CAD Model until its machining process, including the simulation process to optimize the process.

Figure 1 – Manufacturing Steps

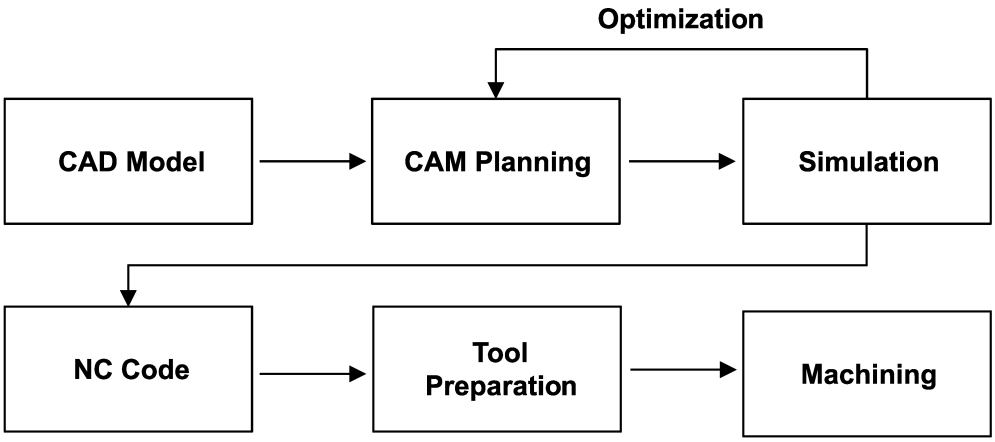

Source: Holst et al [16]

Although after the initial preparation steps, the CNC machine is capable of automatically running milling stages such as roughing, pre-finishing, and finishing, one after the other, the cutting parameters such as spindle speed and feedrate are normally static along each operation [17, p. 237]. Therefore, ideal conditions for each phase of the process might not be achieved during the whole process, given that the geometry of workpiece is continuously changing with the material removal and, thus, the dynamics.

2.1.2 Kinematics of Milling Process

Simultaneous 5-axis milling machines have become each year more and more used, when compared with traditional 3-axis machines [15]. The use of these 5-axis machines results in a five-degree-of-freedom process, given by three linear and two rotatory axis. Both the workpiece and the tool-holder-spindle system move during the milling process, resulting in a relative motion in multiple axes [18]. Therefore, the material removal is defined by the tool movement and this relative motion. Moreover, according to Cabral [8], the kinematics of this process depends on the tool orientation, direction of cutting, and the feed direction.

The movement of the cutting tool used in a milling process is described by Reuleaux [19] as a cycloidal motion which combines both rotational and linear movements, as shown in Figure 2. The translational movement of a point in a cutter tooth

is determine as an extended cycloid path, which depends on the feed rate v_f. The rotational movement is defined by the spindle speed n [8].

Figure 2 – 3-axis milling cycloidal trajectory

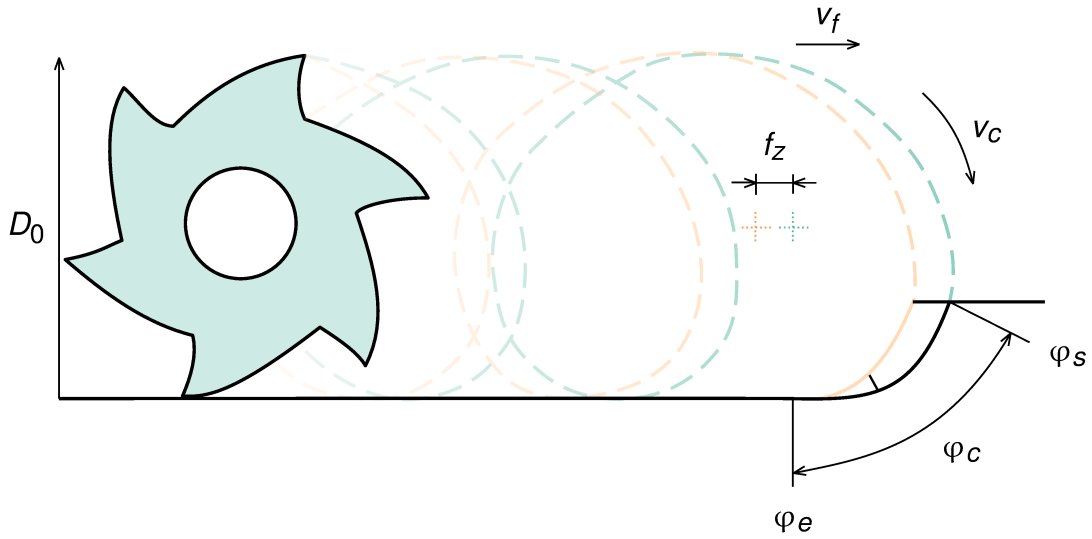

Source: Kienast [20], Cabral [8, p. 26]

Given the cutter diameter D_c and the spindle speed n, the cutting speed v_c is determined [21] [20] .

$$v_c = n \cdot D_c \cdot \pi \tag{1}$$

The cutting speed v_c is, however, only achieved when the cutting edge angle κ is equal to 90°, and it decreases along the tool ball until the tip. Therefore, an average effective cutting speed $v_{c,eff}$ is usually considered, which is calculated based on an average cutting edge angle κ_m and the cutting speed v_c [22] [20].

$$v_c, eff = v_c \cdot \sin(\kappa_m) \tag{2}$$

The spindle speed also impacts in the feed rate v_f, which is calculated based on the number of the cutting tool teeth N_t and tooth feed f_z [20].

$$v_f = n \cdot N_t \cdot f_z \tag{3}$$

The number of cutting tool teeth impacts proportionally the process efficiency. On the other hand, the higher the tool teeth number, the lower the tool stiffness [23] [20]. Different tool geometries and number of tool teeth are selected to achieve a desired process and workpiece result. With the advance of technologies, automated tool changes can be performed during the machining process, according to the process planning or even given tool wear identified by monitoring systems.

The dynamics of milling process using high speed on CNC machines and the technologies applied to them are further discussed in the following sections, with a

main focus on milling hard metals such as titanium for the production of thin-walled turbomachinery components.

2.2 MILLING DYNAMICS

Milling is determined by an interrupted cut with an harmonic force performed by a tool with defined cutting edges. The milling tool is usually mounted in a tool holder connected to a rotating spindle. The workpiece is conventionally coupled in a clamping system and its material is removed to achieve the desired surface by the relative motion between the workpiece and tool [24][18, p. 107]. The dynamic of milling processes is generally described by a delay differential equation (DDE) [25] [24, p. 100]:

$$\mathbf{M}\ddot{\mathbf{x}}(t) + \mathbf{D}\dot{\mathbf{x}}(t) + \mathbf{K}\mathbf{x}(t) = \mathbf{F}_s(t) + K_t a_p \mathbf{A}(t)(\mathbf{x}(t) - \mathbf{x}(t-\tau)) + \mathbf{F}_{pd}(t, \ddot{\mathbf{x}}(t)), \tag{4}$$

where **M**, **D**, and **K** correspond to the mass, damping, and stiffness matrices, respectively, while **x** is the displacement vector in Cartesian coordinates. The left hand side of the equation represents the mechanical milling system composed by the tool, tool holder, spindle, workpiece, damping system, and the machine structure. On the other hand, the right hand side describes three cutting force components. The F_s parameter corresponds to the phenomenon that causes forced vibrations, with K_t being the cutting force coefficient, a_p the depth of cut, τ the regenerative delay, and **A**(t) the Cartesian directional matrix. The second term is related with the regenerative effect that occurs during the milling process. The third one, F_d, is associated with the damping force [25] [24, p. 100].

The phenomena that impact the milling process are presented with more details in the following subsection, with the main focus on vibrations effects. Vibrations generated during the dynamic process are commonly related with the appearance of chatter in the milling process, considering that the tool and workpiece can deflect, specially when milling thin-walled components with long overhanging tools. Those vibrations not only can lead to chatter in the surface, but also cause the system instability [18, p. 121]. The appearance of vibrations is further explained in subsection 2.2.1, while useful techniques to identify the system are described in subsection 2.2.2, and methods to reduce vibrations are presented in subsection 2.2.3.

2.2.1 Vibrations in Milling Processes

Aiming to achieve a more sustainable process with a high material removal rate, and to produce thinner and smaller parts, new technologies and methods have been brought to machining, such as more powerful milling tools and process monitoring [25]. Many studies have been developed with the main goal of improving cutting process, such as turning and milling, being vibrations a prominent field in those research [6].

Tobias [26] classifies three main types of vibrations that might occur while machining. Figure 3 represents the types of vibrations described. The first one, free vibrations, occurs when there is a disequilibrium in the system and an external excited force leads the system to freely vibrate. External disturbances and imbalances, for example, are a possible cause for this disequilibrium. Nevertheless, free vibration amplitude tends to decrease along the time due to the system damping, once the source of imbalance is ceased. [27] [28] [29] [30]

Figure 3 – Metal Cutting Vibrations Types

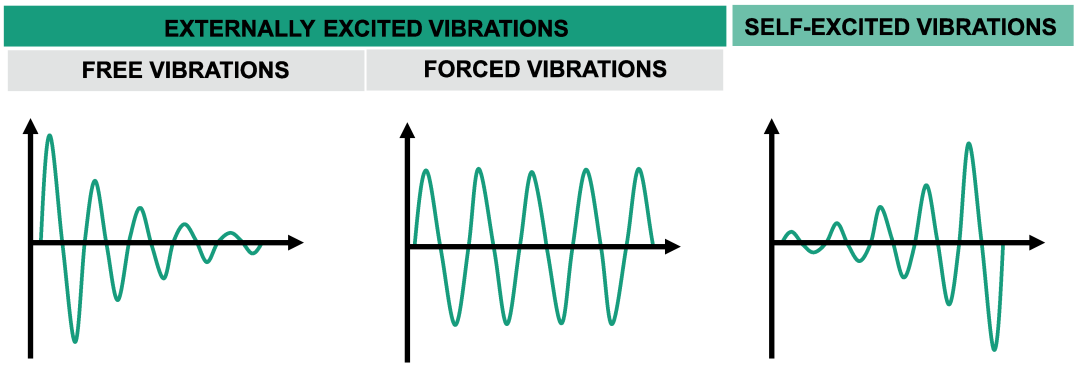

Source: Adapted from Kienast [20]

Secondly, the named forced vibrations can occur when the tool cutting edge moves in and out the workpiece, leading to a vibration of constant amplitude. This type of vibrations is caused in the milling process by external excited harmonics forces induced by the tooth passing frequency f_t [26] [27] [30].

$$f_t = n \cdot N_t \tag{5}$$

There is as well a third type called self-excited vibrations, which are caused by a force between the tool and the workpiece, and tend to increase along the cutting process. They are described as the main cause of chatter marks [27] [28] [29].

Although self-excited vibrations are more commonly known as the source of chatter, this latter phenomenon can be generated by different cutting process conditions, such as forced vibrations as described by Merritt [31]. However, in the case of forced vibrations the detection is possible by comparing chatter frequencies to the ones of vibrations, so the force which causes this type of chatter can be prevented. On the other hand, self-excited vibrations are not that easily discovered. Therefore, self-excited vibrations are commonly known as the primary source of chatter on milling process.

Chatter is a subject that has long been discussed, since it is considered one of the main impediments to achieve a high process productivity and quality [6] [29] [25]. Waves on the workpiece surface known as chatter marks prevent achieving the desired quality and accuracy. Additionally, this phenomenon causes a reduction in the

life cycle of tools and other mechanical components used in the process, and affects the machining safety and reliability [25] [31] [32].

Chatter can be distinguished between the ones caused by physical mechanisms, commonly named primary chatter, and the regenerative chatter. The latter is considered one of the main causes of instabilities in the process, and can occur due to wave regeneration between the workpiece and tool in specific spindle frequencies [6] [28] [7] [33]. Thus, chatter prevention is critical in the production of thin walled parts such as is the case of turbomachinery components.

The flexibility, lack of stiffness, of any part of the machine-tool system can produce chatter [25]. Flexible parts of the workpiece might vibrate due to fluctuating cutting forces. Each tool tooth creates a waviness in the workpiece surface when removing material, known as the outer modulation, as shown in Figure 4. Thus, the next tooth encounters a surface with waviness on it, but the projected cutter path follows a straight line, with a nominal chip thickness h_0, leading to a variable chip thickness [7] [20]. When the depth-of-cut changes while a previously machined wavy surface is touched, vibration amplitudes and cutting force increase, varying the cutting force and generating succeeding vibrations, and affecting the system stability [34] [28]. This loss of stability is then known as caused by the chip regenerative effect, depending of the relative motion between tool and workpiece [35].

Figure 4 – Chip thickness modulation

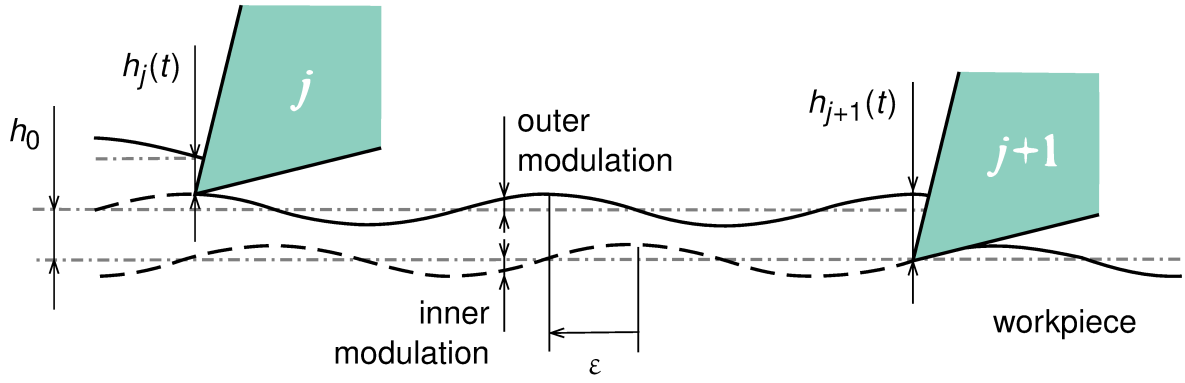

Source: Kienast [20]

Thin-walled turbomachinery components, such as blisks, are commonly designed with flexible parts that lead to the loss of stability when milled. Trends in blades design have lead to thin components with a high aspect ratio. The blade aspect ratio is given by the relationship between blade length from bottom to top, and the chord length (calculated considering the front to back tip part of the blade) [20]. Although compressors with this type of blade geometry tend to be more efficient, thin wall blades with high ratio aspect make them flexible and with a tendency to vibrate [4].

Therefore, given the actual blisks blades design scenario of high aspect ratio, knowledge of the blade dynamics and in-process vibration monitoring are essential to

maintain the high quality required by turbomachinery components. System identification methods to better understand blade dynamics produced on 5-axis milling machines are further discussed in the next subsection.

2.2.2 System Identification

The development of new technologies and intelligence applied to machining and its devices has lead to the study of different techniques to identify the characteristics of a milling system. Experimental Modal Analysis is an example of the techniques that have been broadly applied. As previously described in subsection 2.2.1, those techniques can be used to better understand the dynamic behavior of the machining system and to improve the process design, as well as to study the source of chatter vibrations and to prevent them [24].

Modal coordinates, along with local and design, are one of the coordinate systems used to analyze machining structures. They are typically used to study the behavior of the structure in a specific frequency. Modal analysis is a common methodology in modern facilities to identify modal parameters for all the interesting modes inside a certain milling process frequency range. frequency response function (FRF) can be determine using modal testing techniques, in order to define a mathematical model to be used when designing the milling process [18, p. 39-50] [24, p. 75-98] [20].

For the measurement of FRFs a device that generates a known force $F(\omega)$ exciting the system in an specific frequency is usually required. Commonly used hardware to generate this force input are impulse hammers and shakers. Furthermore, a transducer is necessary to measure the vibrations generated. Accelerometers and other contacting types of transducers are more convenient to install in the system, but they tend to influence the system more than transducers such as laser vibrometers, given the the additional mass. Therefore, the latter is preferred if its installation is possible. A measurement device to quantify the force and vibration signals should be connected to the system so the FRFs can be determined [18, p. 61-63]. A summary of measuring FRFs of a milling system is shown in Figure 5.

Figure 5 – FRFs Measurement

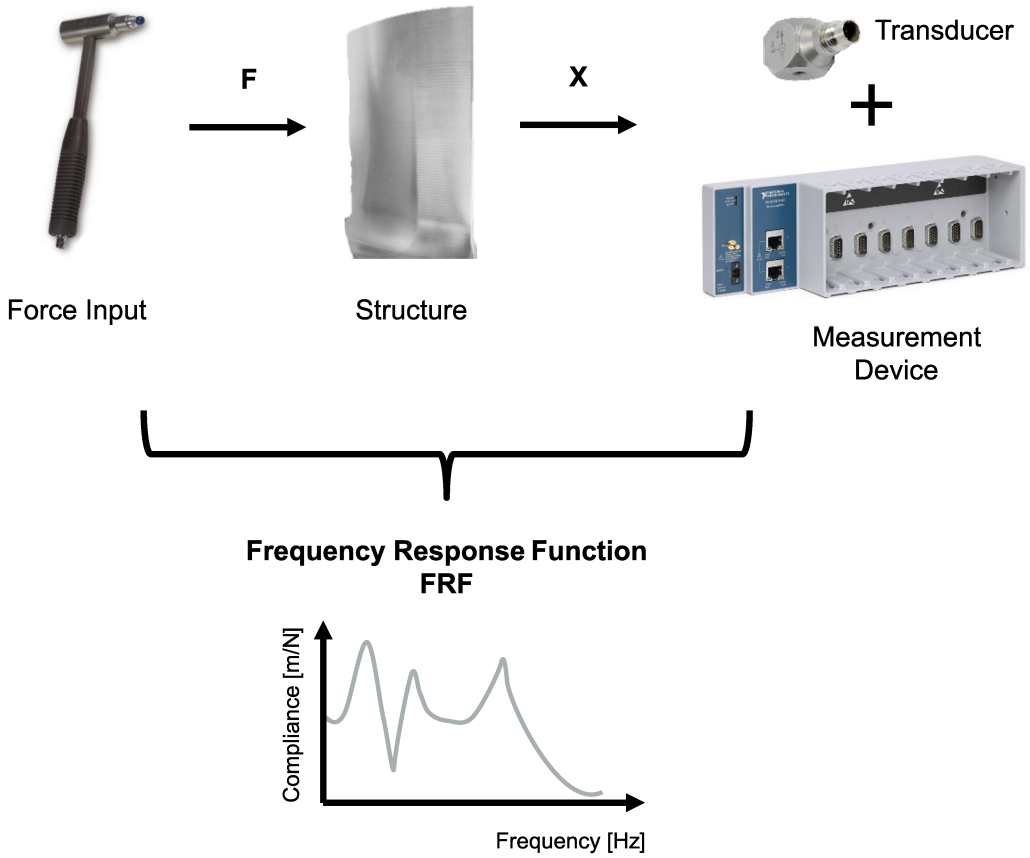

Source: Sinus, [36], Kistler [37], Digi-Key [38]

Therefore, with the required components installed, the response $X(\omega)$ excited by the force $F(\omega)$ is measured. Hence, the FRF of the structure is calculated by the called experimental modal analysis (EMA):

$$FRF(\omega) = \frac{X(\omega)}{F(\omega)}. \tag{6}$$

Identification of peak and its associated frequencies is made based on the measured response signal. Then, modal damping, mass, and stiffness parameters of modal matrices are calculated [18, p. 53-54]. Modal equations can then be determined using modal matrices.

Another possibility of determining the modal parameters is explained by Zhuo et al [39], who applied operational modal analysis (OMA) and compared with the Hammer method to define modal parameters of a thin-walled component milling. With the OMA method, dynamic parameters can be determined while machining. Although commonly applied, the modal analysis components measured at static state are different of the characteristics of the milling dynamic process.

Therefore, an in-process analysis might be necessary to accurately prevent vibrations and improve the surface quality. Different approaches have been applied to

precisely determine milling model parameters, since the analysis depends on the quality of the model [40]. For example, finite element method (FEM) has also been used to obtain modal parameters, such as shown by Maslo et al [41], where FEM was applied to detect the modal parameters in the state-space representation of the dynamic system.

Additionally, the continuous workpiece geometry along the 5-axis milling and the difference between blade blocks should be considered when preventing chatter. Change in parameters such as mass, damping, and stiffness, influences the dynamic behavior of the workpiece. Figure 6 shows how those parameters affect the dynamics of a single-mass oscillator [42] [43].

Figure 6 – Dynamic Parameters Effects

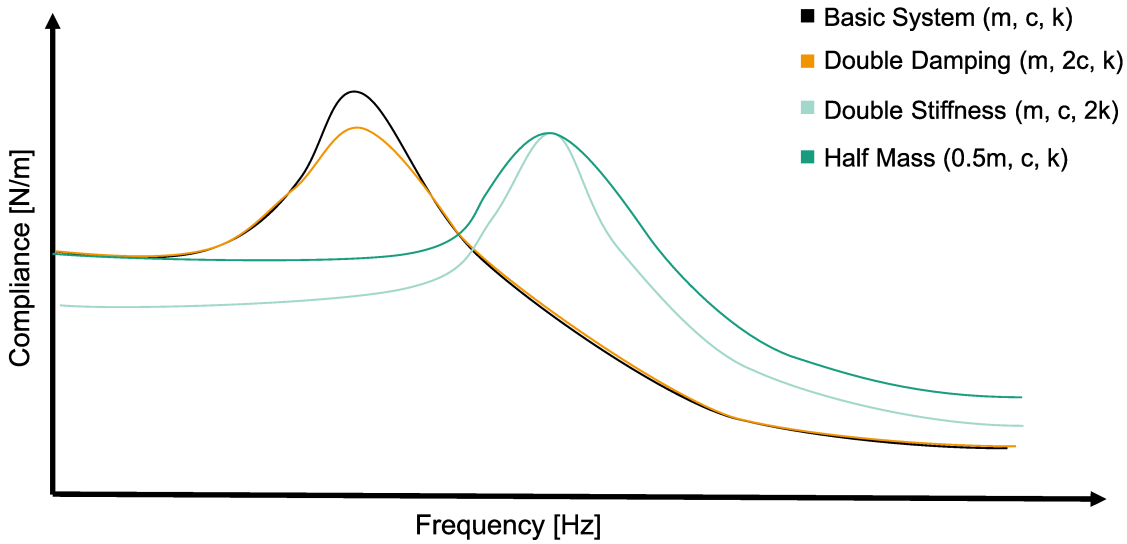

Source: Brecher and Weck [44], Balachandran and Magrab [45], Güden [42], Edler [43]

If the mass is reduced by half, while the other components remain the same, the natural frequency changes and the amplitude is lightly reduced. This same frequency and amplitude is achieved in the case that all parameters are kept the same with the exception of the stiffness, which is doubled. However, the graph is steeper. Additionally, if the damping is doubled, the frequency is kept the same, but the amplitude decreases [44] [45] [42] [43].

Therefore, although the Experimental Modal analysis is typically performed before the milling process, the parameters are continuously changing along the process. However, given the process dynamic information, the process stability can be studied to prevent undesired phenomena such as chatter. The following subsection discusses approaches to achieve a stable process without chatter.

2.2.3 Process Stability

The System Identification stage is commonly used to identify process parameters to achieve a stable process, aiming to obtain a high quality component as planned

earlier in the CAD/CAM phase. Regenerative chatter is considered one of the main causes of instabilities in machining processes. Therefore, many approaches to detect and prevent chatter have been studied along the years.

Five possibilities to reduce vibrations are described by Munoa et al [25], considering the milling Delay Differential Equation (Equation (4)) [42]:

1. Process Damping Increase

   An increase in the process damping would reduce the occurrence of vibrations. This could be achieved by different approaches such as changing the cutting wedge geometry, or by reducing the spindle speed. However, each option has its downside. For example, reducing the spindle speed would affect machining productivity.

2. System Damping Increase

   This approach suggests that vibrations could be reduced by increasing the system damping. This could be done by placing dampers in strategic points, for example, where vibrations with high amplitudes are expected.

3. System Rigidity Increase

   In places where high amplitude vibrations are expected, the system rigidity could be increased, which would prevent the appearance of those phenomena.

4. Process Parameters Selection

   Process parameters such as spindle speed and cutting depth could be determined based on Lobe diagrams, aiming to achieve a process without vibrations. However, FRFs coefficients measured during the system identification stage can vary during the process, leading to the necessity of verifying those coefficients along the process.

5. Regenerative Effect Disruption

   An interruption of the regenerative effect could prevent high amplitude vibrations. This could be achieved with the use of tools with special geometries or by changing the spindle speed during milling. Spindle speed change techniques such as discrete spindle speed tuning (DSST) and the continuous spindle speed variation (CSSV) are used to change the chip thickness modulation period and prevent the regenerative effect that leads to instabilities.

However, most out of process approaches require to know the process dynamics and cutting parameters, and this might be a hard task in the industrial environment [32]. On the other hand, Jemielniak and Widota [46] already mentioned in 1984 the spindle speed variation (SSV) method to decrease the amplitude of self-excited vibrations.

Nevertheless, according to Munoa et al [25], Finite Element Method is highly capable of prediction system parameters, but damping is still difficult to estimate (since it is not easy to predict vibration dissipation behavior of parts such as joints), and damping is one of the main components of stability lobe diagram (SLD). Jasiewicz and Miądlicki [28] describe that the FRF expresses the dynamic of machine-tool-workpiece system, which can be determined by different ways such as using modal synthesis methods. However, coefficients must be determined for each tool-workpiece combination.

The effect of process damping to prevent instabilities decreases at high speeds. Therefore, Stability Lobe Diagrams can be used to predict higher material removal rates at those high speed [7]. An example of SLD is shown in Figure 7, where stable and unstable areas can be selected based on the depth of cut and spindle speed. Although the use of higher rates of material removal makes the process more efficient, it should be balanced with the desired surface quality, since depending of the combination of axial depth-of-cut and spindle speed the system stability is affected [33]. Area C in the figure represents high speed milling zone, which is the main focus of this thesis.

Figure 7 – Stability Lobe Diagram

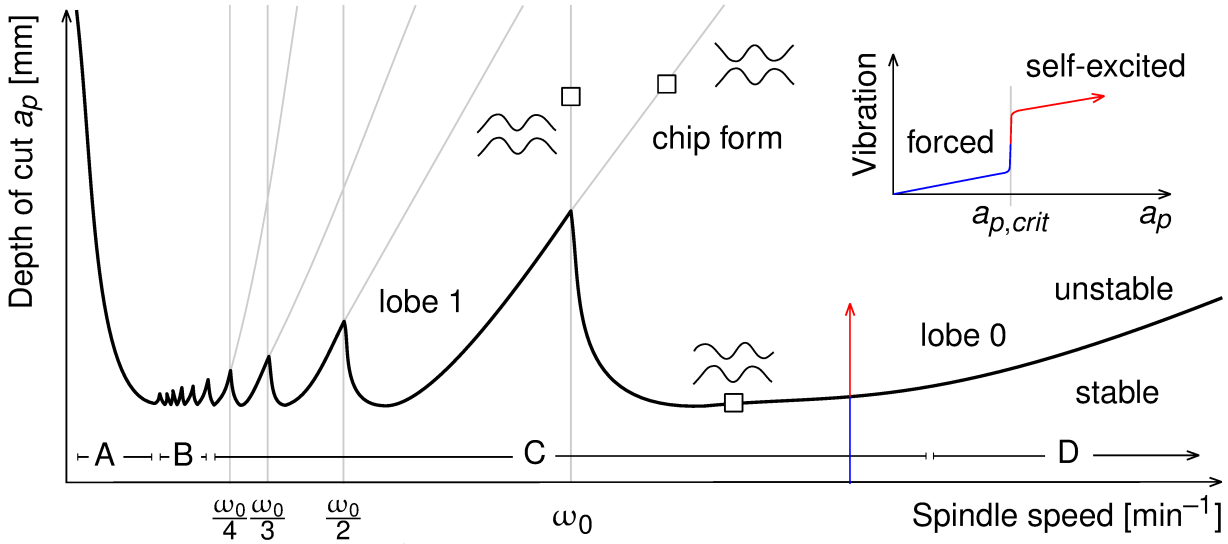

Source: Munoa et al [25], Kienast [20]

Stability Lobe Diagrams are used to visualize stable and unstable combinations of spindle speed and axial depth-of-cut, leading to a definition of machine parameters that lead to a stable system where no chatter is generated. A milling model is used to build those diagrams and to define boundaries among those stable/unstable areas. Faassen et al [33] proposed a milling model to analyze the system stability based on spindle speed variation, where for each spindle speed an axial depth-of-cut value is chosen to achieve an stable process without chatter.

H. E. Merritt [31] already described in 1965 an SLD with width-of-cut and spindle speed. However, he mentions that this method of selecting a spindle speed is not accu-

rate, since many diagrams exist for different orientations of the resulting cutting force and positions of movable process components. To overcome this issue, he presents the representation of self-excited vibrations with a feedback loop.

Delay-differential equations can be used to describe these chatter phenomena and to analyze stability diagrams. Stability diagrams can be combined with frequency charts to study chatter. Insperger et al [27] mention that identifying chatter frequencies when the stability is lost is not an easy task to perform. An experiment was developed were the most dominant frequencies were studied in different scenarios varying the system stability. Tooth pass excitation frequency and its harmonics, and damped natural frequencies were predominant in both unstable and stable scenarios. Additional predominant frequencies showed up with chatter.

Although SLD are used to detect stable regions while machining, material removal implies a continuous workpiece geometry update. Therefore, continuous changes in the milling process dynamics need to be monitored in order to detect and prevent vibrations. Digitalization and new technologies brought to the machining environmental are able to assist in this monitoring, by acquiring the necessary data to perform system analysis and even change process parameters while machining.

2.3 DIGITALIZATION

As the world became more connected and technological, the industrial field has changed constantly to improve performance and attend clients requirements. New concepts, such as internet of things (IoT), cyber-physical systems (CPS), and Cloud Computing, have been incorporated to machining. Virtual representations of physical products known as Digital Twins are used with models and simulations to evaluate the production process and to improve the design of new ones. The digitalization in machines has made process more reliable, accurate, fast, efficient, economical, and sustainable [47] [48].

Data-driven analysis is essential to study the process performance, to evaluate potential changes, and to propose improvements. Modern Machine Tools and Communication Libraries are already able to allow direct data acquisition during process. However, external sensor data are critical to develop further analysis, such as process vibration monitoring.

This section discusses how digitalization can be used to monitor process vibrations, in order to prevent self-excited vibrations known as chatter. Different approaches and implemented research are presented. Techniques to analyze vibration signals are explored, and the digitalization discussion is then expanded to comprehend how it can be used to not only monitor vibrations, but also implement a control loop to prevent them.

2.3.1 Process Vibration Monitoring

Methods to monitor and prevent vibrations have been studied and developed in order to improve the process quality and performance, given the issues caused by chatter in machining [6][29]. Some of those approaches are here discussed.

Depending on the type of chatter, vibration monitoring can be used to reduce chatter and improve the process quality and performance [6]. Perrelli et al [35] divide the approaches to prevent vibrations in two categories: out of process, which involves defining the machining system parameters and creating SLDs; and in-process approaches, in which the parameters are changed while machining.

Chatter prevention can be performed either in the process planning stage, by use of SLD given FRFs for the whole process of flexible workpieces, or by controlling the system when chatter is detected in-process. On the other hand, Bediaga et al [49, p. 385-387] present a hybrid approach to achieve an optimal solution for chatter suppression. A data acquisition system is implemented to acquire data from a microphone while machining. Microphone data are used as input for a chatter detection and analysis algorithm. Signal filtering is used to remove frequency components related to the spindle speed rotation, tooth passing frequency and their harmonics. If chatter vibrations are detected, the process speed is changed.

Furthermore, Kuljanic et al [32] state that spindle speed variation is the most practical methodology to avoid chatter using an in-process approach, since it does not require physical modification of the machine and tool. Additionally, it is mentioned that a control system could be used to detect chatter and send the system back to stability, but an automatic chatter detection in industry is missing.

Process vibration monitoring requires acquiring and analyzing process signals, which vary according to the purpose. Therefore, data acquisition is the first stage towards in-process vibration monitoring [50, p. 3647]. Multiple sensors can have their signal acquired to identify chatter. According to Kratz [51], sensors should fulfill some requirements to successfully generate signals to vibration monitoring. An overview of the requirements is shown in Figure 8. Hence, sensors must be able to measure both workpiece and tool vibrations. Additionally, it must be easy to apply in a good structure to achieve the desired results. The sensor should have also a good bandwidth and resolution, with a high signal to noise ratio. Furthermore, not interesting signals should not be more important than the process ones, and the frequency response to the latter should be high.

Figure 8 – Vibrations Monitoring Sensor Requirements

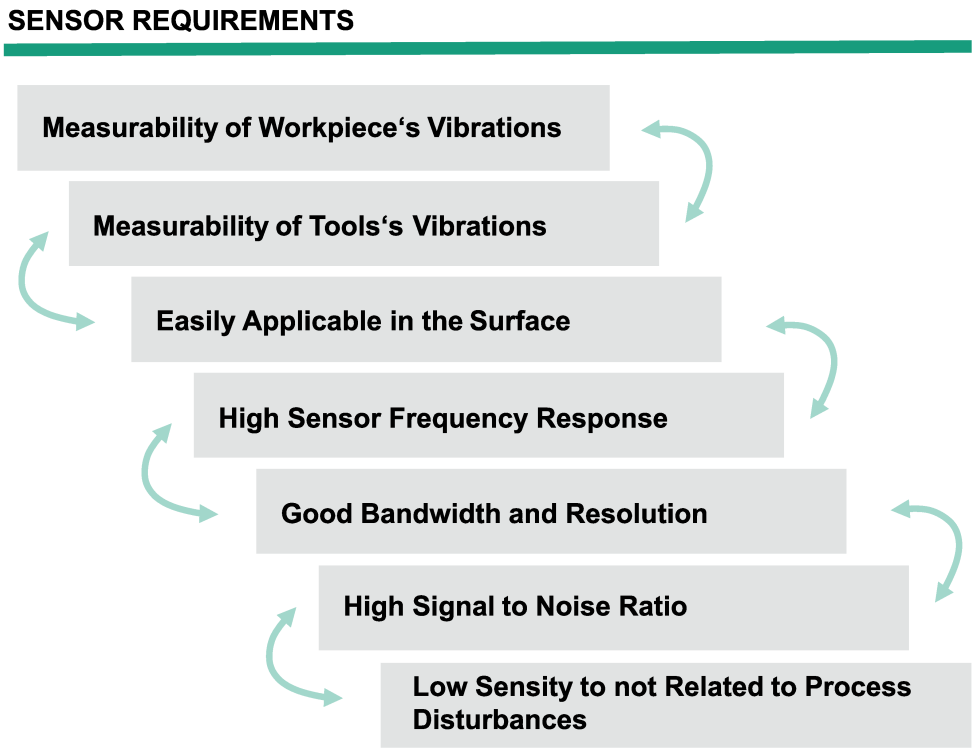

Source: Kratz [51]

Considering the study of which sensor delivers the best results, Van Dijk et al [52] tested chatter detection using a microphone, accelerometers, eddy current sensors to measure tool displacement, and a dynamometer. As a result, acceleration and displacement sensors detected chatter 50 ms before force and sound transducers. According to the authors this result is important considering that with high spindle speed chatter normally grows in 100 ms. Given the fact that eddy current sensors are not easily mounted and they are expensive, an acceleration sensor was selected by the authors to be used for chatter detection.

Kuljanic et al [32] also studied the best sensors to identify chatter. Regenerative chatter seemed to influence cutting force signals measured with a plate dynamometer. Signals from accelerometers in the spindle housing also detect vibrations influences, and acoustic emission alone would not be enough to predict chatter. Additionally, the usage of three or four sensors was recommended to achieve more process accuracy and prevent missing signal with malfunction.

A study of process monitoring articles performed by Iliyas Ahmad et al [50, p. 3647] has shown that 87% of the researches used wired sensors, while the 13% left used wireless sensors. Although the small latter percentage, the authors state that with the technologies being developed and the Industry 4.0, a transition to wireless sensors is being made.

Signal processing techniques are commonly applied to acquired signals by suitable sensory to enable drawing conclusions over the process. Processing techniques

can be performed both in the time, frequency or time-frequency domain. Filtering raw signals might also be required as a pre-processing stage, given the noise and interference caused by machining. Common approaches in the time domain include statistics calculations, such as root mean square (RMS), standard deviation, mean, skewness, kurtosis, among others [50, p. 3647-3653].

Although commonly applied, time domain analysis is limited. Dynamic data are available in the frequency domain, which requires a frequency analysis to evaluate and analyze measured signals before and during milling trials. However, process signals are not stationary, and a frequency analysis along the time is required. In the next subsection, signal processing in the time and frequency domains will be better discussed in order to inspect wave frequency components.

2.3.2 Time and Frequency Domain Processing

Sensory applied for data acquisition during 5-axis milling traditionally results in signals in the time domain. Machine and external sensor data are not always acquired with the same sampling rate, requiring a downsampling of sensors data to use both sources in the same analysis. Analyses in the time domain of external signals implies studying measurements such as the mean and standard deviation, but possible analyses are limited. With the use of frequency-domain transformations, the range of signal analysis is extended, making possible to study phenomena such as vibrations in milling. Therefore, this subsection aims to describe how time and frequency signal processing can be used to study those phenomena.

Fourier Transform is a mathematical transform commonly used to analyze frequency components of a waveform [53]. A signal in the time domain can be represented by a sum of sine and exponential waves of different frequencies and amplitudes [54, p. 528]. The Fourier Transformation is used to discover those cycles that compound a signal by splitting it into sine waves [55]. The Fourier Transform of a signal $x(t)$ is calculated by [54, p. 602]:

$$X(\omega) = \int_{-\infty}^{+\infty} x(t) e^{-j\omega t} dt. \tag{7}$$

STFT, also known as windowed or sliding Fourier Transform, is a technique created to overcome to study signals with frequency components that change over time, which is not possible when applying a Fourier Transformation [56]. This technique was created in 1946, by Dennis Gabor, who started applying the Fourier Transformation in only a small portion of a signal each time [57]. Repeating this transform for short time sections of the signal sequentially, the time information is kept while the frequency components are extracted, resulting in a time-frequency domain analysis. This approach is commonly used to study signals with frequency components that change over time, by measuring their amplitudes for each frequency in a regularly space of time [58].

The STFT algorithm application includes the definition of STFT parameters, such as the signal which will be transformed, and the sampling frequency of this signal. Small sections of the signal that will have the Fourier Transformation applied are usually defined by a parameter called window size, which determines the length of each section. An overlapping between sections can also be set when moving the window sequentially through the signal, as seen in Figure 9.

Figure 9 – Short Time Fourier Transformation

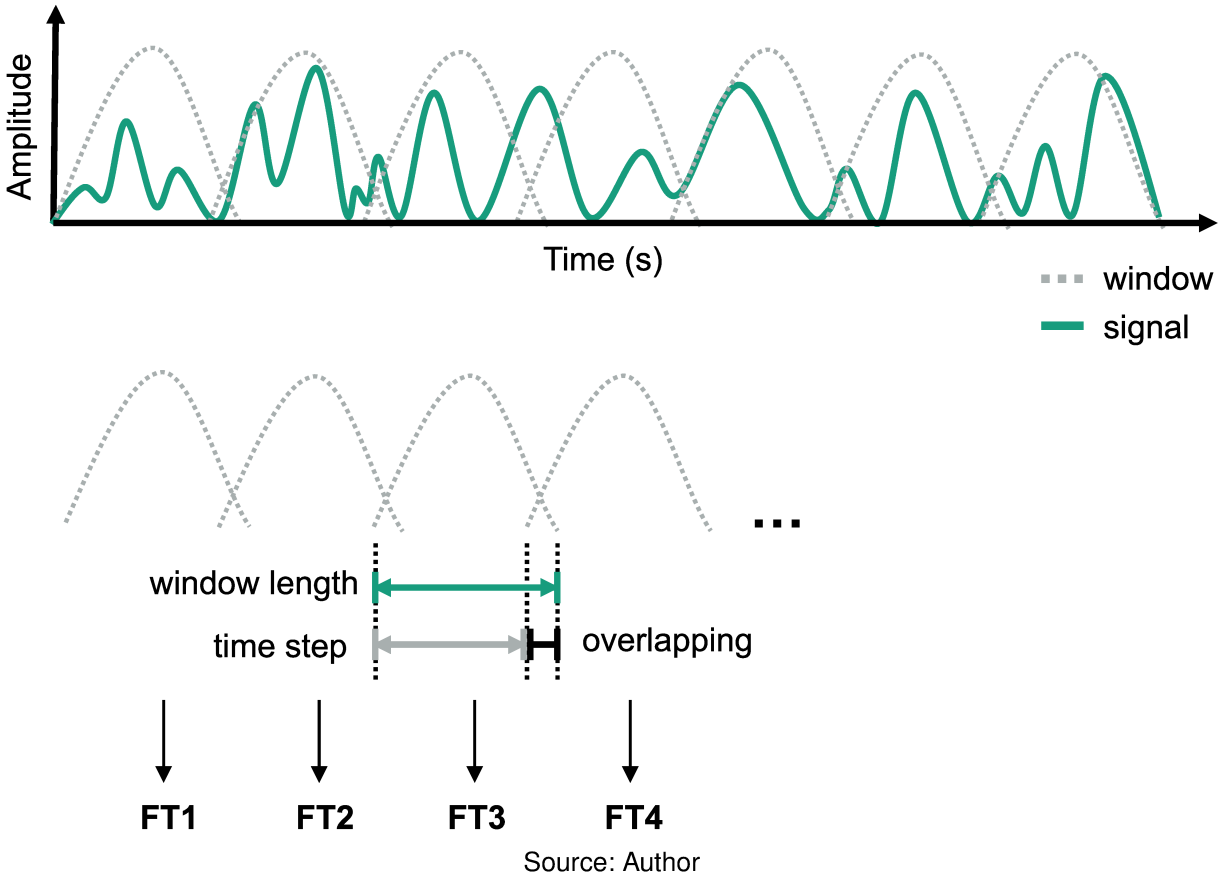

Source: Author

The window size affects the STFT time and frequency resolution. Narrow-width windows results in better time resolution, since the time period that corresponds to that STFT is small. However, this implies in a coarse frequency resolution. The inverse is also true, wide-width windows have a long time duration and therefore a not fine time resolution, but in this case the frequency bandwidth is narrow, resulting in a more accurate frequency resolution [59]. This relation between time and frequency resolution is described by Heisenberg in his Uncertainty Principle, which states that narrow time and frequency windows cannot be achieved at the same time [56][60].

When splitting the signal into windows, the signal might be truncated in the middle of the wave, when it does not has an integer number of repetitions inside a window given the sampling time. Therefore, window functions are used to decrease discontinuities, by reducing the edges smoothly to zero. The window function works

as values (or a single value in case the rectangular window) that the points inside the window are multiplied by, while the samples outside are multiplied by zero [54].

Smooth edges effect caused by window functions can be compensated by overlapping the samples, so no information is lost. However, overlapping requires more computational resources, since more calculations are done. Therefore, it is important to have a balance between information loss and algorithm performance [57].

According to National Instruments [53], to select the best window function it is necessary to estimate the frequency components of the signal. When the estimation cannot be made, the Hanning/Hann has a good frequency resolution and is satisfactory in 95% of the cases, so it can be a good start to compare the performance of different window functions. Depending on the type of signal content, specific window functions are recommended by National Instruments, as seen in Table 1 [53].

Table 1 – Window Functions

Signal	**Window Function**
Sine Waves	Hann
Sine Waves with High Accuracy	Flat Top
Unknown	Hann
Narrowband random signal (vibration)	Hann
Broadband random signal (white noise)	Rectangular

Source: National Instruments [53]

In STFT applications, based on a signal given as entry, an STFT matrix is calculated with frequencies as columns and timestamps as rows, which are displayed in a Spectrogram. The matrix dimensions are defined by the number of samples and sampling rate of the signal, as well as STFT parameters such as window length, time steps, and frequency bins [61].

The frequency values go from zero until half the sampling rate, and are divided by the number of frequency bins, resulting in the frequency resolution. Given a specific frequency resolution (f_e) to be used in the STFT and the signal sampling rate (f_s), the frequency bins (N) can be determined by:

$$N = \frac{f_s}{f_e}. \tag{8}$$

Considering n_s as the number of samples, t_s the time steps, and l the number of time lines, the size of the time dimension can be calculated by:

$$l = \frac{n_s}{t_s}. \tag{9}$$

With l calculated, and considering the time duration T, time resolution (t_r) is then:

$$t_r = \frac{T}{l}. \tag{10}$$

Based on the time duration and the number of samples, the distance between each sample on time (d_t) is calculated:

$$d_t = \frac{T}{n_s}. \tag{11}$$

In the case that an specific time resolution is used, the number of time steps can be calculated to achieve this value:

$$t_s = \frac{t_r}{d_t}. \tag{12}$$

Additionally, the overlap is calculated by the window length and time steps using the following equation by National Instruments [61]:

$$O = 100 \cdot \frac{l - t_s}{l}, \tag{13}$$

where O is the overlap and l is the window length. Therefore, the window length that should be used to get an specific overlap can be calculated, given a specific time step:

$$l = \frac{t_s}{1 - \frac{O}{100}}. \tag{14}$$

Different algorithms of Fourier Transformation can be applied with STFT, such as the fast fourier transform (FFT). Cooley and Tukey developed the FFT in 1965, when trying to achieve a faster Fourier Transformation algorithm. The FFT reduced number of calculations makes it possible to use it with applications that would require too many computational resources if applying a traditional Fourier Transformation, such as digital processing of signals [54]. Therefore, to calculate the STFT of a signal, a Fourier Transformation algorithm such as FFT is applied sequentially to sections of the signal.

Since the STFT returns amplitudes in the time-frequency domain, 2D graphs are not enough for representing its values. Therefore, special graphs are used. Spectrograms are charts that are commonly used to represent STFT values. A common representation in this type of graph is the time in the horizontal axis, the frequency in the vertical axis, while the amplitude is displayed by colors [62].

Figure 10 displays an example of spectrogram generated based on the STFT of an acceleration signal from a blisk process. The color scale is represented by a gradient, where red represents the highest signal amplitudes and blue the lowest ones. As previously described, the frequency range should go up to half the sampling rate, which in this case was 25.6 kHz, but the graph limit was restricted at 12 kHz. The

first approximately 70 s of the spectrogram are not related to the process, since data acquisition started before the process.

Figure 10 – STFT Spectrogram

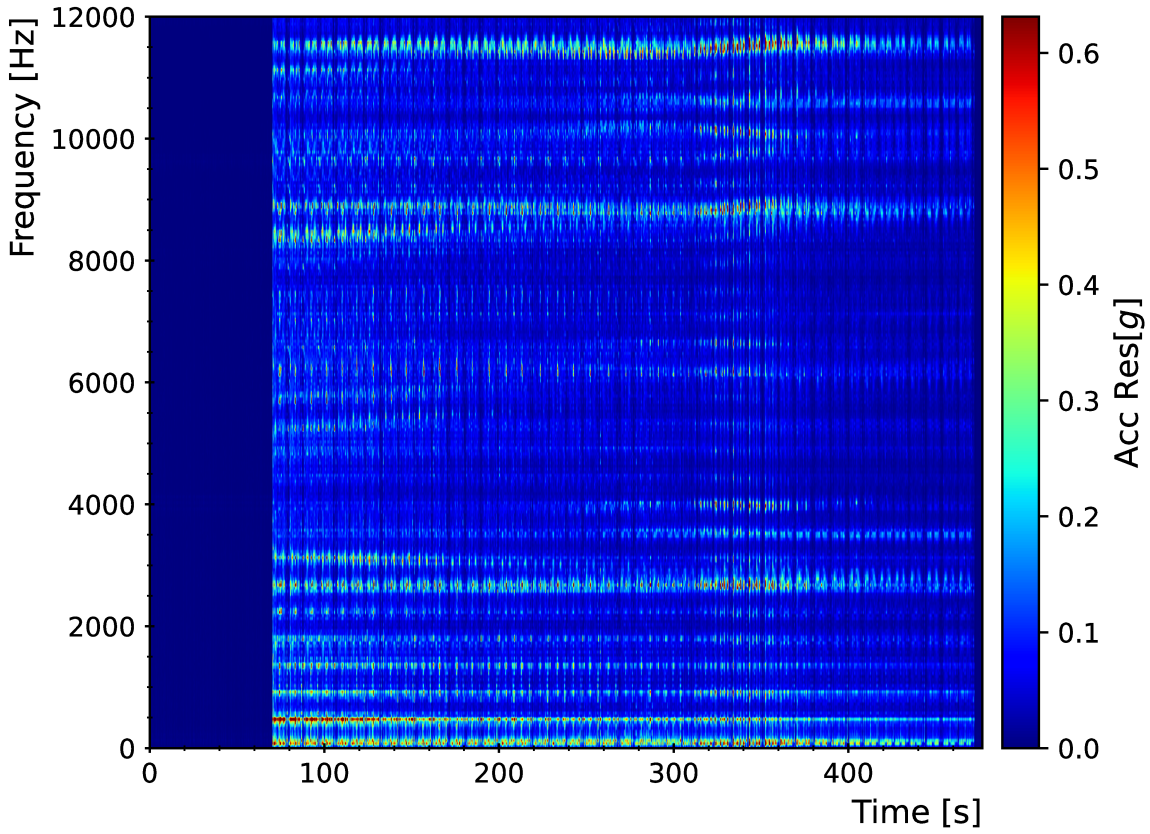

Source: Author

Knowing the expected tooth passing, workpiece and tool frequencies, an analysis of possible vibrations is possible. For example, with the knowledge that the tooth passing frequency is 446 Hz, its harmonics could be detected, and other frequencies such as workpiece eigenfrequencies could be evaluated.

This time-localized frequency information that STFT provides is important in the context of 5-axis milling process to detect the moment in which potential vibrations are caused. STFT can be applied in digital systems when acquiring data from a 5-axis milling process. With data from sensors connected to the milling machine, the STFT can be applied to those signals in order to study the frequency components and identify vibrations.

An example of Fourier Transformation application is presented in a research conducted by Alexandre et al [63], where an accelerometer is used to monitor chatter caused by self-excited vibrations in a grinding process, and signals are treated by an amplifier connected to an oscilloscope. In this study, time domain process data

are transformed to the frequency domain using Fast Fourier Transformation with the Hanning window function, after machining. The whole signal is then compared with a digital visual inspection of the workpiece manufactured. Thus, the signal showed higher amplitudes in the region with chatter.

The Fourier Transformation with vibration signals is also applied by Huang et al [64]. More specifically, STFT is used to obtain a time-frequency analysis of vibration signals. Then a neural network is implemented to build a prediction model as a bridge between the time-frequency representation of vibration signals and tool wear. The first step of this method consists of acquiring vibration signals, measuring the tool flank width, converting the signals using STFT and creating a predicting model. With the model defined, the online phase is initialized: accelerometer sensors are used to acquire vibration signals, which are transformed to the frequency-time domain process-parallel and then used as inputs for the model to predict tool wear during a milling process.

Krishnakumar et al [65] also describe the prediction of tool wear in milling processes. The study acquires vibration signals using an accelerometer as well, and machine learning algorithms to correlate statistical values of the FFT of the signal read to tool wear condition.

In the scope of this thesis, Short Time Fourier Transformation is used to analyze external sensory data in the time and frequency domains in order to identify and prevent chatter in a 5-axis milling process. External sensory data are used as parameters to determine how the process should be modified. Therefore, a control loop is implemented to achieve a desired state given the sensory data. The next section discusses how this data acquisition and control products can be used along with sensors to control a system process-parallel.

2.3.3 Control Loop

Control systems is a wide field that has been taking everyday more space in our daily life; since temperature controlling by air conditioners, until the control of autonomous cars [66]. Given inputs and a desired condition of the system, a control loop calculates one or more output signals that act over the system to achieve a reference point, such as the one shown in Figure 11. Sensors are usually used as input for this loop, while parameters or actuators receive the output signal. In the vibration scenario, a possibility of control loop is applied to prevent vibrations that cause chatter while machining.

Figure 11 – Control Loop Diagram

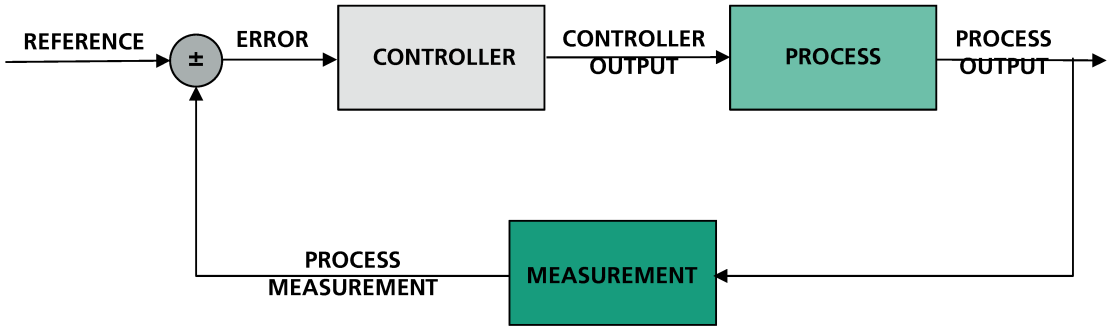

Source: Author

An example of cutting force control loop applied in a milling process is presented by Cus et al. The feed rate is controlled during the milling process using Siemens Sinumerik Feedrate Override function. This same functionality can be implemented to spindle speed control. For this purpose, the machine is connected to a personal computer (PC) with a control loop that sends the override value by an RS-232 protocol [67].

Another possibility of control loop with vibrations is presented by Alharbi [66]. Assisted monitoring vibrations have been proved to enhance the performance of milling processes. In his thesis, a control loop was created to apply vibrations during 5-axis milling process of a CNC to improve the process quality. The data acquisition software and control loop were created using LabVIEW and implemented using Real-Time and field-programmable gate array (FPGA) programming modes, with a compact reconfigurable input-output (cRIO) controller by National Instruments (NI). Input/output (I/O) modules were used connected to the controller, in order to receive signals from the accelerometer and dynamometer sensors and send them to the vibration system used. A LabVIEW program was developed in a computer which communicates with the cRIO controller, to get and send signals to it and then to the sensors.

As shown by Alharbi [66], data acquisition performs an important part in the control loop, since input signals are required to understand the current system state and to perform decisions. Data acquired can be used to understand points of improvement and how to increase performance.

Data from multiple sources, and not only from the direct connection with the machine, are generally important to make the necessary analysis and optimize the process [68]. External sensors such as accelerometers can be used to monitor vibrations, as discussed in subsection 2.3.1. A data acquisition system could be implemented to acquire those signals, and used as input for a control loop. In the context of 5-axis machining process of turbomachinery components, vibration signals can be used as input to analyze the system and to identify parameters that could be changed with a control loop to prevent chatter.

Ganser et al [48] describe edge-based data acquisition of 5-axis milling process, using a proprietary LabVIEW application to acquire, monitor, and store data from milling machines. Data from external sensors are also integrated and synchronized with this application. Spindle speed, axis position, and position in workpiece coordinate system (WCS) are among data acquired using this data acquisition system.

Cus et al [17, p. 238] implemented a feedrate control using a feedrate override function on a 4-axis machine. The adaptive controller was based on a initial peak force, which is used to calculate the following feedrate values as a product a percentage of this reference value. If no changes should be made, a override of 100% should be implemented.

Van Dijk et al [52] developed two different automatic and in-process chatter control approaches, to achieve the required surface quality while maintaining a high material removal rate. The first strategy consists of changing a spindle speed harmonic to be the same as the dominant chatter frequency, which aims to limit chatter but not minimize chatter vibrations. The second one aims to adapt spindle speed and feed while machining automatically. For the machine control, feed and spindle override machine functions were used. A new spindle speed setpoint is defined by the controller in case chatter detection, and the feed is changed to keep a constant feed per tooth. However, it is important to notice the response time given the fact that chatter detection algorithm and spindle speed adaptation control must be fast enough to be used in high-speed milling.

Bleicher at al [69] built a tool holder sensory to detect and control chatter while machining. The tool holder system was developed to transmit data from an accelerometer, in order to monitor the system and to change the process speed. A National Instruments hardware was used to receive the sensory signals, and the LabVIEW software was applied to run algorithms to machine control and data analysis. The tests were made considering three different control systems, being one of them a Heidenhain iTNC 530 CNC control system implemented with a Hermle machine. LabVIEW communicates with a Heidenhain direct numerical control (DNC) software using COM communication ports to link the algorithm to the machine parameters. An experimental setup described by the authors has shown that the control logic developed is capable of reducing chatter in-process. The solution presented seems to be more economically advantageous when compared with ready-to-use products, given the low cost of the tool-holder sensory system.

Ready-to-use products capable of acquiring machine and sensory data, monitoring, and even controlling variables such as feed rate are already available at the market. MARPOSS Group (ARTIS) has a product called CTM that is capable of monitoring in-process cutting machining, by acquiring electronic or external sensor data. A visualization system is integrated with the system to inspect the machine process and tool

condition. The control functionality comes with the product AC function, which allows an adaptive continuous feed rate control that changes the feed rate along the process to achieve an optimum performance state, given security limits [70] [71] [72].

Companies such as Komet have also been using technologies advances to create tools able to monitor machining process. Komet BRINKHAUS ToolScope is not only able to monitor, but to control as well. The adaptive control is applied to change the feed rate during process, in order to optimize the process and minimize chatter vibration [69] [73] [74].

Although ready-to-use products to monitor and control machining process, this thesis aims to develop a personalized in-process control to reduce chatter vibrations during 5-axis milling of a thin-walled turbomachinery component. The process requires a time-frequency domain analysis to detect peaks of vibrations, and differ the high amplitudes from expected machining frequencies, along the process.

2.4 CHAPTER CONCLUSION

As discussed along the State of Art chapter, chatter is one of the main impediments to achieve an efficient high-speed milling process while maintaining a high quality workpiece production [52]. Therefore, approaches to predict and prevent chatter have become of great value in the machining field in the last decades.

Although the approaches here presented are highly capable of monitoring and detecting vibrations, there is still space to develop more research on not only identifying chatter but also operating the process while machining to prevent it from happening. Iliyas Ahmad et al [50, p. 3657] reviewed 60 articles from 2010 to 2019 related to machine monitoring, and stated that:

> However, the integration between signal processing and the control system to develop an intelligent machine monitoring system is still new and is considered to be a new direction for future implementation. [50, p. 3657]

Between the approaches here presented to prevent chatter, the approach of changing the spindle speed to prevent machine vibrations is mentioned by Perrelli et al [35] as a established one, along with the possibility to change feed rate or depth cut:

> The scientific community has widely accepted that the spindle speed, the feed rate, and the depth of cut may be tuned in order to control machining vibrations [35].

Therefore, this thesis presents the development of control loop with an online vibration monitoring, to automatically change process parameters to prevent chatter. More specifically, a control loop with spindle speed in process variation method is implemented to improve a 5-axis milling process of a thin-walled turbomachinery component.

3 OBJECTIVES AND METHODOLOGY

The State of the Art chapter discusses the current situation of 5-axis milling process of thin-walled turbomachinery components, and how vibrations can lead to unstable systems, resulting in bad quality surfaces. With the digitalization of 5-axis milling and data acquisition technologies, process-parallel control of machine variables is capable of preventing those vibrations from surging, and therefore achieving the expected surface quality. This thesis is then formulated to implement a process-parallel spindle speed control, having its objectives further elaborated in section 3.1, which are met by following the methodology described in section 3.3.

3.1 MAIN OBJECTIVE

The main objective of this thesis is to develop a data-based spindle speed control for a 5-axis milling machine, aiming to reduce vibrations during finish milling of thin-walled turbomachinery components. Suitable processing techniques for the process-parallel acquired data are analyzed to detect occurring vibrations during milling by using suitable key performance indicator (KPI). The spindle speed control is validated within milling trials.

3.2 SPECIFIC OBJECTIVES

Considering the objective of controlling the spindle speed during 5-axis milling of a thin-walled component, specific tasks were defined aiming to achieve this main goal:

- Define and setup suitable sensory;
- Acquire and process machine and sensor data;
- Perform offline sensitivity analysis of KPIs for vibration detection;
- Determine dynamics properties of the mechanical system;
- Monitor vibrations process-parallel during milling;
- Send new spindle speeds to a 5-axis machine process-parallel, based on vibration KPIs;
- Conduct milling trials to evaluate the control developed;
- Analyses of process data and final workpiece quality.

3.3 METHODOLOGY

In the first step, the state of the art is presented on the basis of a literature research (chapter 2). Subsequently, a sensor setup is designed for milling trials of a demonstrator blisk blade, and a procedure for data acquisition of machine and sensor signals is used (chapter 4). The acquired signals are processed using filtering, statistical calculations, Fourier transform, and peak tracking algorithms. Suitable techniques for the derivation of vibration KPIs are evaluated by sensitivity analyses, which are performed in two steps: first, simulated vibration signals with irregularities, i.e. change in amplitude, frequency, noise or disturbances, are used to derive KPIs capable of detecting these vibration phenomena. Then, data already obtained from a previously milled blisk blade is used to calculate and analyze the KPIs offline to identify irregularly occurring vibrations. Functionalities for the process-parallel calculation of KPIs and for the control of the spindle speed are integrated into the already existing data acquisition system in LabVIEW and validated within milling trials. Before actual machining, the dynamic properties of the mechanical system are determined by Experimental Modal Analysis (EMA). Changes in the dynamic behavior during the machining process are detected by the selected KPIs, so that the adaptation of the spindle speed leads to reduced vibrations during milling. The control performance is measured by comparing the results of a blade machined with and without taking actions over the process to reduce such vibrations. Finally, the implementations and results are documented (chapter 6).

Figure 12 – Document Structure

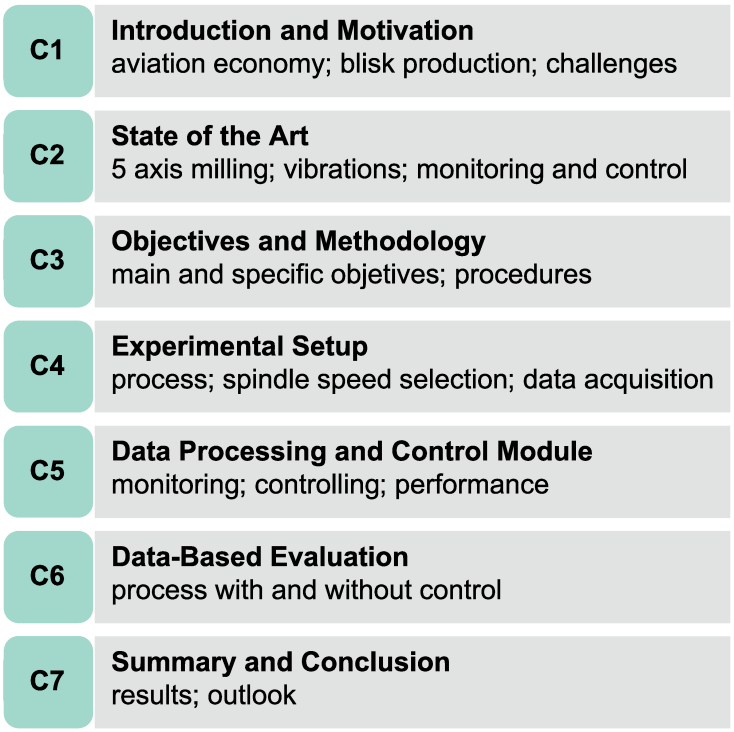

Source: Author

4 EXPERIMENTAL SETUP

This chapter presents the experimental setup to machine a blisk blade, aiming to test the effects of controlling the spindle speed in the quality of the final workpiece. The process stages and parameters are planned given the designed blade model. Dynamics of the tool-holder-system and the workpiece are measured between each stage of the process. Therefore, the spindle speed that will lead the system to a stable process without vibrations is selected, considering the high aspect ratio that blades have been designed. Process-parallel and after process analysis are performed with the application of a data acquisition system, and suitable external sensors.

4.1 BLADE GEOMETRY AND PROCESS PLANNING

The 5-axis milling spindle speed control is performed parallel to a thin-walled turbomachinery component with tendency to vibrate while machined. The control performance is measured by comparing the results of a blade machined with and without taking actions over the process to reduce such vibrations. Therefore, an essential stage of the experimental trials is the design of the workpiece that will be machined and the process planning that will lead the initial stock to the final geometry.

4.1.1 Blade Geometry

The state of art of 5-axis milling process of thin-walled turbomachinery components called blisks is described in chapter 2. Blisks are composed by several blades combined into disks, resulting in a complex geometry with long process to achieve the desired high-quality surface (chapter 1). Therefore, given the required time that would be necessary to machine a whole blisk, the experiments described by this thesis consist of a single blade design, which is used to study the effects of data processing and control developed in this project.

The designed blade is composed by three circular rings known as blocks. The use of blocks in blisks design leads to shorter lengths milled, since the total blade height is divided between the blocks. Shorter height manufacturing areas result in increased stiffness, thus reducing vibrations along the process (subsection 2.2.1). Figure 13 shows the three blocks of the designed geometry.

Figure 13 – Blocks Division

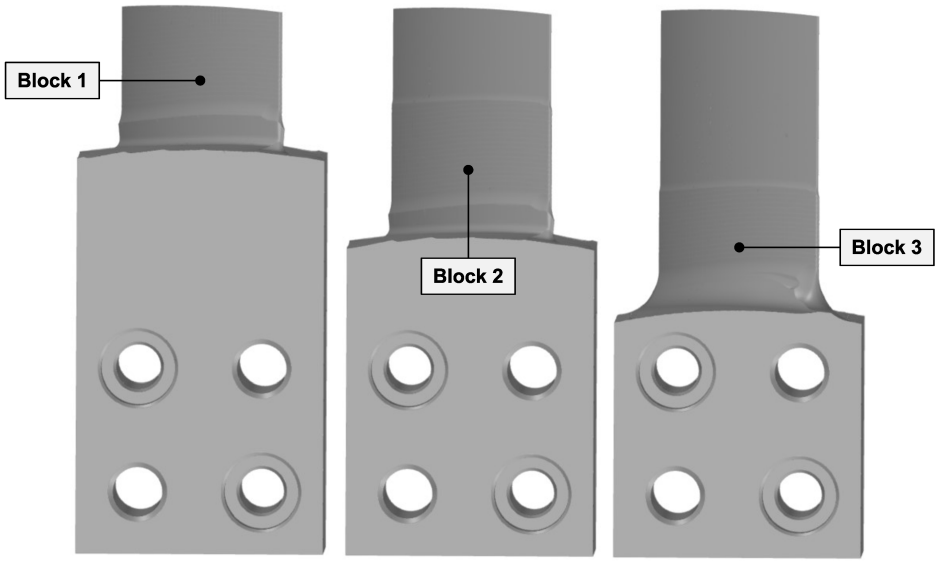

Source: Author

An initial stock material, displayed in figure 14, is used to obtain the designed blade geometry shown in the right-hand side of the image. The finalized blade has a chord length of 45 mm and a total height of 60 mm, with a minimum thickness of 0.7 mm and maximum of 2.9 mm. The height is equally divided by the three blocks, and the third block is followed by a transition area called fillet and the hub area.

Figure 14 – Initial Stock Material and Final Blade Geometry

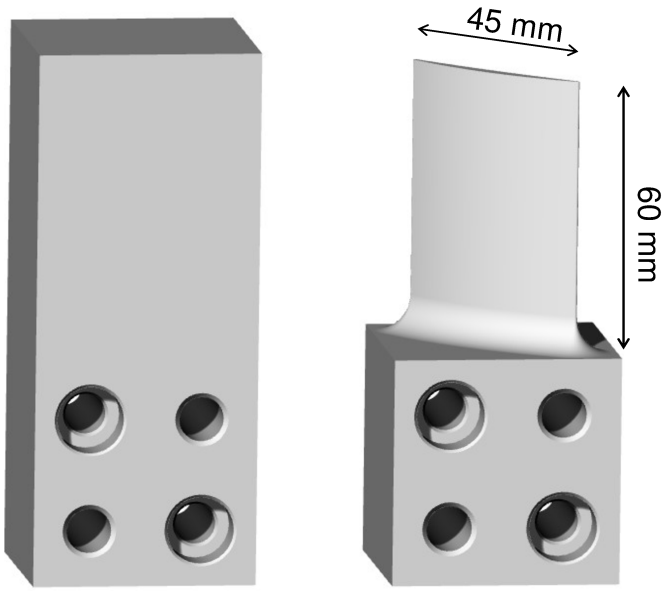

Source: Author

The initial stock material geometry contains a base that is fixed in a clamping block, which is then mounted in the milling machine adapter plate. The blade was

designed to have an accelerometer attached to the base surface, so data are acquired during the machining process. Based on the CAD model and CAM Planning, the stock material is milled in a 5-axis milling machine to obtain the desired final geometry.

4.1.2 5-axis Milling Process

The milling trials were performed in a Mikron Vertical Machining Center with five axis, model HPM 800 U HD, with a spindle speed of up to 36 000 min^{-1} and the SINUMERIK 840D sl control system. The milling tool moves along three linear axis, X, Y, and Z, while the workpiece mounted rotates with the table along axis A and C. Figure 15 shows each axis orientation and the machine used.

Figure 15 – Mikron Vertical Machining Center with Five Axis

Source: Author

The blade milling process consists of multi-stages to achieve the desired surface and geometry. Three main operations (roughing, semi finishing, and finishing) are executed sequentially for each block. When the operations are performed, the next block is then milled. The main goal of the first operation, roughing, is to remove the huge majority of material possible of a raw block, achieving a geometry close to a blade. Operations for each side are performed to remove material of both left and right-hand blade sides. After roughing, the semi-finishing is then performed, aiming to prepare the surface for the third operation, finishing. The latter defines the final surface and geometry of the piece, being the most important step when controlling vibrations. However, although finishing is the milling process that more influences the final blisk surface quality, the choice of parameters for steps such as roughing are also important to define the process productivity [75].

A milling cutting tool is specified for each operation, considering the specifications of the process in the planing stage. Ball end mill and end mill tools were used in the process as shown in Table 2. A Pro-Micron tool holder (further described in subsection 4.3.2) was used to clamp the tool in finishing operations, while a Rego-Fix (HSK-A 63 / PG 25 x 100 H) tool holder was used in the other operations.

Table 2 – Milling Tool Specifications

Operation	**Tool type**	**Number of teeth**	**Tool diameter [mm]**
Roughing (1-2)	End mill	4	16
Roughing (3)	End mill	4	16
Semi finishing	Ball end mill	6	16
Finishing (1-2)	Ball end mill	4	12
Finishing (3)	Ball end mill	4	12

Source: Author

The engagement process parameters such as axial and radial depth of cut are also defined in the CAM planning stage, as shown in Table 3. Later milling trials are performed to define kinematic process parameters as the feedrate and cutting speed. A spindle speed for each operation is calculated given the tool diameter and the cutting speed.

Table 3 – Process Parameters

Operation	**Feedrate [mm/teeth]**	**Cutting speed [m/min]**	**Spindle speed [1/min]**	**Axial depth of cut [mm]**	**Radial depth of cut [mm]**
Roughing (1)	0.9	80	1592	4	2
Roughing (2)	0.6	80	1592	4	2
Roughing (3)	0.6	80	1592	6	-
Semi finishing (1)	0.6	215	4277	1	0.4
Semi finishing (2)	0.6	210	4178	1	0.4
Semi finishing (3)	0.6	235	4675	1	0.4
Finishing (1)	0.6	268	7109	0.4	0.2
Finishing (2)	0.6	252	6685	0.4	0.2
Finishing (3)	0.6	344	9125	0.2	0.1

Source: Author

A first blade is produced in a 5-axis milling process, and used as a reference for a second blade, in which the control was applied. Therefore, the two processes and final blades are compared to ensure the effects of the control on the process and surface quality. Given that finishing is the most relevant stage for the final product quality, and the fact that the coolant used in the first two operations is the most dangerous aspect to sensors, the control and external sensors acquisition were mainly used in the finishing stage.

4.2 SPINDLE SPEED SELECTION

Thin-walled turbomachinery components such as blades have a tendency to be influenced by phenomena such as vibrations, which lead to undesired effects on the surface. Dynamic properties of the process are analyzed to avoid such phenomena by, for example, selecting parameters such as spindle speed that will lead the process to a stable operating condition. The system identification is performed to determine the dynamic properties of the process and apply a suitable stability prediction method.

4.2.1 Experimental Modal Analysis of Dynamic System

The Experimental Modal Analysis is carried out after each operation of the milling trials, so the measurements are used to determine a mathematical model of the tool-toolholder-system and thin-walled blade by system identification, as described in subsection 2.2.2. Particularly after semi-finishing, the EMA of the blade is performed to select an advantageous spindle speed in a stable region to reduce vibration effects and chatter formation while finishing, given that this step of the process results in the final surface.

The blade is excited with an impulse hammer Polytec GmbH OFV-5000, and the response is measured with a laser vibrometer PCB Synotech GmbH 08A17, as shown in Figure 16. The laser vibrometer was selected as measurement device given the fact that this equipment is mounted without contact with the workpiece, preventing influencing the measurement with the attached mass. Eigenfrequencies of the finishing tool and workpiece are determined by FFT based on the signal measured.

Figure 16 – Experimental Modal Analysis Setup

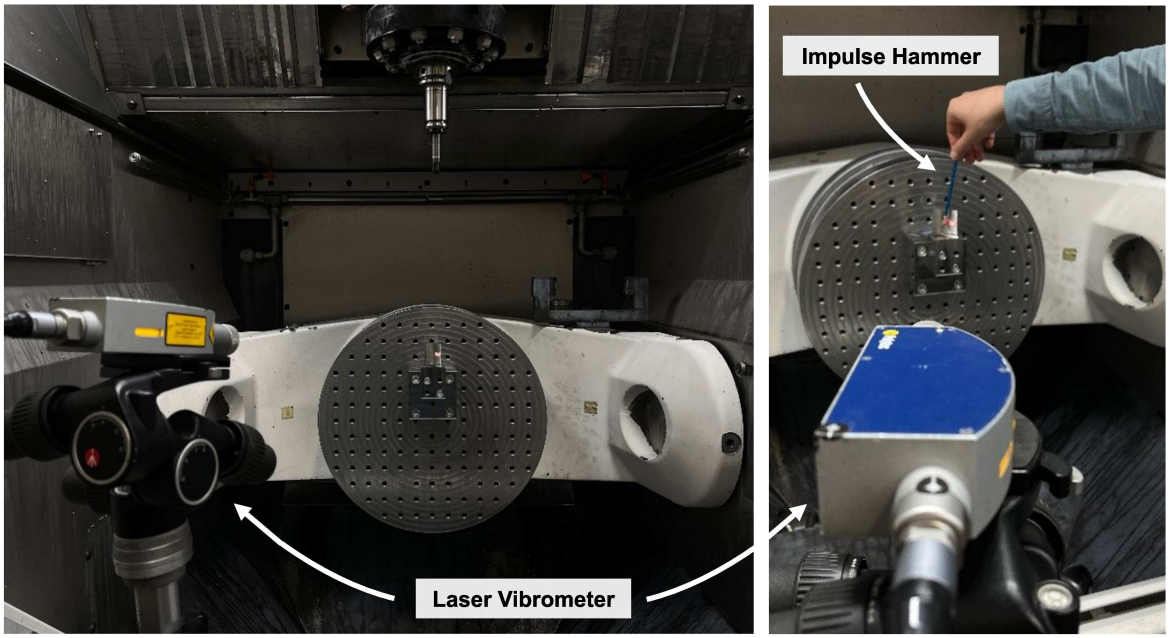

Source: Author

The EMA was performed to get the characteristics of the finishing tool. The impulse hammer Polytec GmbH OFV-5000 and an accelerometer PCB 352C22 were used in the experiment. The same dominant eigenfrequency of 780 Hz was identified for the finishing tool measuring in both X and Y directions, with a slight difference in the amplitude of approximately $1.17\,10^{-6}$m/N, as shown in Figure 17.

Figure 17 – Experimental Modal Analysis of Finishing Milling Tool

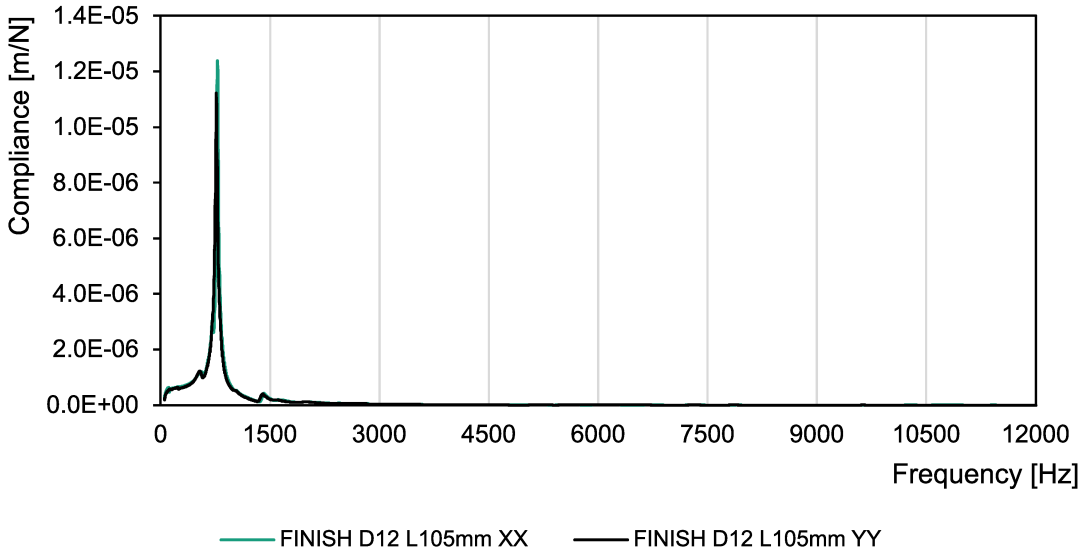

Source: Author

The dominant eigenfrequencies identified for the workpiece before finishing are shown in Figure 18. For the first block, the two eigenfrequencies with highest amplitudes were: 3960 Hz and 6266 Hz. For the second block the highest amplitude eigenfrequencies found were 1906 Hz, 3908 Hz, and 7676 Hz. Finally, for the third block: 1168 Hz, 2630 Hz, and 5222 Hz.

Figure 18 – Frequency Response Function of the In-Process Workpieces Before Finishing of Blocks 1 to 3

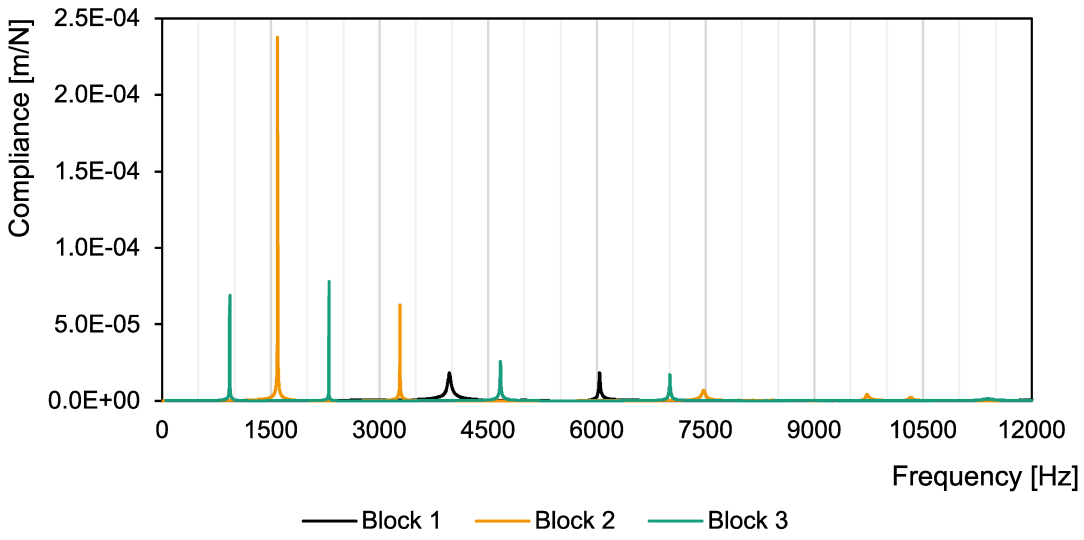

Source: Author

With the eigenfrequencies determined, the spindle speed is defined in order to achieve a stable process. Figure 19 shows a graph that displays the tooth passing frequency and its harmonics, considering the selected spindle speed for finishing the first blade block. In terms of stability, the workpiece frequencies should be ideally between two tooth passing frequency harmonics and not overlapping one of them.

Figure 19 – Experimental Modal Analysis of Operation Finishing of Block 1

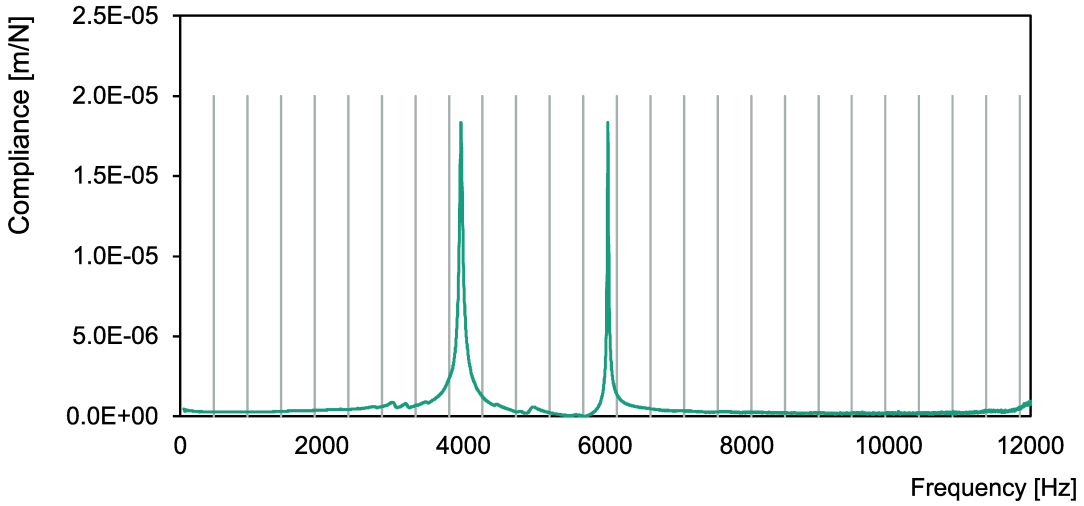

Source: Author

Considering the system identification and following the relation given by Equation (5), the spindle speeds and tooth passing frequencies shown in Table 4 were selected for each block finishing operation.

Table 4 – Spindle Speed and Tooth Passing Frequency for Finishing Operation

Block	**Spindle Speed [m/s]**	**Tooth Passing Frequency [Hz]**
Block 1	7109	474
Block 2	6685	446
Block 3	9125	608

Source: Author

Although a initial spindle speed that would lead the system to a stable process is determined, the dynamics are constantly changing by material removal of the workpiece. Therefore, a process-parallel analysis is still necessary to monitor the stability of the system and ensure the desired final blade quality.

4.2.2 Stability Prediction

Many approaches to detect and prevent chatter have been studied along the years, as discussed in subsection 2.2.3, resulting in different methods to predict the stability of a process. Although Stability Lobe Diagrams are a common method for detecting machining stable regions, material removal leads to a continuous workpiece geometry update so the dynamics are constantly changing. Therefore, process monitoring and stability prediction parallel to milling are better applied methodologies to identify and achieve the process stability.

Existing procedures to predict milling process stability include the minimal frequency method, which has a reasonable balance between stability precision and computational resources. This procedure is applied for specific spindle speeds of a determined range. Therefore, the selection of process parameters such as spindle speed leads the process initially to a stable region. The minimal frequency difference method is applied based on the system identification performed with EMA, by considering the identified eigenfrequencies of the tool and workpiece. The latter frequencies are together considered the natural frequencies of the total system, and the tooth passing frequency is an external harmonic excitation.

The possible spindle speed range of the system is used to evaluate the stability of the system. For each considered spindle speed inside the range, the minimal frequency difference is calculated, and a state in the frequency domain is related to it. Figure 20 shows an example of the method applied to a blade. The middle graph displays the minimal frequency difference calculated for the whole spindle speed range, where the vertical axis value represents the smallest distance between a natural frequency and the tooth passing frequency harmonics. Upper and bottom graphs show the calculation of the minimum distance for two different spindle speeds.

Figure 20 – Example of Minimum Frequency Difference Method Application

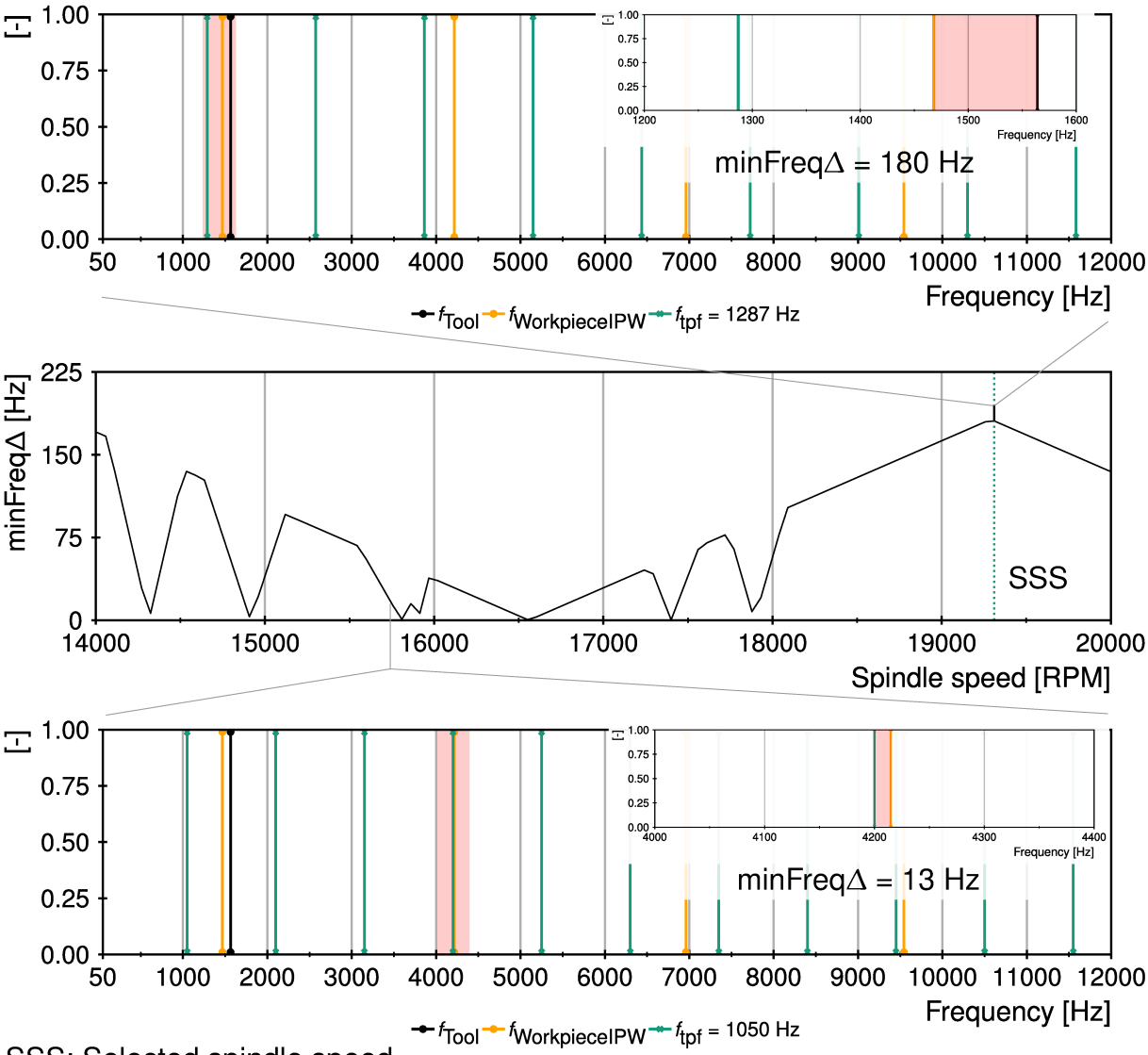

SSS: Selected spindle speed

Source: Kienast [20]

Small values of the minimum frequency difference method indicate a tendency to instability, since the distance between an eigenfrequency and an harmonic is small. As seen in Figure 20, a spindle speed of 15.750 m/min has a minimum frequency difference of only 13 Hz, while if a speed of 19.311 m/min is selected, the minimum value increases to 180 Hz, representing an advantageous spindle speed that tends to lead the process to a stable condition.

4.3 DATA ACQUISITION AND SENSOR SETUP

Machine data acquisition and processing from the 5-axis milling process is necessary for the process-parallel spindle speed control. Not only the acquired data allows the parallel control, but it also allows after analysis and improvements in the process

by storing data in files. Suitable sensory is used to perform further analysis over the process, that would not be possible using only machine data.

4.3.1 Data Acquisition Hardware

A data acquisition on LabVIEW was previously developed in the High Performance Cutting department. The system implemented is capable of acquiring both machine and external sensory data. The data acquisition runs continuously in a PC or industrial personal computer (IPC) (which typically is stored inside the machine electrical cabinet, where it is protected and constantly connected), which is then connected to the data sources to obtain the desired information.

Machine data are acquired directly from the machine Programmable Logical Controller (programmable logic controller (PLC)) and Numerical Control Kernel (numerical control kernel (NCK)) using the ACCON-AGLink library, which is capable of exchanging data between machines and IPC/PCs. Furthermore, different external sensory data acquisition (DAQ) modules can be integrated to the system by using communication protocols such as message queuing telemetry transport (MQTT), or by connecting with USB a data acquisition chassis to the PC. Figure 21 shows the connection schema between the PC running the Data Acquisition system and data sources.

Figure 21 – Data Acquisition Schema

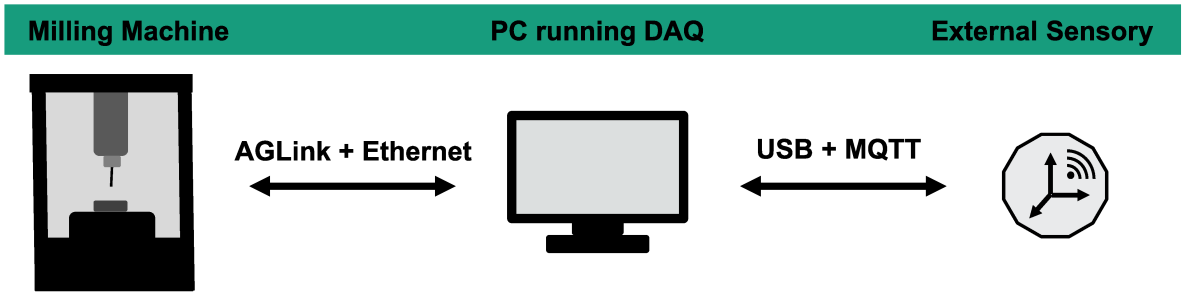

Source: Author

The ACCON-AGLink is a communication library that comes with ready-to-use functions to allow a smooth data exchange between PLC and IPC/PC. Therefore, large amounts of data can be processed and stored in a PC, while the connection to the machine to acquire such data is retained. The ACCON-AGLink supports the connection between different machine controllers, including the SINUMERIK PLC of the 5-axis milling machine used. The goal of this software is to handle multiple languages and technologies, so different communication protocols can be employed, assuring data transferring. An Ethernet cable is used to connect the machine with the PC or IPC running the data acquisition system, then the machine Internet Protocol (IP) address is configured in the PC/IPC, allowing both reading and writing machine data. [76] [77]

External sensory data are acquired by connecting a National Instruments cDAQ-9178 chassis with space for up to 8 I/O modules to the PC or IPC running the data acquisition system. The compact data acquisition (cDAQ) line from National Instruments is compound by hardware created to be compact and portable, so they can be mounted near the industrial process being monitored. Its main goal is to measure and validate data from any environment, with integrated data processing, by connecting sensors with data storing software such as LabVIEW. cDAQ is easily scalable with its chassis and I/O modules, making it suitable to DAQ applications with a large number of signals [78]. The cDAQ hardware is connected directly to a PC using USB or Ethernet, so the PC is able to read and send signals to the modules. Figure 22 shows an overview of National Instruments components and sensors commonly used to acquire data.

Figure 22 – National Instruments Data Acquisition Schema

Source: Kistler [37] [79], Digi-Key [38], National Instruments [80] [81], DirectIndustry [82], AMC [83]

Sensors such as accelerometers, acoustic emission, and force sensors are connected using National Instruments I/O modules to the cDAQ module, thus they have their signal translated to inputs that the LabVIEW is capable of reading by using a function specific to read real-time data of DAQ modules. An initial task is created in the National Instruments measurement and automation explorer (NI MAX) software, where specifications of each sensor are defined, such as the scale and units measured, the sensor sensitivity, and the physical position of each sensor in the cDAQ module. A USB interface is used to connect the cDAQ chassis with modules to the IPC/PC running the Data Acquisition software on LabVIEW, so sensor data are read and then stored in the same file as machine data.

Other types of external sensors might be connected to the Data Acquisition system by using communication protocols, such as MQTT. Although machine data are essential for the data acquisition system, external sensors are optional. Thus, sensors definition and required connections vary with the process and desired analysis.

4.3.2 Suitable Sensory

Suitable sensory is used to complement data acquired directly from the machine. Thus, additional analysis can be performed. Subsection 2.3.1 discusses suitable

sensors for process vibration monitoring, stating that the huge majority of sensors yet applied are still wired. Furthermore, accelerometers have shown a good performance when looking for detecting vibrations in the milling process, considering the desired requirements of a good vibration monitoring sensor.

A large variety of accelerometers are available, differing by their characteristics such as size, resolution, and range. Selected sensors should be able to measure the process dynamics, as identified in the EMA. However, frequency range of accelerometers and sensitivity are inversely proportional. A wide frequency range implies in increasing the resonant frequency and, therefore, decreasing the seismic mass. On the other hand, low seismic mass means that the sensitivity is also low. Therefore, a balance between those characteristics should be achieved [84].

Figure 23 shows a typical frequency response curve for an accelerometer excited by a constant acceleration. Although the characteristics of an accelerometer can vary, for example if a long cable is used, typically the recommended frequency to be used with an accelerometer is one-fifth of its resonant frequency f_r [85]. When looking at the frequency response curve, $0.2\,f_r$ indicates a measurement error of 5 % when compared with the reference frequency f_0 [84].

Figure 23 – Accelerometer Frequency Response Curve

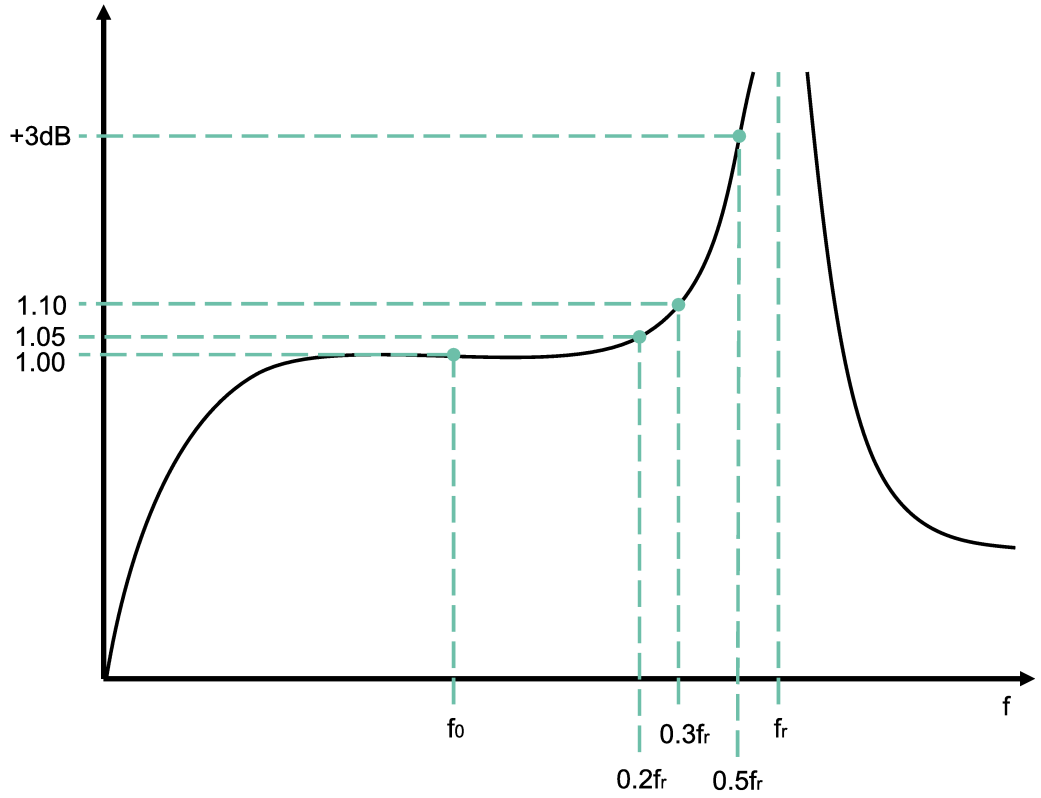

Source: Wagner and Burgemeister [84]

Additional sensor characteristics include the number of axis in which the acceleration is detected. Considering the desired process analysis, triaxial accelerometers

were selected for this experimental setup, so the acceleration on three axis (X, Y, and Z) are measured, considering the sensor attached position. Furthermore, the integrated electronics piezo-electric (IEPE) technology was selected for the experimental setup. IEPE accelerometers are commonly adopted in industrial applications, with built-in electronics that allow integrated signal conversion from the charge output of piezoelectric transducers to a voltage signal [86].

Given the desired characteristics, two IEPE triaxial accelerometers were mounted in the milling machine, as shown in Figure 24. The first accelerometer used, a PCB 356A15 accelerometer with a measuring range of $\pm$ 50 g, was attached to the workpiece. The second one, a Kistler 8764B050BB accelerometer with the same measuring range, was mounted in the spindle speed fixture.

Figure 24 – Sensor Positioning

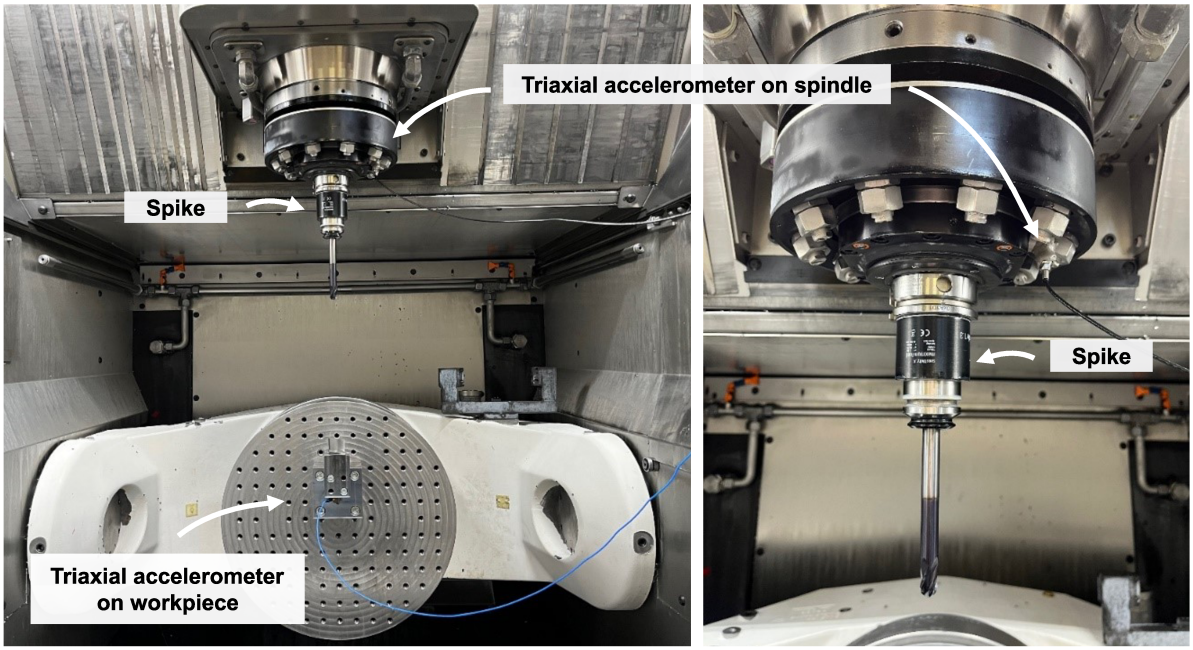

Source: Author

Additionally, a spike mobile from Pro-Micron was used during finishing operation, as shown in Figure 24. The spike is a wireless intelligent tool holder that is able to measure the cutting force and moments directly in the tool by integrated sensory in the tool holder. Not only raw data of measurements such as bending moment, torsional moment, axial force, and temperature (figure 25) are send, but the spike is also capable of calculating and sending statistical values of the variables being measured [87]. Data are sent wireless from the tool holder to a receiver, which is connected by USB with a computer which is running the Tool Control Center software. Then, the communication protocol MQTT is used to send data to the Data Acquisition system running on LabVIEW.

Figure 25 – Pro-Micron Spike

Source: Pro-Micron [88]

Suitable sensory data, such as the ones sent by the accelerometers and spike, are constantly acquired by the data acquisition system. Storing the external sensory data allows further analysis even after the process is finished, leading to improvements in future trials.

5 DATA PROCESSING AND CONTROL MODULE

Process-parallel vibration monitoring is typically based on process data acquired, which are processed and analyzed to identify and avoid vibrations. A data acquisition system is necessary to obtain data used as basis for the analysis. Statistical calculations and transformation from time to frequency are performed to allow analysis of the process. Processed data are then used to identify changes in the system that would lead to vibration reduction, by implementing a control module capable of sending data back to the machine. Therefore, an integration between data acquisition, calculations, and data writing is necessary, with a performance fast enough to change the process correctly.

5.1 TIME-FREQUENCY DOMAIN ANALYSIS APPLICATION

Subsection 2.3.2 introduces how the transformation of signals to the time-frequency domain allows additional analysis of the process, since the components in the frequency domain can be analyzed to detect vibrations, for example. A data acquisition system was already developed in LabVIEW, which is able to acquire process-parallel data. Therefore, the further development of this system is proposed to process external sensory signals and apply stability analysis and calculations. An offline application was first developed to read technical data management streaming (TDMS) files and apply the transformation over the read signal (subsection 5.1.1), which is then used to track vibrations in the process (subsection 5.1.2). Offline tests using previously machined blisks data are performed to test the application and its ability to detect process vibrations (subsection 5.1.3). The offline application was then integrated with the data acquisition system (subsection 5.1.4). Thus, signals are acquired and processed while machining.

5.1.1 Key Performance Indicators Application

The software named Key Performance Indicators (KPI) application (Figure 26) was previously developed at the High Performance Department at Fraunhofer IPT using LabVIEW, aiming to perform sensitivity analyses on simulated vibration signals. Three different simulated waves can be defined in the interface, with different frequencies, amplitudes, types of wave, noise, and phase. Additionally, a disturbance might be applied to the simulated system, with specific frequency, amplitude and phase, in a certain period of time. The application is capable of running multiple simulations, where parameters of each wave can be modified to perform sensitivity analysis.

Figure 26 – KPI Application Used as Basis

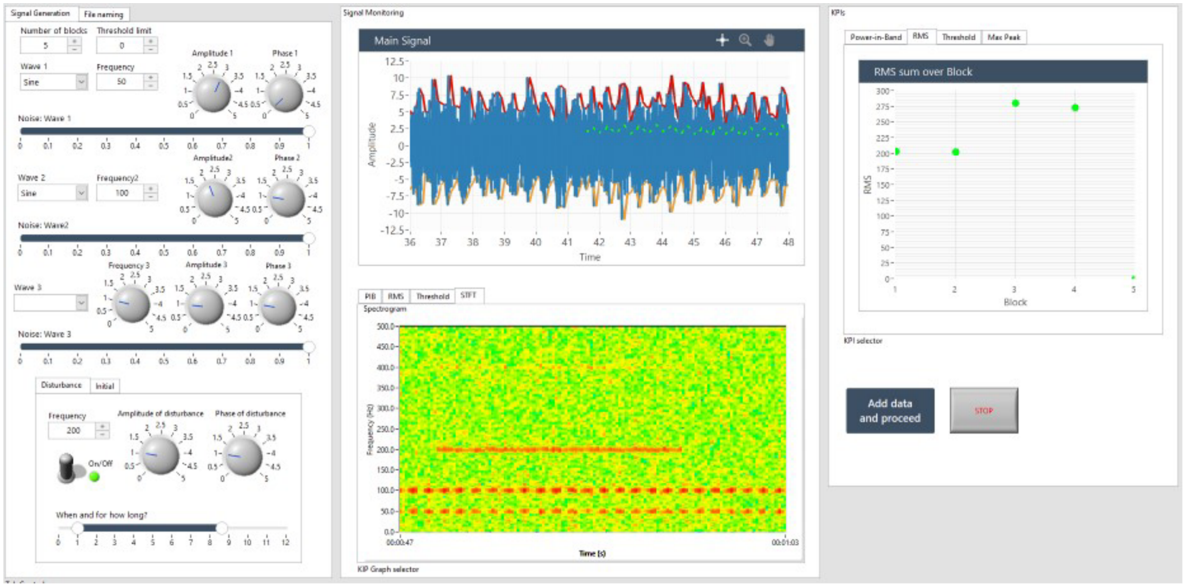

Source: Author

STFT is applied to the sum of each simulated wave and disturbance, and displayed in a Spectrogram in the KPI application. The frequencies of the waves with highest amplitudes are identified in the Spectrogram with the red color (considering a scale from blue to red). Given the signals in time and time-frequency domain, KPIs are calculated by the application, which includes power-in-band (PIB), RMS, Threshold, and Maximum Peak. The KPI application is used to simulated signals with irregularly vibrations, in which sensitivity analysis can be performed to identify vibrations using certain KPIs. Kienast [20] presents a study using the application that shows RMS and PIB are efficient to identify dynamic vibrations.

New functionalities were then implemented to the KPI application, aiming to apply the KPIs to process-parallel signals instead of simulated ones. The STFT functionality was further developed to enable performing sensitivity analysis of the STFT parameters. For example, in the new application it was added the possibility to change the window size simultaneously. Also, more controls such as the signal sampling rate and number of samples were added in the front panel. With the analysis and development of KPI application finalized, and based on studies on how the time and frequency resolution are affected by each input of the STFT module on LabVIEW, a new application was created. The Time-Frequency Domain Analysis application (Figure 27) has the same functionalities as the KPI application, but instead of using simulated signals created on LabVIEW, this application is capable of reading TDMS files to get signals as inputs for the STFT. TDMS is a National Instruments type of file. The previously developed data acquisition system stores data from 5-axis milling processes in these files.

Figure 27 – Time-Frequency Domain Analysis Application

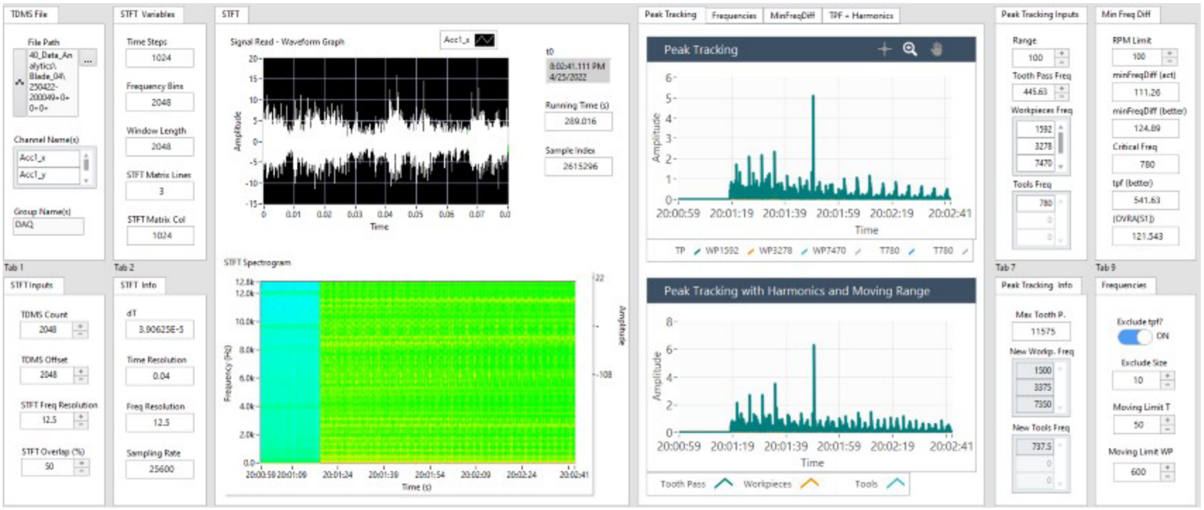

Source: Author

A TDMS file path and the variable which will be read are selected in the front panel, in the Time-Frequency Domain Analysis application. With the signal read from the file, the offline KPIs of this new application are used to identify irregularly occurring vibrations in previous processes. The reading and KPIs were first implemented for the whole signal, but to simulate the real-time environment the TDMS reading and processing was developed to read a certain number of samples, since in the real process data new data are acquired one after the other. The number of values that should be read from the TDMS file and the overlap between packages are defined in the front panel.

The STFT is then calculated for each package of elements read from the TDMS file. Based on the choice of STFT parameters, time and frequency resolution are defined. This resolution is automatically calculated by the STFT module used on LabVIEW, which has as inputs the time steps, frequency bins, and window length. However, frequency resolution and overlap between STFT windows are generally more easily understood. Therefore, variable manipulations are made inside LabVIEW so the the frequency resolution and overlap are defined in the front panel, and the necessary inputs for the STFT module are defined considering them.

Based on the time-frequency domain transformation of signals read, a matrix is generated such that the rows are time values and the columns are the frequencies, with the specific resolution of each calculated. The time-frequency domain signals are then displayed in a Spectrogram, as data are read from the TDMS, which is used to a visual analysis of signal amplitude along the time for each frequency. Additionally, based on this time-frequency transformation matrix values, further functionalities are develop in order to identify irregular vibrations in the signal read.

5.1.2 Peak Tracking

The peak tracking functionality is one of the functionalities implemented in the Time-Frequency Domain Analysis application. Its goal is to track signal amplitude along the time for specific frequencies, using STFT transformed data as input. Considering the usual frequencies of a blisk 5-axis milling process, tooth passing frequencies, workpiece, and tool frequencies are defined in the front panel. For the tooth passing frequency, the peak tracking functionality compares the amplitude of all the harmonics and plots their highest value for each timestamp,. As for the other two types of inputs (workpieces and tools frequencies), the maximum amplitude of each category is determined for each time value and displayed in a waveform graph to visualize peaks. The list of the frequency with highest amplitude for each category is presented in a waveform chart.

A range is also defined for the peak tracking functionality. Considering the range, frequencies around the specified ones have their value read to verify which magnitude value is the highest inside the range. Therefore, for each timestamp, the highest value is detected for each one of the categories (tooth passing, workpiece, and tool frequencies), and then used as the value to calculate the range in the next timestamp. As a result, only the highest value of each category considering a moving range is plotted.

Figure 28 shows part of an example of STFT Matrix and how the moving range would work for the frequency of 50 Hz and its harmonic 100 Hz, to exemplify how the peak tracking and moving range works. Considering a range of 16 Hz and with a frequency resolution of 4 Hz, the figure shows how the range (highlighted numbers) and the highest values (bold numbers) in each range move along the time, since the range is based on the last highest value.

Figure 28 – STFT Matrix - Example of Columns with Highest Amplitude

index	***0***	***...***	***10***	***11***	***12***	***13***	***14***	***15***	***16***	***17***	***18***	***19***	***20***	***21***	***22***	***23***	***24***	***25***	***26***	***27***	***28***
***f* (Hz)**	***0***	***...***	***40***	***44***	***48***	***52***	***56***	***60***	***64***	***68***	***72***	***76***	***80***	***84***	***88***	***92***	***96***	***100***	***104***	***108***	***112***
0s	5	...	5	6	8	9	**10**	4	5	5	5	5	4	4	4	4	5	**6**	5	5	4
0,01s	9	...	9	11	12	**13**	8	7	9	9	9	9	9	8	8	7	**10**	9	9	9	9
0,02s	11	...	11	7	**10**	9	9	8	11	11	11	10	10	9	9	8	11	11	**12**	10	10
0,03s	11	...	11	**12**	10	9	9	8	11	11	11	10	10	9	9	8	11	11	**12**	10	10
...	...	...	...	...	...	...	...	...	...	...	...	...	...	...	...	...	...	...	...	...	...
10s	11	...	11	10	10	9	9	8	11	11	11	10	10	9	9	8	11	11	11	10	10

Source: Author

The moving range functionality works on the back-end of the Time-Frequency Domain Analysis application, by identifying the highest value in each range on every

iteration. The application then displays the information in the front panel for visual analysis. Figure 29 shows two graphs generated by extracting data from the graphs in a simulation with data of a previously-milled finishing stage of the reference blade. The graph on the left shows the amplitude for the selected frequencies only, but the right-hand one considers the harmonics of the tooth passing, and a range around the selected frequencies. Since the latter graph considers the maximum value in a certain range and the harmonics, its amplitudes are higher than the ones in the former.

Figure 29 – Offline Peak Tracking Graphs

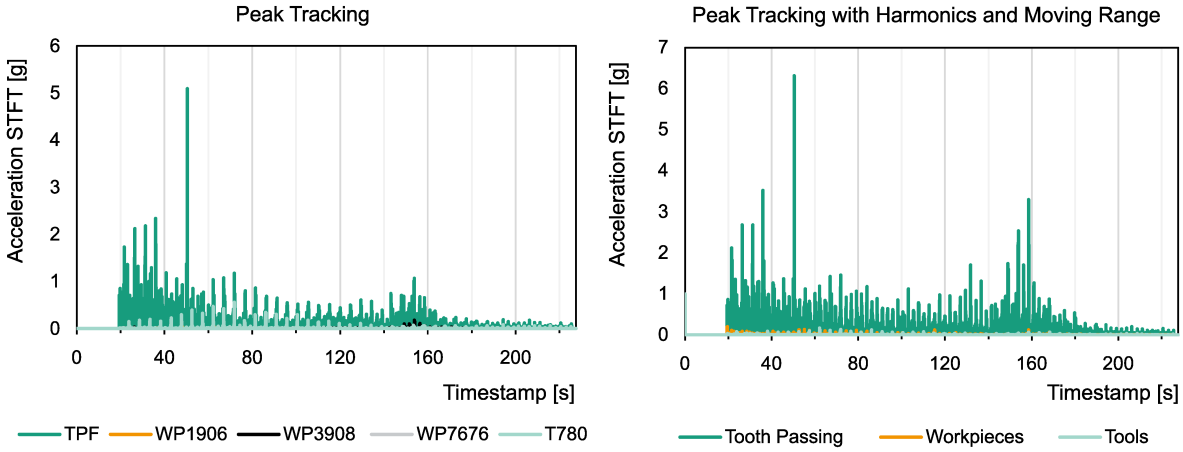

Source: Author

Additional graphs in Time-Frequency Domain Analysis application allow the analysis of identify how the maximum frequency of each category (tooth passing, workpieces, and tools) changes along the time (left graph in Figure 30), as well as tracking changes of the tool and workpiece frequencies (right-hand graph in Figure 30).

Figure 30 – Moving Frequencies graphs

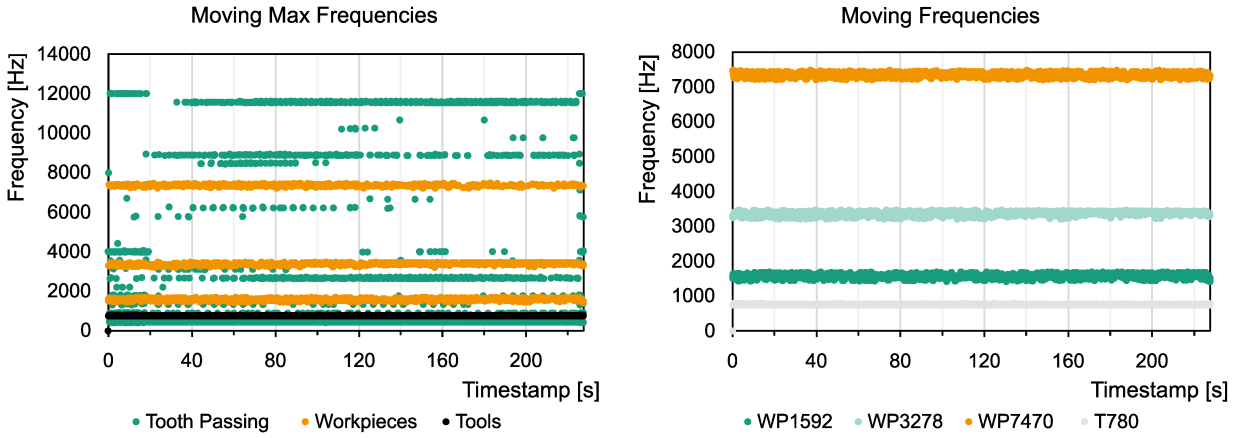

Source: Author

Since the workpiece and tool eigenfrequencies move along the process, moving frequency limits were also implemented for them. Therefore, even though a moving

range is applied, the workpiece and tool moving frequencies do not exceed the frequency limits defined. Without this functionality it was analyzed that for a specific workpiece or tool frequency the moving range could detect one of the other workpiece/tool or a tooth passing harmonic frequency that has the highest amplitude inside the range, and consequently no longer monitor this frequency.

An additional functionality was developed given this fact that a tooth passing harmonic frequency with high amplitude could be detected instead of a tool or workpiece frequency. A range around each tooth passing and harmonics frequency can be defined, so they are not considered as a possible choice for the highest amplitude for the workpiece and tool moving range functionality. Therefore, when activated, this functionality avoids the case where workpiece and tool frequencies overlap one of the tooth passing harmonics, since this condition should ideally be avoided. However, after some tests it was observed that depending on the exclude size, the workpiece frequency is limited between two harmonics and would not achieve the desired final value. The offline tests performed are further explained in the following subsection.

5.1.3 Offline Tests

Sensitivity analysis of the Time-Frequency Domain Analysis application parameters was performed while new functionalities were implemented, aiming to verify the best values to identify process vibrations. The application analysis is made by using data from previously manufactured blades, which are imported by the application. Figure 31 shows a previously milled blisk, which data are used for testing the Time-Frequency Domain Analysis application. Data from the finishing operation of two different blades are used for testing: the first one was milled with a new tool, while an old tool was used for milling the second blade.

Figure 31 – Previously Milled Blisk Used for Offline Tests

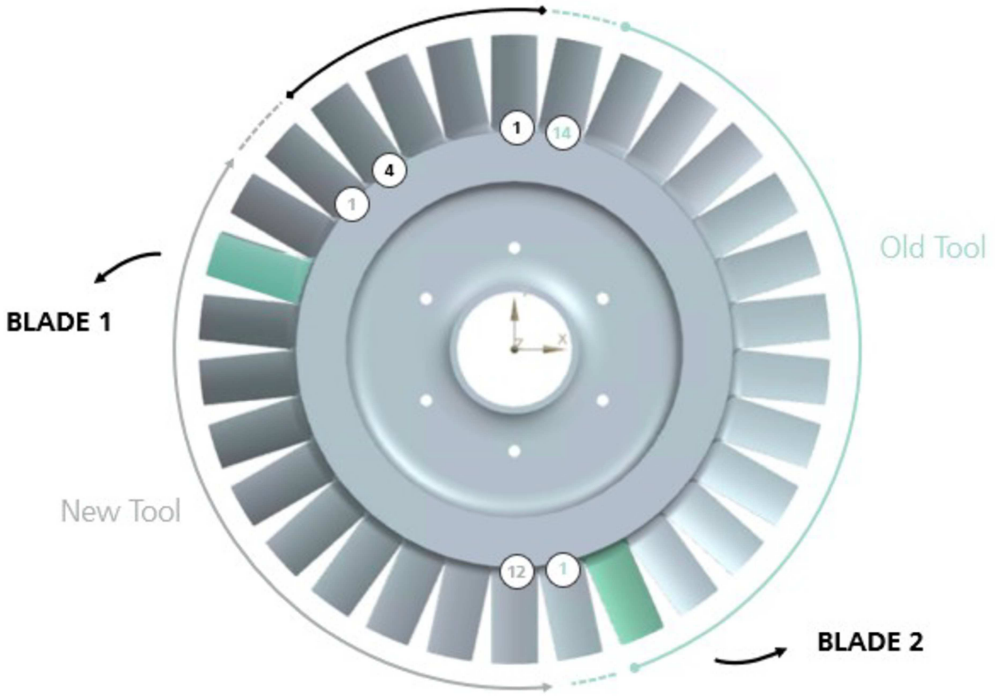

Source: Author

Figure 32 displays the two blades of the manufactured blisk that were used for sensitivity analysis. The numbers displayed indicate the four blocks of each blade. As seen, the second block of the blade on the left-side was not affected by chatter, resulting in the desired surface quality. On the other hand, the right-side blade shows marks of vibrations effects on its surface.

Figure 32 – Chatter Effects on Blade Surface

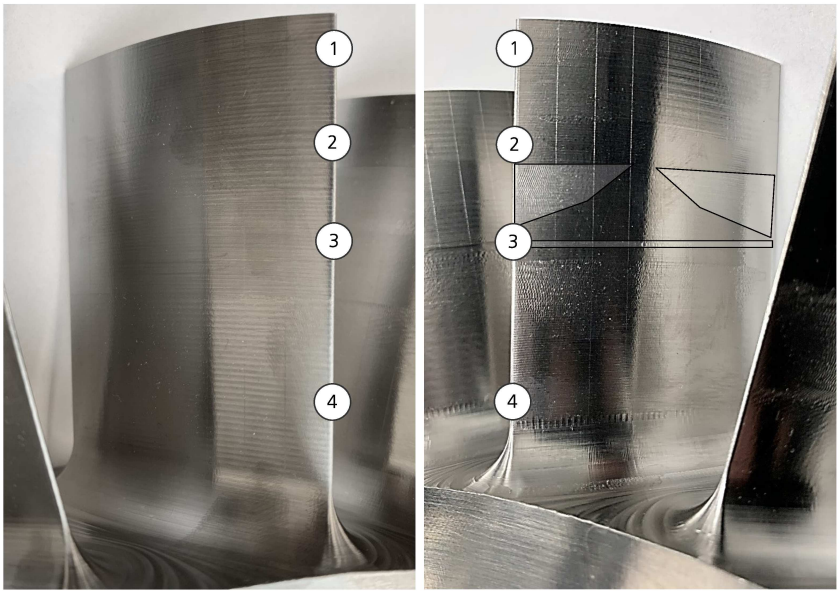

Source: Author

Figure 33 shows an example of a test performed to check if the application is capable of tracking peaks of blades with chatter, considering the blades shown in Figure 31. The left-hand graph shows peak tracking functionality values for a blade without chatter, while the right-hand one shows the influence of vibrations. When comparing both graphs, higher amplitudes were displayed considering workpieces frequencies for the blade with chatter, indicating that the process was influenced by vibrations leading to chatter.

Figure 33 – Peak Tracking Offline Test

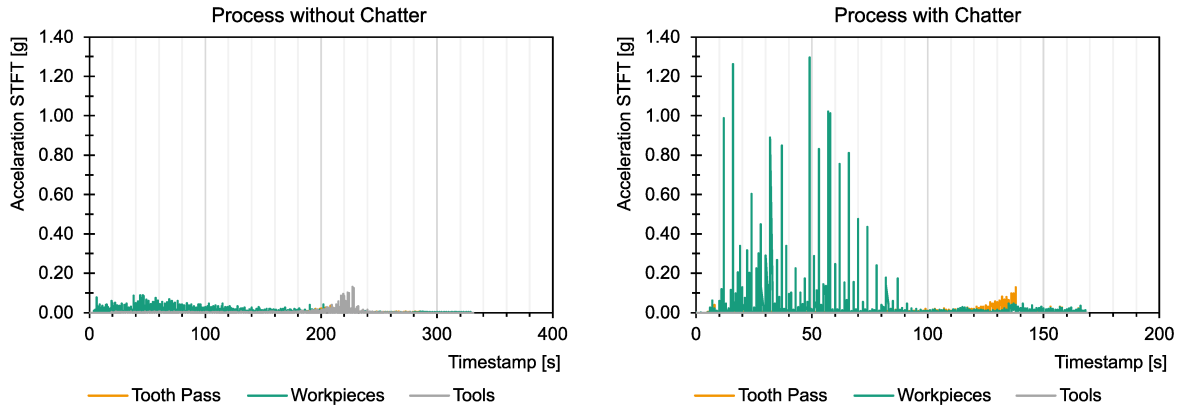

Source: Author

Further applications were developed in the Time-Frequency Domain Analysis tool, with the goal of avoiding to reach unstable regions, such as the exclude tooth passing frequency and exclude size. They were implemented to avoid frequencies around the harmonics to be considered as potential better workpiece frequencies. However, it was observed that this functionality could limit the workpiece frequency, and the spindle speed control, since its difference cannot be higher than the tooth passing frequency.

A sensitivity analysis of exclude size parameter was performed using data from the reference blade described in chapter 4, more specifically from the finishing operation of block two. Considering the blade eigenfrequencies before and after the operation, with a tooth passing frequency of 445.63 Hz, it was expected that the workpiece frequencies changed from 1592 Hz, 3278 Hz, and 7470 Hz, to 1460 Hz, 2968 Hz, and 7314 Hz. The left graph of Figure 34 shows the tooth passing frequency and its harmonics (in green) and workpiece and tool frequencies (in orange), considering a exclude size of only one, around each harmonic. On the right-hand side, the same parameters are used for the same operation, but the exclude size is changed to ten. As observed, in the right-hand side graph, the workpiece frequencies are limited to the initial harmonics where they started, as the exclude size is set to ten. On the other hand, when this value was set to one, the frequencies move across the harmonics, while the harmonics are still excluded from the moving range.

Figure 34 – Frequencies Tracking with Different Exclude Sizes

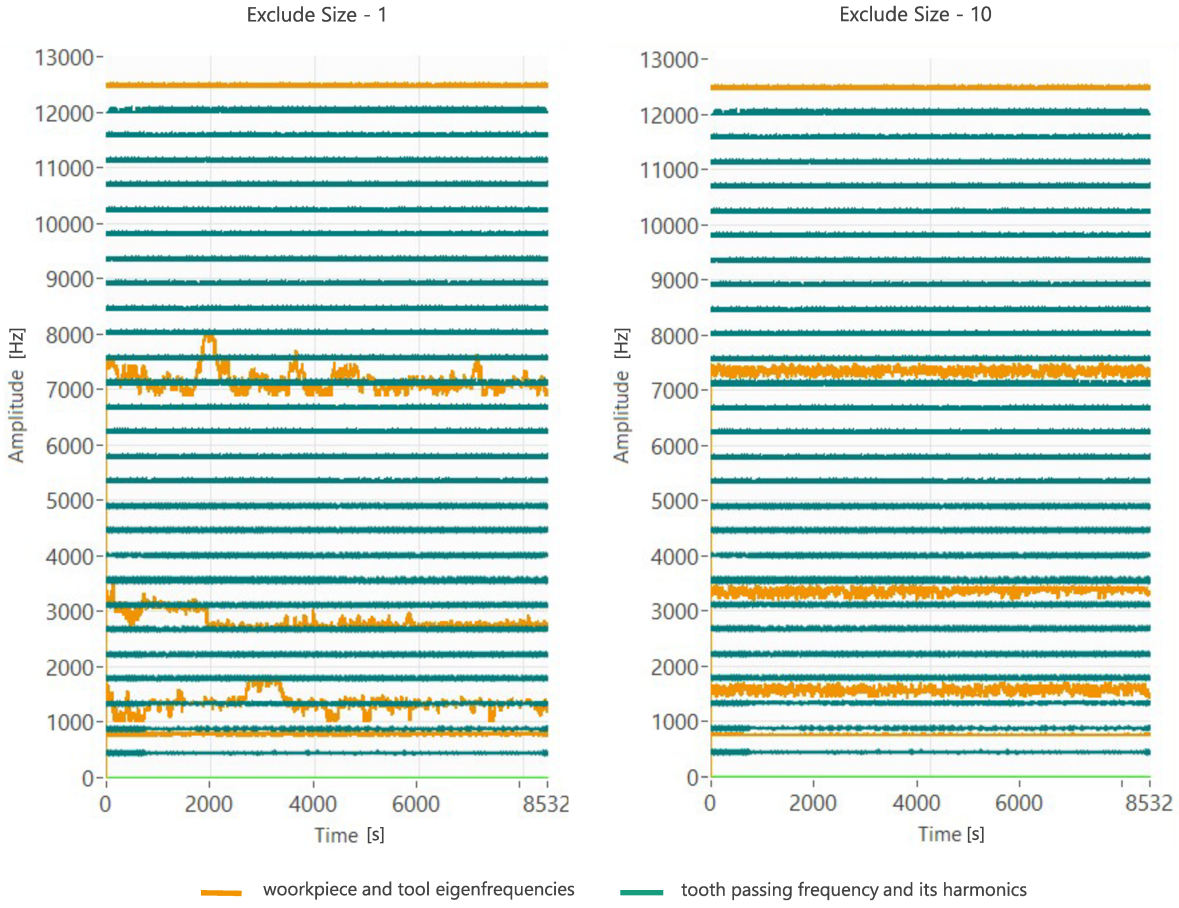

Source: Author

The frequency tracking graphs should ideally display the initial workpiece frequencies smoothly going to the final values, and not limit this change by not correctly defined limits. Figure 34 is an example of how the correct definition of application variables should be tested to achieve the desired results. A wrong exclude size selection would avoid that a better spindle speed is achieved, affecting the control performance. For example, when using a value as high as ten, the frequencies are limited between harmonics. This leads to not correctly tracked frequencies changes as, for instance, the second eigenfrequency movement, which should cross the 3119.4 Hz harmonic to change from 3278 Hz to 2968 Hz. However, this change was also not correctly tracked by the exclude size equals to one, as frequencies next to the 2673.4 Hz harmonic were tracked in the end of the process, instead of 2968 Hz. A balance between the two cases should be aimed. For the studied case, a exclude size of two or three has proven to be more suitable.

STFT variables are also critical for achieving the correct peak tracking and process analysis, since the time-frequency transformation is used as a base for the graphs shown in the front panel (presented in subsection 5.1.2). Offline tests were also performed to identify correct STFT parameters. However, the STFT spectrogram has a

better visibility with process instabilities, and machining design goal is to achieve a stable process to produce the desired surface and geometry, avoiding the excitement of blade frequencies. Therefore, the visibility of the system frequencies in the spectrogram is inversely proportional to the process stability, it depends on the STFT parameters and the sensor position. In summary, application variables change from process to process, and should be verified when starting monitoring to achieve the desired outcomes.

5.1.4 Monitoring Integration

The Time-Frequency Domain Analysis application was integrated in the previously developed data acquisition system, after offline tests had been performed to ensure the application functionality. Therefore, process-parallel external sensory data are acquired and monitored by implementing the same Time-Frequency Domain Analysis application functionalities in the data acquisition system. These implemented components are named the monitoring part of the whole new application developed. A control functionality is also implemented to allow sending data back to the machine, which is further explained in section 5.2). Both monitoring and controlling functions were developed in a way that they need to be activated in the front panel to be enabled. Thus, it is possible to just monitor and extract time-frequency domain analysis, without writing new spindle speeds. Figure 35 shows the resulting front panel system, with the monitoring and controlling integrated with the data acquisition.

Figure 35 – Control and Monitoring Integrated with DAQ

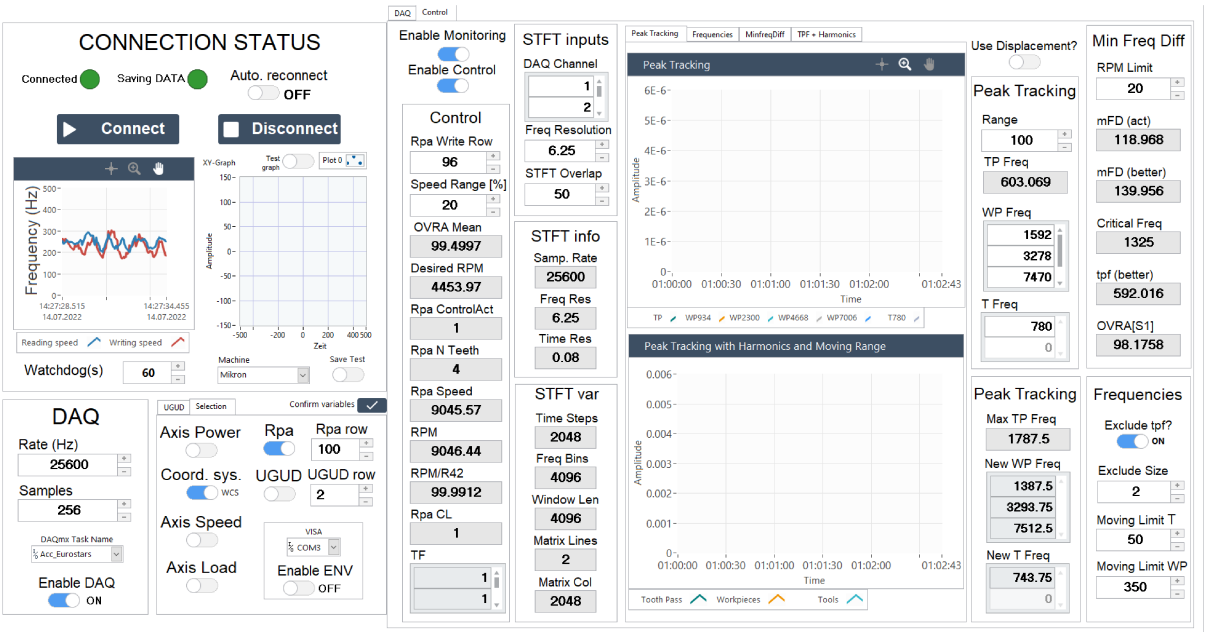

Source: Author

As a result of the application integration, now not only is it possible to acquire and visualize machine and sensor data acquired, but also to analyze time-frequency domain

KPIs of acquired data. The time-frequency transformation is then used as a base for the graphs shown in the control part of the front panel (the same graphs presented in subsection 5.1.2), which expand the process-parallel analysis of the machining.

Additionally, since process-parallel data are acquired with the integration, it is possible to select in the front panel which of the external sensor channels acquisition are going to be used in the monitoring. Therefore, the resultant of the selected channels is calculated. The three channels of a 3-axis accelerometer are selected for the milling trials, so changes in all the directions measured are considered in the analyses. Considering three channels (x, y, and z), the resultant is calculated by:

$$r = \sqrt{x^2 + y^2 + z^2}. \tag{15}$$

The automatic calculation of the actual tooth passing frequency f_t was also implemented in the integrated data acquisition system. In each iteration, the spindle speed n and the tool number of teeth N_t are read, which are used to calculate the tooth passing frequency, following Equation (5).

The Spectrogram was also developed in this new integrated application. However, it was observed that the computational resources required by this graph were too high, and it was hanging the computer program. Therefore, although the STFT is applied in the background, the time-frequency domain transformation is not displayed in a Spectrogram in this integrated application. Other types of applications could be developed in the future to support this visualization. Further performance analysis of the tool are described in section 5.3.

5.2 CONTROL MODULE

Control systems are typically composed by a reference input, a desired state that the system should achieve based on the reading inputs and the recommended action over the system. The Time-Frequency Domain Analysis application integrated with the data acquisition performs part of this control loop, by processing data that are used to control the system. A control module needs then to be developed, so the acquired data lead to changes in the process with the goal of achieving a process with less vibrations. Thus, the minimum frequency difference method (introduced in subsection 4.2.2) is used as stability criterion for a more suitable spindle speed, and the calculated values are then written in the machine, following a path-wise logic.

5.2.1 Process-Parallel Selection of Advantageous Spindle Speed

The minimum frequency difference method (described in Figure 4.2.2) is implemented for the selection of advantageous spindle speeds along the milling process. A Python script is called inside the application on LabVIEW, which implements this

method. As described in subsection 5.1.2, a peak tracking with moving range was implemented, which calculates the new tooth passing and workpiece frequencies, as the process is dynamically changing with material removal. This dynamic change is considered in the minimum frequency difference method, which is used as a stability criterion to identify when the spindle speed should be overwritten and with which value, so a better tooth passing frequency can be achieved and vibrations during the milling process can be reduced.

The control is implemented inside the data acquisition system integrated with the Time-Frequency Domain Analysis application, as the time-frequency domain transformation and moving range of peak tracking are used as input for analyzing the process dynamic. The program is constantly running, while reading new data from the sensors, and time-frequency transformations are made for each data package. Therefore, in each iteration, after new tooth passing and workpieces frequencies are calculated by the moving range algorithm, these frequencies are used as inputs to a Python script. The script calculates the actual minimum frequency difference, considering the new frequencies calculated and the new tool frequency. Considering a certain limit, the algorithm searches for the ideal minimum frequency difference which could be achieved by changing the tooth passing frequency for a better one. This better frequency is then used to calculate a value called *OVRA*, which is calculated based on the actual tooth passing frequency f_i and the desired one f_d:

$$OVRA = 100 \cdot \frac{f_d}{f_i}. \tag{16}$$

OVRA calculation results in a percentage value, which is used to define the spindle speed that should be sent to the machine for adaptation, when the control is enabled in the LabVIEW application. Thus, the value represents which percentage of the initial spindle speed would leads the system to have a better tooth passing frequency, aiming to reduce instabilities.

The control calculations were also implemented in the Time-Frequency Domain Analysis application, allowing offline analyses of the process. Graphs related to the control were implemented only in the Time-Frequency Domain Analysis application, as the performance of the integrated application with process-parallel data acquisition is affected with additional plots. The offline application is then able to display the actual and better minimum frequency difference, the OVRA value, and the critical frequency (that represents an inadequate tooth passing value that could be coincident with a tooth passing frequency harmonic) in the form of graphs, so the values along the time are easily monitored. Figures 36 and 37 show graphs built based on the extracted values of the originals one in the Time-Frequency Domain Analysis application.

Figure 36 – Offline Calculation of Actual and Better Minimum Frequency Difference

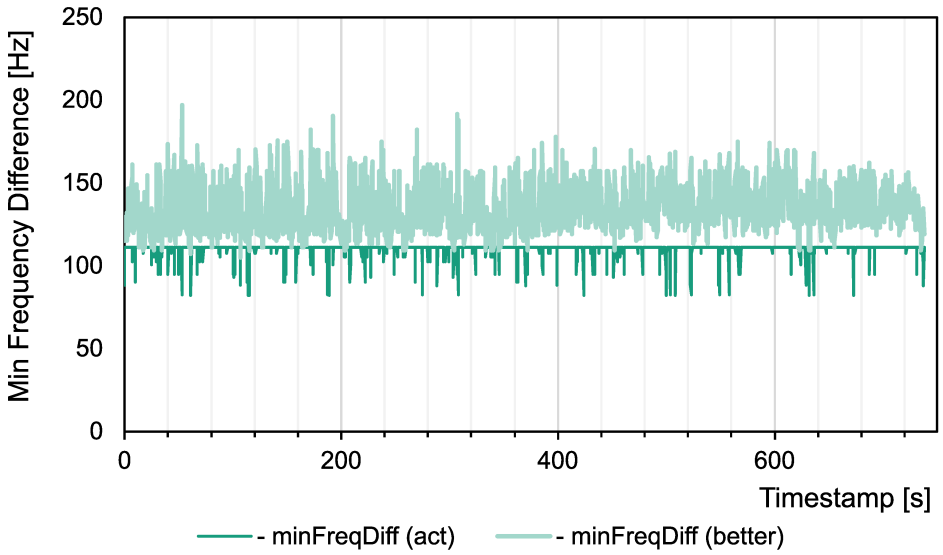

Source: Author

Given the minimum frequency difference values displayed in Figure 36 and better tooth passing frequency calculated each iteration, the OVRA values displayed in Figure 37 were determined. Values less than 100 % indicate that the spindle speed should be reduced, when comparing with the initial process value. On the other hand, values higher than 100 % suggest an increase in the speed, which would be accomplished with a spindle speed writing functionality.

Figure 37 – Offline Calculation of Spindle Speed Overwritten Values

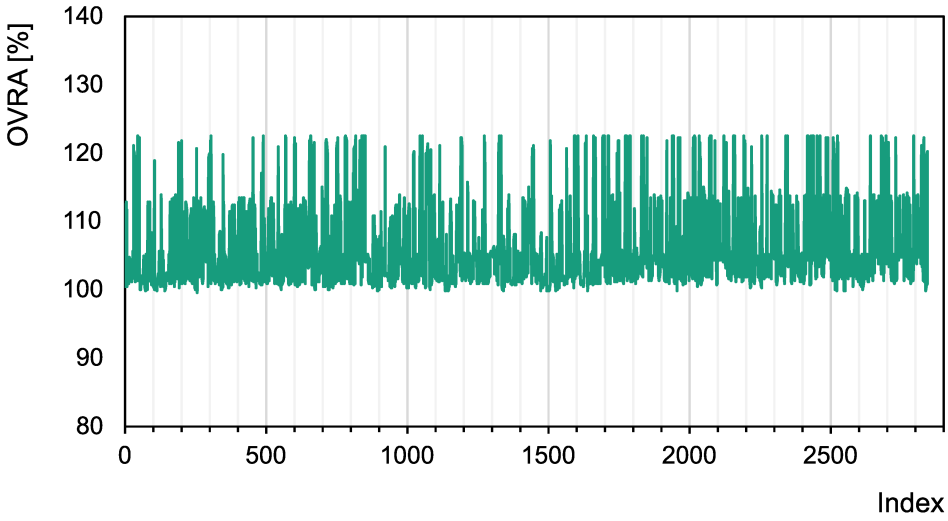

Source: Author

A limit is defined in the front panel as a percentage value of the speed range. This value is used to define a limit which the spindle speed is changed by the control,

based on the initial spindle speed. Thus, the spindle speed does not change by a value distant from the original one with the control implementation, which could affect the process and machine. For example, if a value of 10 % is selected, considering a spindle speed of 8000 1/min, then the control has a limitation of maximum speed suggested of 8800 1/min. On the other hand, if limit value of 100 % is selected, a overwritten value 16 000 1/min is possible, which could affect negatively the process. Therefore, it is important to know the ideal spindle speed range for each process where the control is used. A limit of 20 % is used in the milling trials.

As a result of the reading variables, time-frequency transformation, monitoring functionalities, control calculation, and writing function, the initial data acquisition was further developed in an integrated system capable of acquiring both sensor and machine data, and sending to the machine a better spindle speed to avoid vibrations in the process.

5.2.2 Spindle Speed Overwritten Function

The 5-axis milling machine writing functionality is an important feature in terms of controlling a blisk manufacturing process. Thus, the machine used in the process should not only be able to send data process-parallel, but also to receive signals indicating how the process may be changed to achieve a desired outcome. Aiming to include this functionality in the already developed data acquisition system, the other communication side of ACCON-AGLink library was used to write on the machine data sent by the data acquisition system running on a PC/IPC process-parallel in a time-sensitive and reliable way.

R parameters, also known as Arithmetic Parameters, are machine variables dedicated to be freely used in the NC program by users. R parameters are applied to overwrite the spindle speed in synchronization with the machine loop. Therefore, instead of directly overwritting spindle speed, the data acquisition system uses ACCON-AGLink library to write an specific R parameter. The spindle speed is then defined in the NC program as equal to this specific R parameter by using the machine synchronized action functionality. The spindle speed is then modified in the process, when the R parameter read in the NC program indicates that a different spindle speed should be used.

The control logic is supported by an additional R parameter which is read by the data acquisition and used to define when the writing functionality should be activated. Three different values of this R parameter are used to indicate which control function should be performed. Figure 38 shows when these values are modified along the finishing process of block two. Firstly, represented by the black color, the R parameter is changed to one, indicating that the process started and the OVRA values should start to be stored, if the control is enabled. Then, next to the edge of the blade, on

each path, the R parameter is changed to two, indicating that the mean value between the OVRA values stored until that point should be calculated and sent to the machine. A writing time is expected to perform this calculation and send data to the machine, where no OVRA values are stored. Afterwards, the R parameter is changed back to one, indicating the initial data storage for calculating a new mean spindle speed.

Figure 38 – Control Activation Points for Finishing Block 1

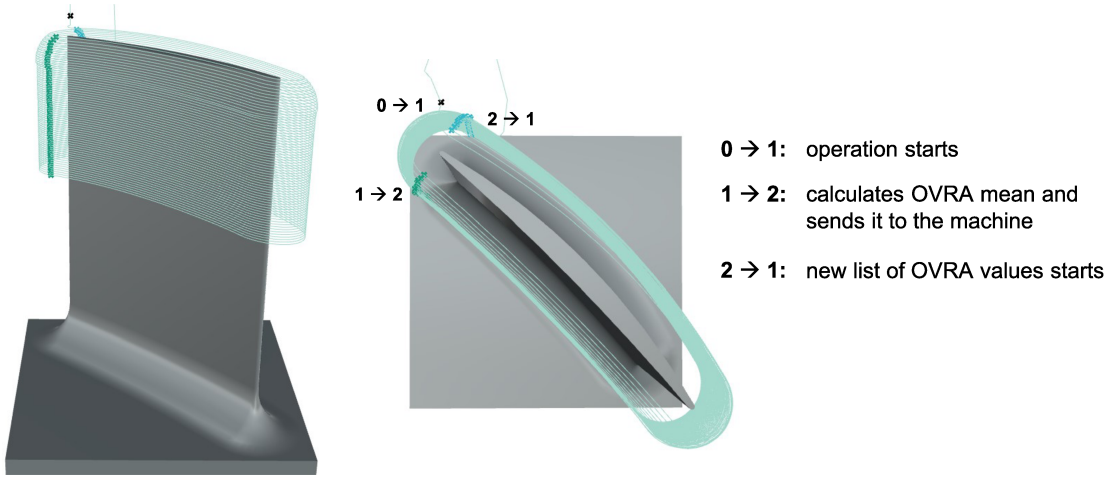

Source: Author

A logic was implemented in the DAQ system so the OVRA calculation would be stored in a list along the path, until it reaches the front edge of the workpiece being machined. The average between OVRA values stored is then calculated, so a smooth transaction of the spindle speed is expected. The program checks if this average value is inside a user-defined range around the initial spindle speed of the program. In case the average is outside the range, the closest limit is used as value to overwrite the spindle speed. Otherwise, the calculated average is sent to the machine.

Hence, the spindle speed writing happens when the R parameter is modified from one to two, and considering different calculated values along each path. A machine synchronized action functionality is adopted in the NC program. Therefore, once the R parameter that receives the new spindle speed is modified, the machine spindle speed automatically changes, as it is defined in the NC program as equal to this parameter that is continuously verified by the synchronized action. A continuous change of spindle speed could be also implemented with this synchronized action. Though, a path-wise logic was implemented in the milling trials, considering a mean of the calculations along the path. Other types of writing logic could be also implemented, such as blade-wise, in the case of a whole blisk production. However, the performance of the monitoring and control application must be first evaluated, since an increase in the machine writing points impacts in the communication rate between PC/IPC and machine.

5.3 CONTROL AND MONITORING PERFORMANCE ANALYSIS

Machine and sensor data are the base for the vibrations monitoring and process control. Therefore, the developed Time-Frequency Domain Analysis application was integrated with a process-parallel data acquisition system. A requirement for the integrated system is the ability to acquire data fast with a considerable time and position resolution, so the process is correctly modified and vibrations reduced by the implemented control. On the other hand, writing and reading fast enough for the control application impacts in the machine performance, as will be discussed in this section.

A digital twin of the blade milled is built with the data acquired, by associating sensory data such as acceleration to cutting position. The digital twin allows further analyses of the process performance. However, downsampling of sensory data is necessary for this position-oriented analysis.

The data acquisition system previously developed is able to store both machine and external sensors data in a same file that is later used for process analysis. However, milling machine data are typically in a frequency much lower than that of the external sensory. Considering a sampling rate of 250 Hz for the milling machine used, and a frequency of 25 600 Hz for the accelerometers, every time that machine data are acquired, a package of approximately 102 sensory data is sent.

Downsampling of external sensory data is then used to allow a position-oriented analysis of sensory data, which links the acquired sensory data to the tool tip points in the blade. Since for one timestamp of the machine, multiple values of each sensor are normally obtained, statistics of each sensor data packages are calculated. The data acquisition software developed automatically calculates the following statistics: Mean, Median, Maximum, relative standard deviation (RSD), and Standard Deviation. Therefore, a specific machine position has one single value of each statistic calculated based on the data package acquired in the period between one machine data acquisition period. Downsampled sensory data are then saved in a file in the same frequency as machine data. Raw data are also stored for further analysis and statistical calculations. Both external sensor raw data and downsampled statistics are stored in a single TDMS file, along with machine data and metadata. The acquired TDMS files are then used for analyses and improvements of the process.

5.3.1 Monitoring Time Resolution

Subsection 5.1.4 discusses the high computational resources required by the Spectrogram when the data acquisition and control were integrated. To better understand how the other background monitoring calculations and graphs affect the software performance, a time monitoring analysis was performed.

Monitoring performance was analyzed by implementing points of time measure-

ment along the data processing steps, which are displayed in Figure 39. The time is recorded before and after acquiring external sensors data, which is then used to the following monitoring calculations. After acquiring data, the resultant of all the selected cDAQ channels is calculated, and time after this calculation is also recorded. Then, considering that the STFT parameters selected in the front panel are not exactly the ones necessary as inputs STFT module, a calculation is performed based on the selected values. Therefore, time is measured after both this STFT parameters calculation and the transform. Then, both the peak tracking and moving average are performed in parallel, and data are displayed in graphs. The next step is then calling the Python script and performing the minimum frequency difference calculation. Finally, data are saved in a TDMS file for further analysis. The stages then repeat as long as external sensors data are acquired.

Figure 39 – Monitoring Stages

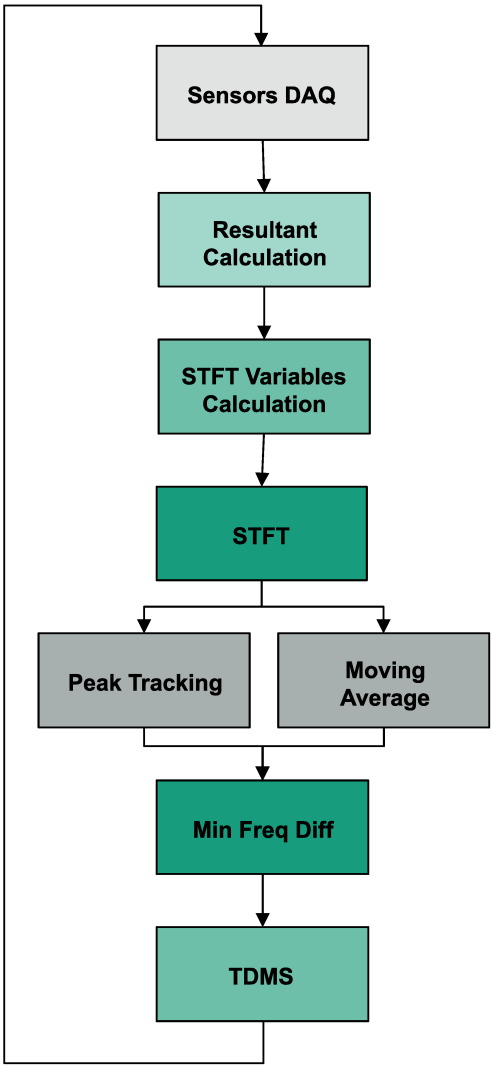

Source: Author

The duration of monitoring steps was recorded while performing air cuts with the

5-axis milling machine. The minimum, maximum, and mean time duration of each stage were calculated and are displayed in Table 6.

Table 5 – Monitoring - Time Resolution

Step	**Mean [ms]**	**Min [ms]**	**Max [ms]**
Sensors DAQ	0.57	0	1.08
Resultant Calculation	48.66	41.89	69.81
STFT and Parameters Calculation	1.23	0	20.95
Peak Tracking and Moving Average	58.95	31.92	99.74

Source: Author

The data acquisition of external sensors has shown to be fastest stage of the monitoring, as it only receives data from the input/output (I/O) modules connected to the cDAQ and sends to the further stages. The short time Fourier Transform has also a considerable low mean time duration. The resultant calculation and peak tracking and moving average have a much higher time durations compared with the other ones. The resultant calculation is performed for all the signals acquired by the cDAQ, since more than one value is acquired for each channel in one iteration. The peak tracking and moving average stage is the most time requiring one, as it was expected, since multiple calculations are performed to track all the defined workpiece and tool frequencies, while also avoiding the tooth passing frequency harmonics.

5.3.2 Position Resolution

The integration of monitoring and control functionalities in the data acquisition system led to a change in the performance of the whole system, as new calculations were added. Ideally, the system would be able to acquire data continuously, in every single tool tip position. However, more computational resources are necessary to process and store all the data acquired, which might lead to a lower data acquisition rate. The comparison of the density of data acquired for the same milling operation with different functionalities is related with this change in the data acquisition rate. A visual representation of this data density is conducted by displaying the tool tip positions from process data files in the blade CAD model.

Data for position resolution performance evaluation were acquired by performing air cuts in the machine. Air cuts allow to analyze the process in a fastest way and without cutting material, when comparing with performing the real process. The same milling operation was executed with air cuts four times, by sequentially activating the following functionalities:

1. Machine data acquisition
2. Machine and external sensors data acquisition

3. Monitoring

4. Control

Therefore, the impact in the density of data acquired is analyzed for each scenario. Figure 40 shows the blade model, in the software Rhinoceros 3D, with the tool tip positions acquired for each one of the air cuts.

Figure 40 – Data Acquisition, Monitoring, and Control Functionalities - Position Resolution

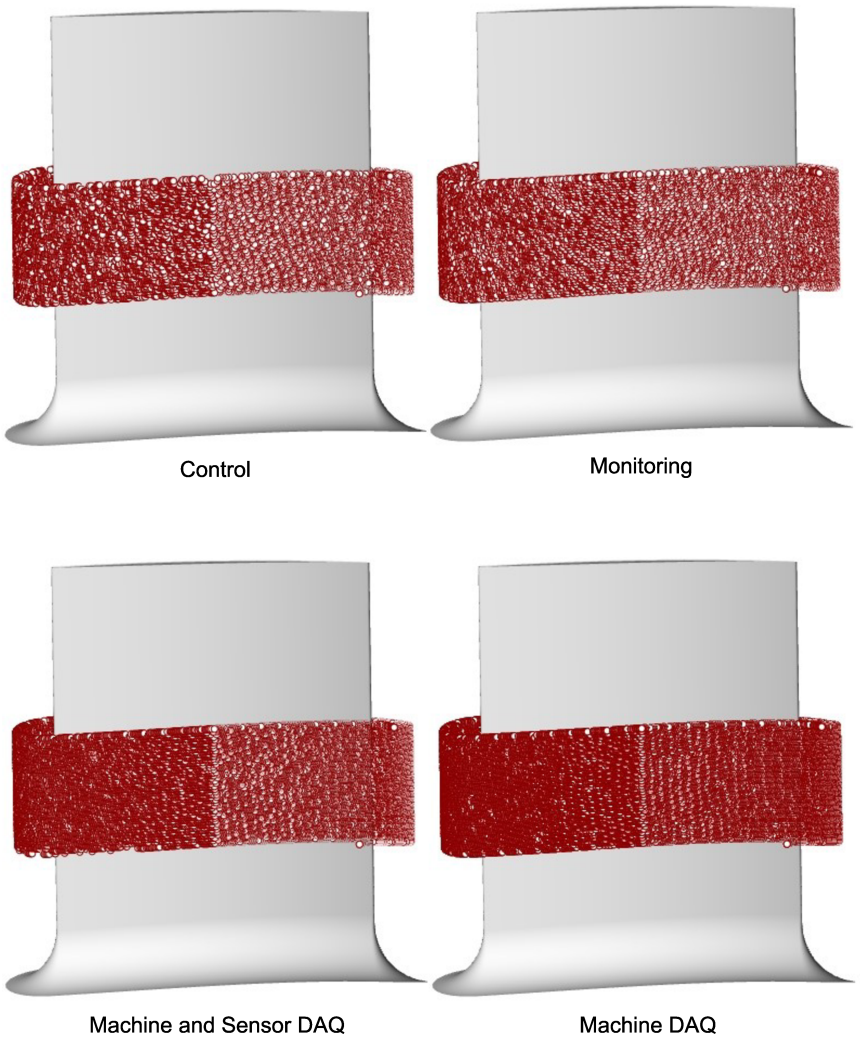

Source: Author

The visual inspection of points density is supported by the calculation of average and median distance between two points in the blade. Therefore, they are used as a metric for evaluate how the quantity of points acquired is affected by each operation. Table 6 shows the values obtained.

Table 6 – Distance Between Points

Functionality	**Average Distance [mm]**	**Median Distance [mm]**
Machine DAQ	0.15260	0.10699
Machine and Sensors DAQ	0.15552	0.10700
Monitoring	0.26003	0.10715
Control	0.27104	0.10707

Source: Author

As a result, DAQ with external sensory seems to interfere little in the system performance. And, as expected, the control requires much more computational resources, as it is an integration of all the other acquiring and processing data stages, with the addition of machine writing functionality. However, the average value for the monitoring is very close to the one obtained when the control was activated, especially when comparing with the other two functionalities. Subsection 5.3.1 showed the time that each step for data processing requires for performing the process-parallel monitoring. Optimizations applied to these steps could improve the application position resolution overall.

5.3.3 Writing Functionality Performance

Writing data from the computer to the machine is an essential functionality to perform a spindle speed control in a 5-axis milling process. However, this feature integrated with the reading machine data requires a communication in both ways with the machine, increasing the computational resources necessary to perform all the essential activities. Thus, the frequency in which the writing functionality is activated impacts in the system performance, as it is here discussed.

The same position-oriented analysis in Rhinoceros 3D described in subsection 5.3.2 was performed to compare the effects of multiple writing points. The monitoring and control application performance was first evaluated by defining writing points path-wise, every two paths, and only 5 times in each operation. Air-cuts were performed in the milling machine, where the finishing operation of block two was uploaded to the machine. The control functionality integrated to the data acquisition system was enabled. Data acquired is then further analyzed in Rhinoceros 3D, using a Grasshopper script. The position-oriented spindle speed values are displayed in Figure 41 for each one of the scenarios.

Figure 41 – Spindle Speed Writing Approaches

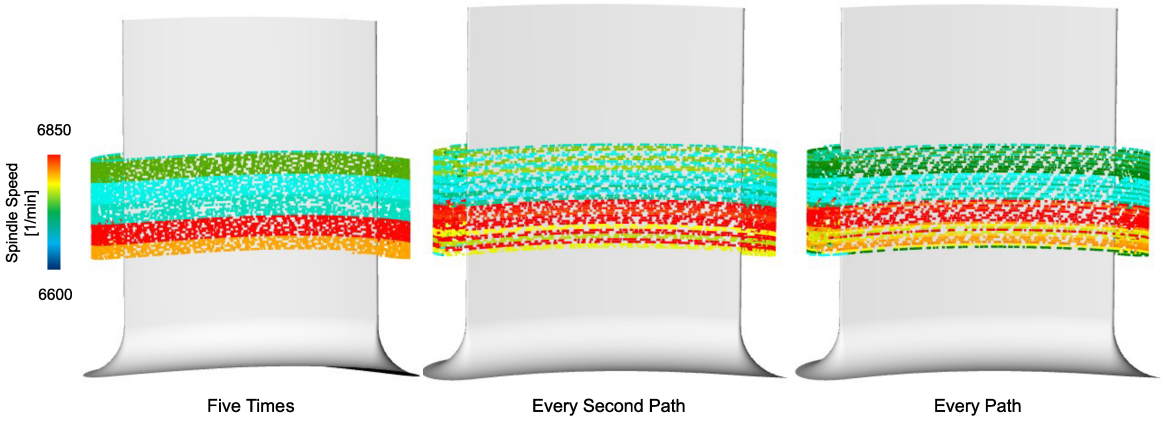

Source: Author

The average distance between every two points was also calculated considering the three different scenarios. Table 7 shows the values obtained.

Table 7 – Spindle Speed Writing - Average Distance Between Points

Approach	**Average Distance [mm]**
Five Times	0.238195
Every Two Paths	0.249907
Every Path	0.240406

Source: Author

Therefore, it was observed that the performance of the data acquisition and control application is impacted by how many times data are written into the machine. However, the number of tool tip points acquired seems to fluctuate each time the operation runs.

An additional communication is necessary for overwriting the spindle speed. Furthermore, NC commands are added to the program to indicate when to calculate the mean OVRA value and send to the machine, and to start storing those OVRA values again. These additional NC commands could be impacting the data acquisition performance. Considering the results, it was defined that the control milling trials would be performed by writing every five paths. Therefore, data transfer frequency is still high, but the performance is not that impacted by path-wise writing.

Additional tests were performed to evaluate how these NC commands to write data in the machine impact in the control performance. A synchronized action functionality of the machine is used to continuously read the R parameter that indicates which new spindle speed should be applied. A possible alternative to read this R parameter is by adding an NC command in a specific program points where the writing should be performed.

The position-oriented analysis of data acquired has shown that the monitoring without synchronized action resulted in a better performance, as more data were acquired. The average distance between two points acquired of the control with synchronized action was approximately 0.07 mm higher than without this functionality. However, the synchronized action was still implemented in the milling trials, as it is a safer scenario. Tests would have to be performed showing how long it takes to calculate the OVRA value and write the value back to the machine, so the correct R parameter reading position in the NC program is selected. With the synchronized action this is not necessary, as it is constantly reading the R parameter. Furthermore, the selected approach would also work for continuous spindle speed change, in case it was implemented.

6 DATA-BASED EVALUATION OF SPINDLE SPEED CONTROL MODULE

The integration of the Time-Frequency Analysis application with the existing data acquisition system was implemented aiming to perform a process-parallel spindle speed control during 5-axis milling. The main goal of this control is to reduce the vibrations that appears while milling turbo-machinery components. Although air cuts are efficient to test the application performance and functionality, the control is only truly evaluated with real milling trials, where the dynamics of the system are continuously changing. Therefore, the experimental setup with suitable sensory (described in chapter 4) was carried out to validate the developed monitoring and control application. The analysis of the reference blade is first discussed in section 6.1. The reference blade results are then compared with the demonstrator blade with spindle speed control applied, in section 6.2.

6.1 DEMONSTRATOR BLADE WITHOUT SPINDLE SPEED CONTROL

The demonstrator blade was first milled in a 5-axis machine without the spindle speed control, so the performance of the developed application could be evaluated. A position-oriented analysis of data acquired during the process is possible given the suitable sensory and the down sampling to connect sensor data to tool tip positions. A time-frequency analysis is also performed by reading the TDMS files with process data in the offline Time-Frequency Analysis application developed. Therefore, the surface quality is linked with the acquired and processed data.

6.1.1 Position-Oriented Analysis of Demonstrator Blade

A position-oriented analysis of the demonstrator blade, with no control, is performed such that sensory data acquired in each tool tip position is displayed. The 3D model of the blade is first uploaded in the Rhinoceros 3D software. The programming language Grasshopper 3D is then used to display data in the specific tool tip points, considering a down sampling when necessary.

Figure 42 shows a position-oriented analysis made in Rhinoceros 3D, considering data from the finishing operation of block two of the reference blade. Data from the accelerometer in the workpiece were displayed considering each tool tip position, in the blade 3D model, as shown in the left side of the figure. The statistic mean values were considered for the down sampling of sensory data. A scale of colors is used to indicate low and high amplitudes.

Figure 42 – Position-Oriented Analysis of Finishing Operation of Block Two

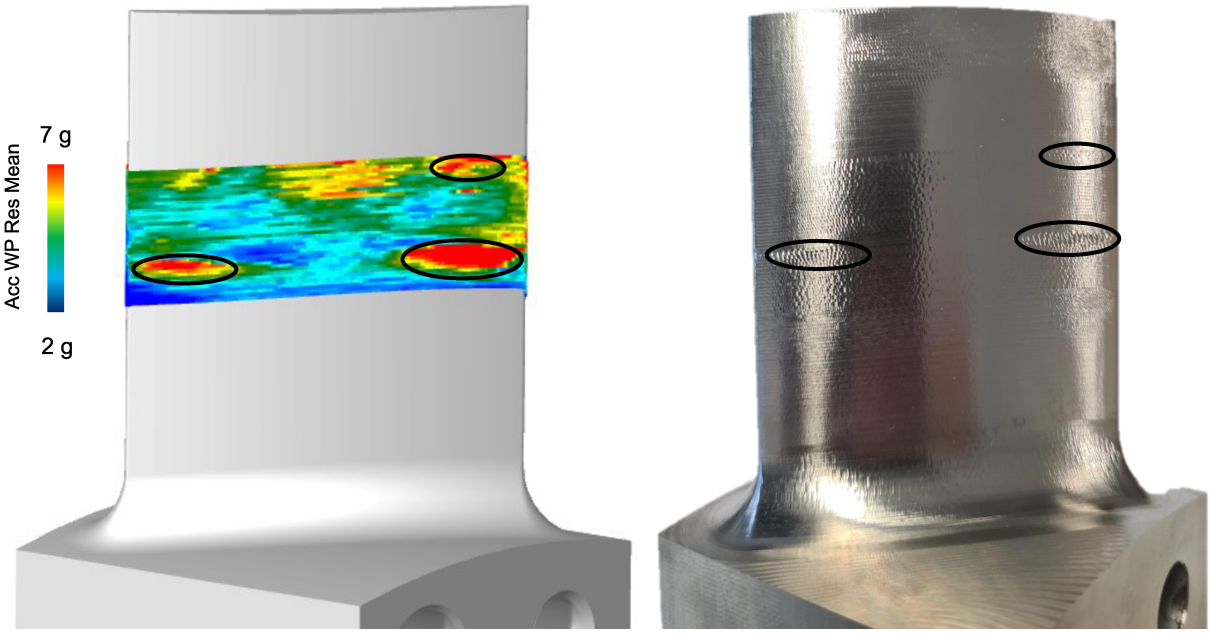

Source: Author

The after process position-oriented analysis is compared with the real blade surface, in the right-hand side of Figure 42. As shown by highlighting circles, sensory data with high amplitudes are linked with chatter in the final blade surface. These values show a possible influence of vibrations, which could be reduce by applying the spindle speed control process-parallel.

A position-oriented analysis considering the Short Time Fourier Transform of sensory data, which is a base for the developed control module, is also conducted. Workpiece accelerometer data acquired in time is transformed for the time-frequency domain, allowing analyses of specific frequencies. Figure 43 shows the amplitudes of accelerometer data, considering the cutting position in time and a frequency of 1600 Hz. This frequency is close to the workpiece eigenfrequency of 1592 Hz, which was measured using EMA for block two before finishing.

Figure 43 – Position-Oriented Analysis Considering the Frequency of 1600 Hz

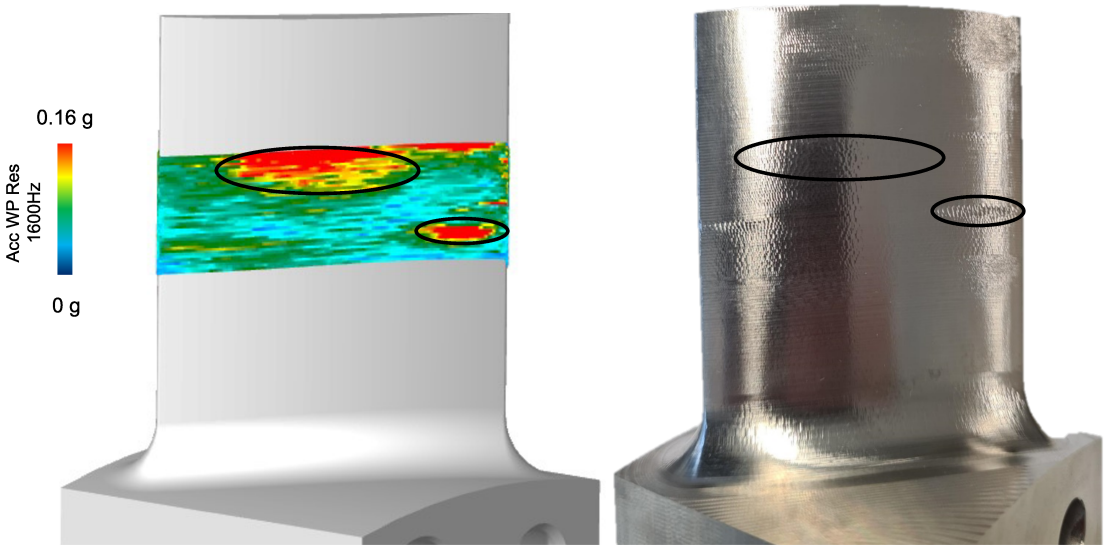

Source: Author

As observed in Figure 43, the frequency considering the first workpiece eigenfrequency also shows evidences of vibrations effect. The circled areas show high amplitude measured with the accelerometer while milling, in the 3D model, and the effects on the final surface. As seen, the final surface did not achieved the desired final quality, which might be achieved by controlling the vibrations along the process.

6.1.2 Time-Frequency Domain Analysis

The Time-Frequency Domain Analysis application described in section 5.1 is used to evaluate the milling after the process, with acquired sensory data. Knowing the initial workpiece eigenfrequencies before and after the operation, as identified and described in subsection 4.2.1, the spectrogram was used to check if the system would be able to detect the dynamics change. The STFT is then used for the peak tracking, which is essential for the minimum difference method used to control the system. Thus, the wrong detection of eigenfrequencies could lead to mistaken changes in the process, and not prevent vibrations.

Figure 44 shows the spectrogram considering the STFT of data from the finishing operation of block two. The tooth passing frequency measured for this operation was 446 Hz, which can be identified in the spectrogram as having high amplitudes along the time, as well as its harmonics. Furthermore, considering FEM results, the simulated paths of the first three workpiece eigenfrequencies were highlighted in the spectrogram. Therefore, the evaluation of the identification of those eigenfrequencies is possible, which is necessary for the peak tracking functionality.

Figure 44 – Spectrogram of Finishing Operation of Block Two with Workpiece Eigenfrequencies

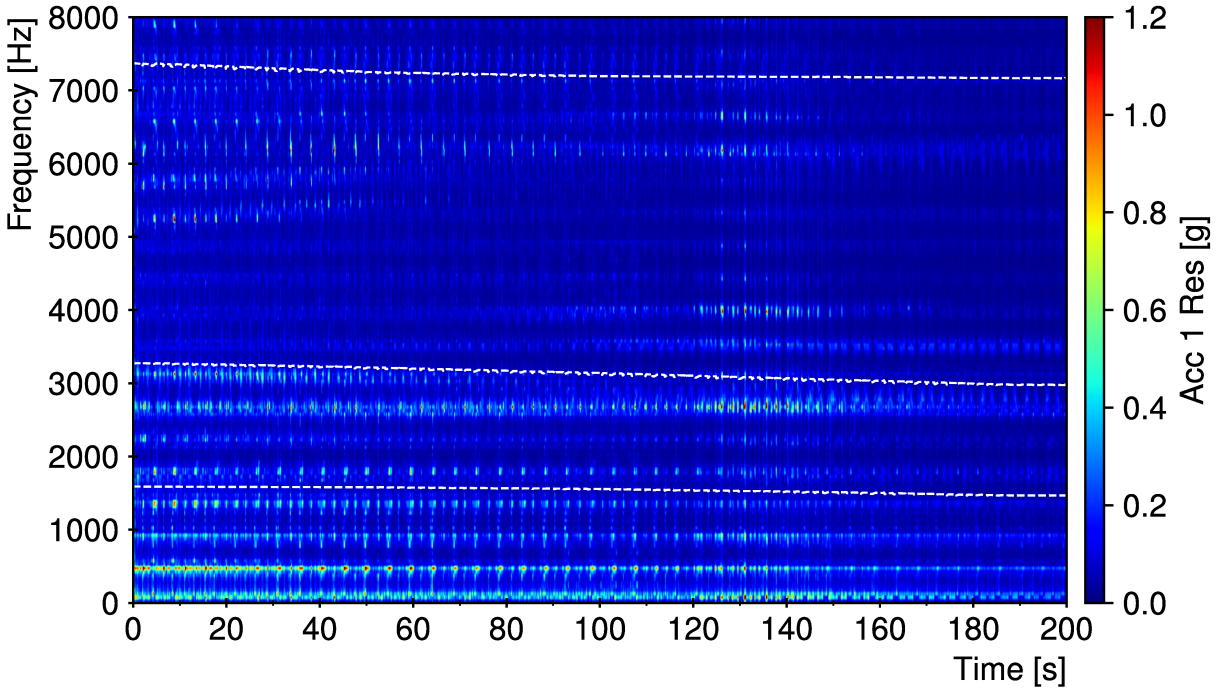

Source: Author

Comparing the high amplitudes in the spectrogram and highlighted eigenfrequencies change in time, it was observed that the workpiece eigenfrequencies are not easily identified. The tooth passing and its harmonics were much more evident. As a possibility to improve the visualization, high-pass and low-pass filters were implemented. In the case of block 2 finishing, the lowest limit was defined as 1000 Hz, which is higher than the tooth passing frequency and excludes low frequencies that have high amplitudes, but are not important for the peak tracking. As for the low-pass filter, a limit of 12 Hz was set, considering sensor limitations. The filter implementation was tested directly in the Time-Frequency Domain Analysis application, with offline data, as shown in 45.

Figure 45 – Spectrogram of Finishing Operation of Block Two with Filters

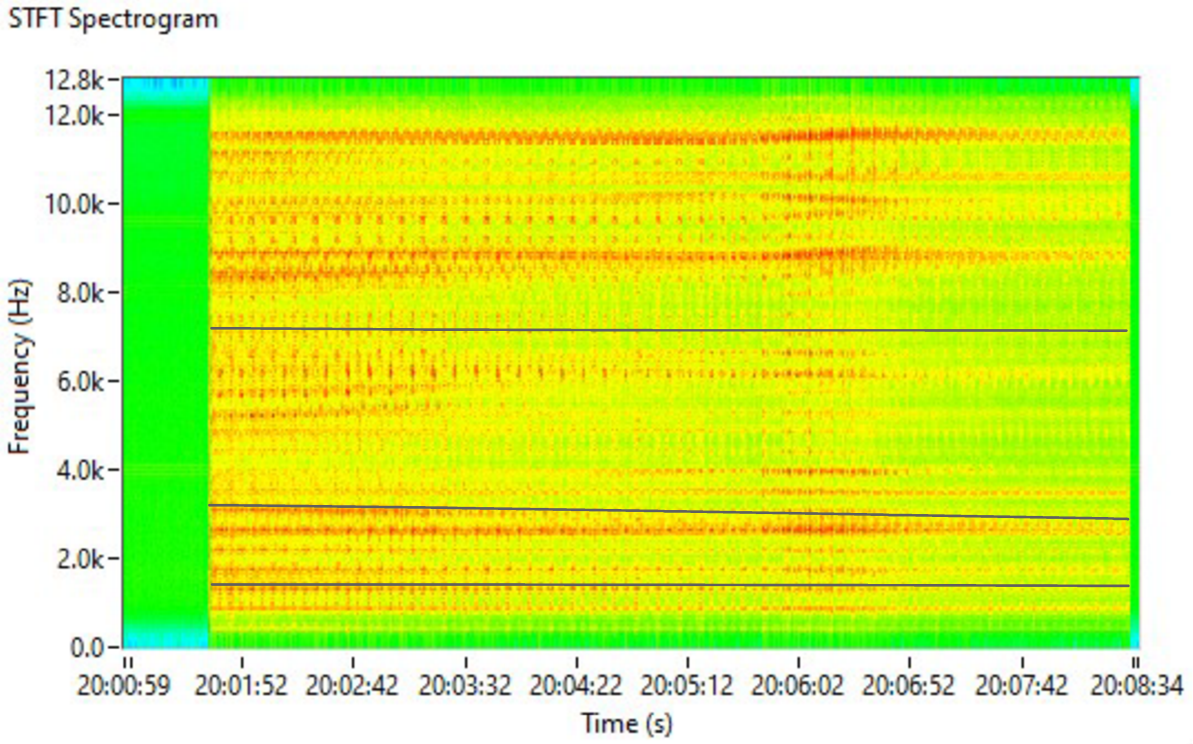

Source: Author

The eigenfrequencies identification seems to be improved by applying the filters, as low frequencies with high amplitudes are not considered in the spectrogram. The change in first three eigenfrequencies based on simulated data is highlighted with black lines. Although the visualization was improved with the application of the filters, the peak tracking identification still need improvements. The acceleration sensor needs to be in a protected position, not exactly in the current cutting zone, which impacts in the acquired results. Given that the sensors are usually not in the cutting zone, a transfer function could be implemented to do the transition between the sensor position and the real cutting and EMA measured region.

6.2 DEMONSTRATOR BLADE WITH SPINDLE SPEED CONTROL

The analysis of data acquired when milling the reference blade has shown the influence of vibrations in the process, which lead to irregularities in the surface. Therefore, a spindle speed control is implemented to reduce the vibration effects in the 5-axis milling process. Different control strategies were implemented for the three blade blocks, so the control could be evaluated with multiple approaches. The results are then compared with data obtained from milling the reference blade.

6.2.1 Control Strategy Operation-Wise

The strategy for 5-axis milling of a blade with spindle speed control process-parallel is defined considering the control and monitoring application performance, described in section 5.3, and the reference blade milling analysis, developed in section 6.1. The writing functionality was activated by the use of R parameters every five paths, and with the implementation of the machine synchronized action.

Different approaches are possible when defining the initial spindle speed to use with demonstrator blade with spindle speed control applied. A wrong spindle speed could be used to achieve an unstable process, so a test could be performed to check if the control is able to lead the process to stability. On the other hand, the reference blade was milled considering spindle speeds selected to achieve good process results. So the same spindle speed could also be used with the control implementation to compare how it performs with already stable processes. However, since the reference blade already had influence of vibrations, as shown in subsection 6.1.1, the same spindle speeds used in the reference blade were applied initially for the blade with control.

The control and monitoring application parameters were defined by sensitivity analysis, as further described in subsection 5.1.3. The STFT was performed with a frequency resolution of 6.25 Hz and an overlap of 50 %. Thus, considering an external sensors sampling rate of 25 600 Hz, a time resolution of 0.08 s is achieved. The exclude size functionality was applied with a value of two. Moving workpiece limits were defined for each operation, considering the expected initial and final workpiece eigenfrequencies, as shown in Table 8.

Table 8 – Workpiece Frequencies Moving Limit by Operation

Operation	**Moving Limit [Hz]**
Block 1 Semi Finishing	240
Block 1 Finishing	150
Block 2 Semi Finishing	640
Block 2 Finishing	320
Block 3 Semi Finishing	560
Block 3 Finishing	290

Source: Author

Furthermore, after analyzing spectrograms with reference blade process data, it was observed that the use of a transfer function could improve the control. Therefore, based on simulation data of the process, a transfer function was identified. The transfer function was used to generate values that are read in LabVIEW, considering the sensor and tool tip position. Different cutter locations were defined, and the way they are affected by the modes is different, resulting in different values that need to be multiplied by the STFT. Therefore, an additional data source for the control system was generated with all the different cutter locations and the values for each frequency, considering a

frequency resolution of 6.25 Hz, and frequencies of up to 12 800 Hz. Commands were then added to the NC program, so the LabVIEW is able to read an R parameter that indicates the cutter location number. Then, the additional data source is accessed and the values from the specific cutter are read and multiplied by the STFT ones. Thus, the sensor location is compensated by changing the STFT amplitude, considering the current cutter location.

However, adding multiple commands in the NC program impacts the application performance, as previously described in subsection 5.3.3. Therefore, a position-oriented analysis was performed. Figure 46 displays the two different cutter locations positions used in the analysis. The left side displays the 3D model of the blade with the finishing operation of block two paths, considering a total of 50 cutter locations which are written in every path by NC commands added in the orange points. On the other hand, the right-hand side blade displays only five cutter location, at the edge. The location of R parameters writing used for the spindle speed overwrite (described in subsection 5.2.2) is also displayed by black and blue symbols, already considering an every five paths approach.

Figure 46 – 3D Blade Model with 50 and 5 Cutter Locations

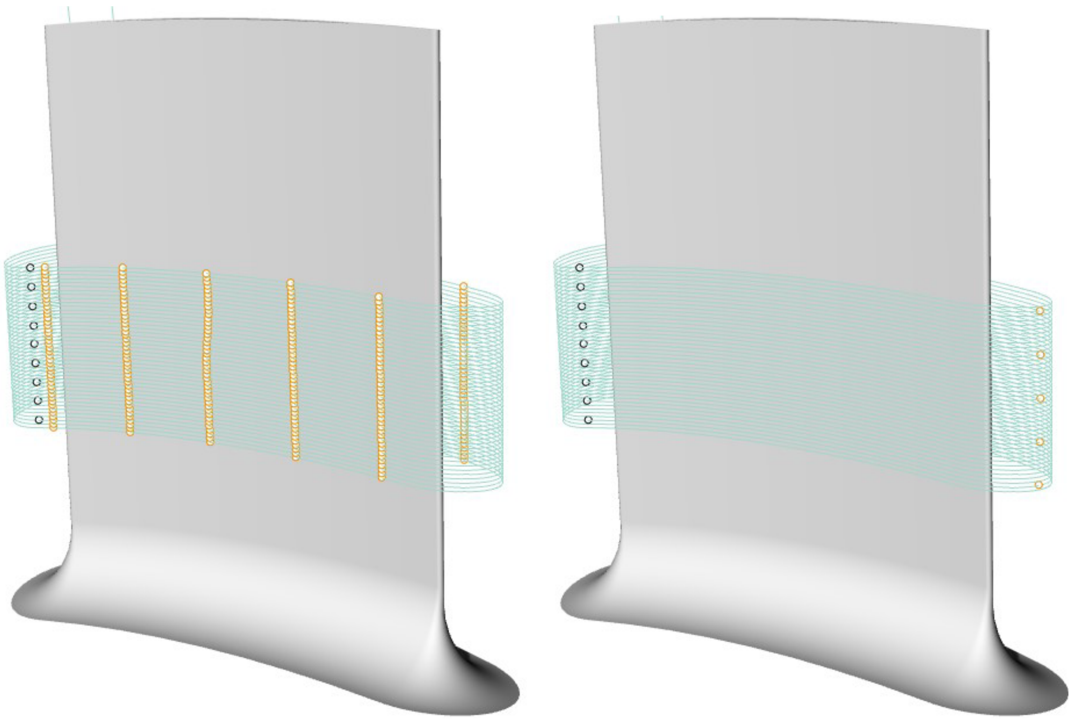

Source: Author

Aircuts were performed considering finishing operation of block two. Data acquired during aircuts with 50 and 5 cutter locations were used to perform a position-oriented analysis to evaluate the impact on feed rate. Figure 47 shows the feed rate at

each tool tip point. Additionally, the average feed rate was calculated for each scenario. Considering 50 cutter locations, the average feed rate obtained was 1713 mm/min, while for five cutter locations this value was 1716 mm/min.

Figure 47 – Transfer Function Cutting Locations Impact on Feed rate

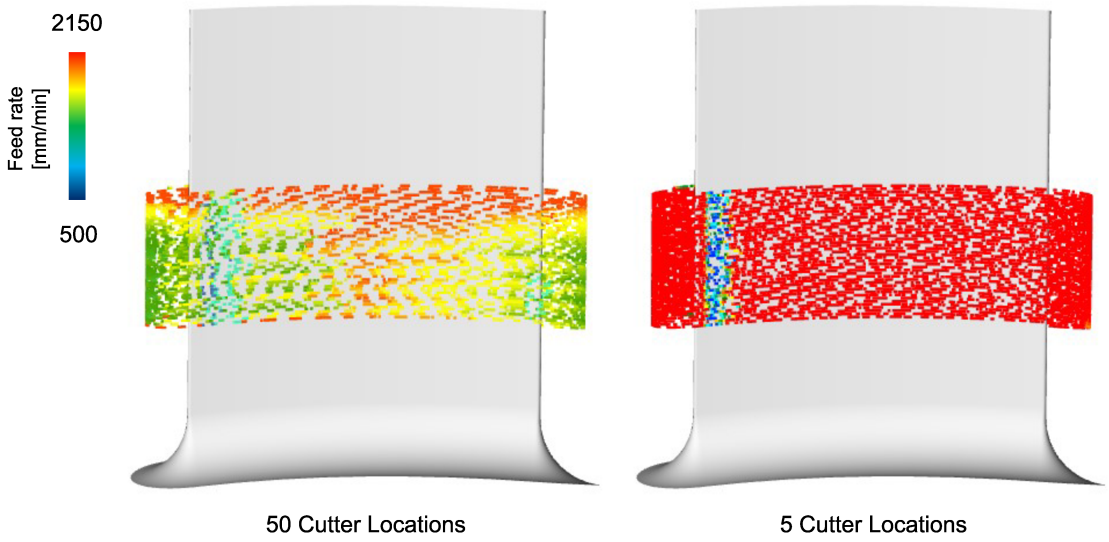

Source: Author

As shown in Figure 47, the feed rate was affected by the addition of multiple commands in the NC program to indicate the cutter location. A more constant feed rate value is obtained with only five cutter locations. However, the ideal feed rate still decreases when the writing command is added. Therefore, the control was implemented in the three semi-finishing operations without the transfer function. On the other hand, aiming to achieve better surface results, the three finishing operations were performed with the transfer function functionality.

6.2.2 Comparing Blades with / without Application of Control

The milling trials were performed aiming to evaluate the performance of the developed spindle speed control, while milling a thin-walled turbomachinery component. The results of the first milled blade, the reference blade without control, were discussed in section 6.1. Here, the first demonstrator is compared with the final blade machined with the control strategy applied process-parallel.

The final front surface of both demonstrator blades are displayed in Figure 48. Evident chatter marks are circled and named in each blade. One of the goals of 5-axis milling process of thin-walled turbomachinery components, such as the demonstrator blade here presented, is to achieve the desired smooth final surface. Thus, observing only superficially Figure 48, it is possible to say that the demonstrator blade with control achieved the best results. Not only less chatter marks were produced, but the existing marks are more gentle, when compared with the other blade.

Figure 48 – Front Surface of Demonstrator Blades with and without Control

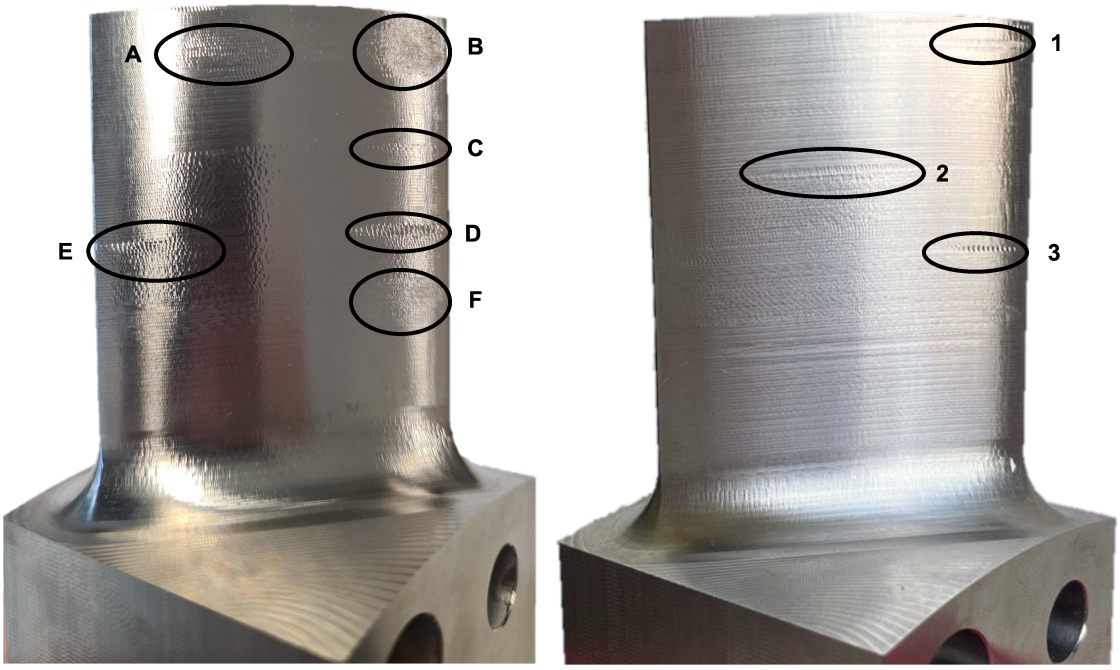

Demonstrator Blade without Control Demonstrator Blade with Control

Source: Author

The final back surface of both demonstrator blades also displayed chatter marks, as shown in Figure 49. The front surface analysis applies to the back, as the demonstrator blade with control displayed a visible reduction of chatter marks, when compared with the reference blade surface.

Figure 49 – Back Surface of Demonstrator Blades with and without Control

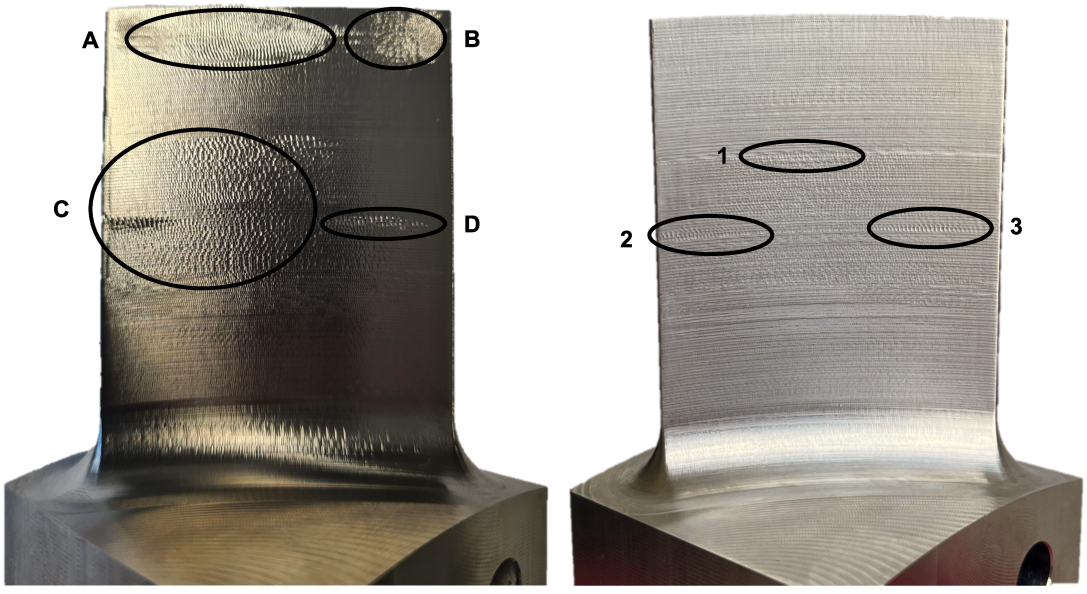

Demonstrator Blade without Control Demonstrator Blade with Control

Source: Author

When analyzing each blade block by block, the third block is the one that has

shown less chatter marks already in the reference blade. In the blade with control, the block three surface also did not contain a high presence of those marks.

On the other hand, the second block was the one that was most affected by vibrations, in both demonstrators, as it contains the huge majority of chatter mark. Nonetheless, it is possible to observe that there are less chatter marks considering the whole block two area. Reference blade front marks *C*, *D*, and *E* were reduced drastically, as well as the whole *C* area in the back surface.

A possible reason for the still considerable chatter marks shown in block two is that the initial spindle speed selected was already not appropriate, and the control did not had enough margin to select a better one. In fact, Figure 50 shows the measured workpiece frequencies both after semi finishing and finishing, as well as the tooth passing frequency harmonics. Since in the demonstrator blade the tooth passing frequency is constant, the second eigenfrequency ends up reaching one of the harmonics, while following the path to achieve its final value. This could be a possible cause of vibrations influence on the second block.

Figure 50 – Workpiece Eigenfrequencies Before and After Finishing Block 2

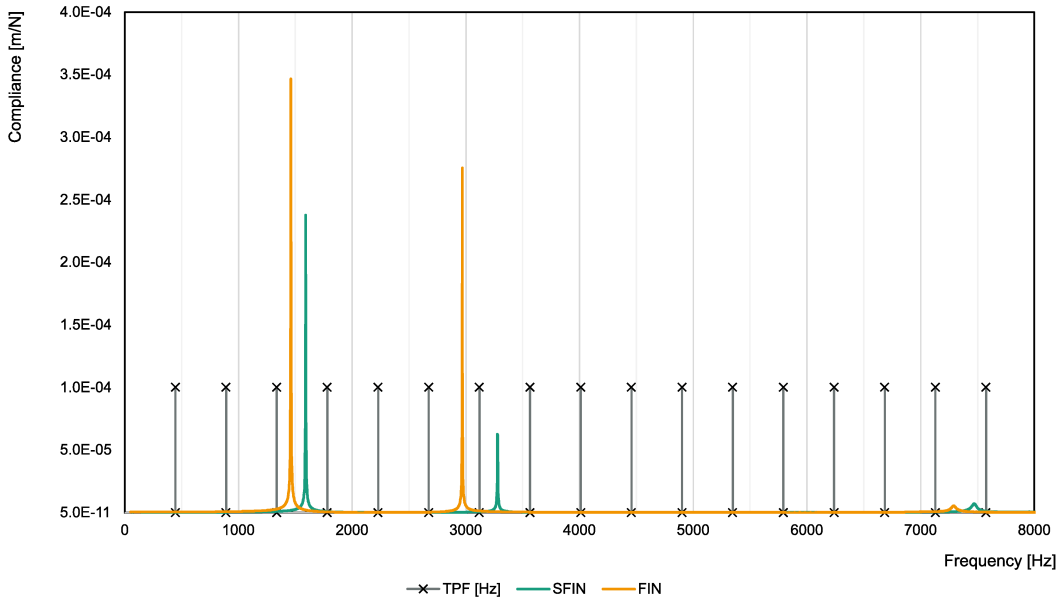

Source: Author

On the other hand, the tooth passing frequency is modified in the process with control, as the spindle speed is overwritten to achieve a better value. Figure 51 shows how the tooth passing frequency changes along the finishing operation of block two with control, considering the mean OVRA value calculated. The control aims to avoid that a workpiece eigenfrequency reaches one of the tooth passing frequency harmonics.

Figure 51 – Tooth Passing Frequency Changes while Finishing Block 2 with Control

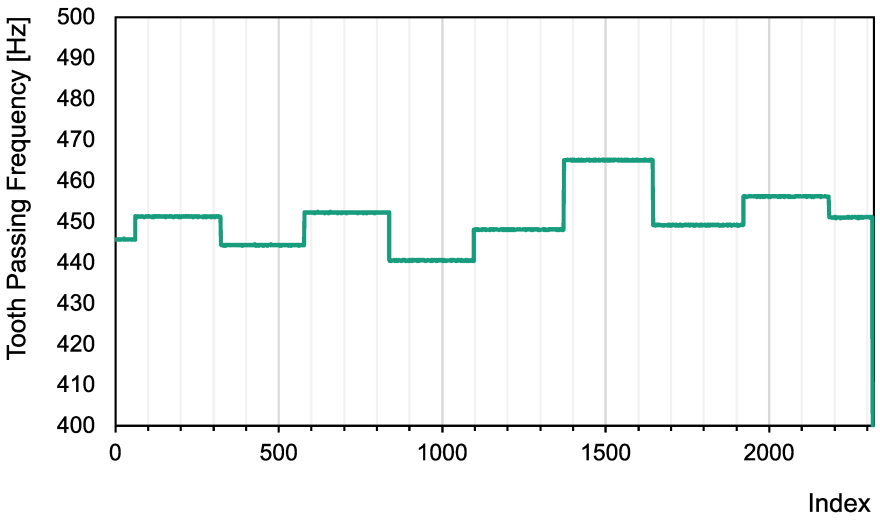

Source: Author

Furthermore, the first block is the one that resulted in a major change in the final surface quality considering both demonstrator blades. On the front surface, mark *A* disappeared completely, and the area of mark *B* was reduced. Furthermore, the chatter marks in the back of the blade did not show up in the control blade, resulting in a smooth surface. An analysis of the characteristics of the processes is possible by studying the sensory data downsampled to the machine frequency. Figure 52 shows the values of the resultant of the acceleration in three axis in the workpiece each tool tip point, considering the three blocks finishing operation of both the demonstrator with and without control.

Figure 52 – Workpiece Accelerometer Resultant Values each Tool Tip Point

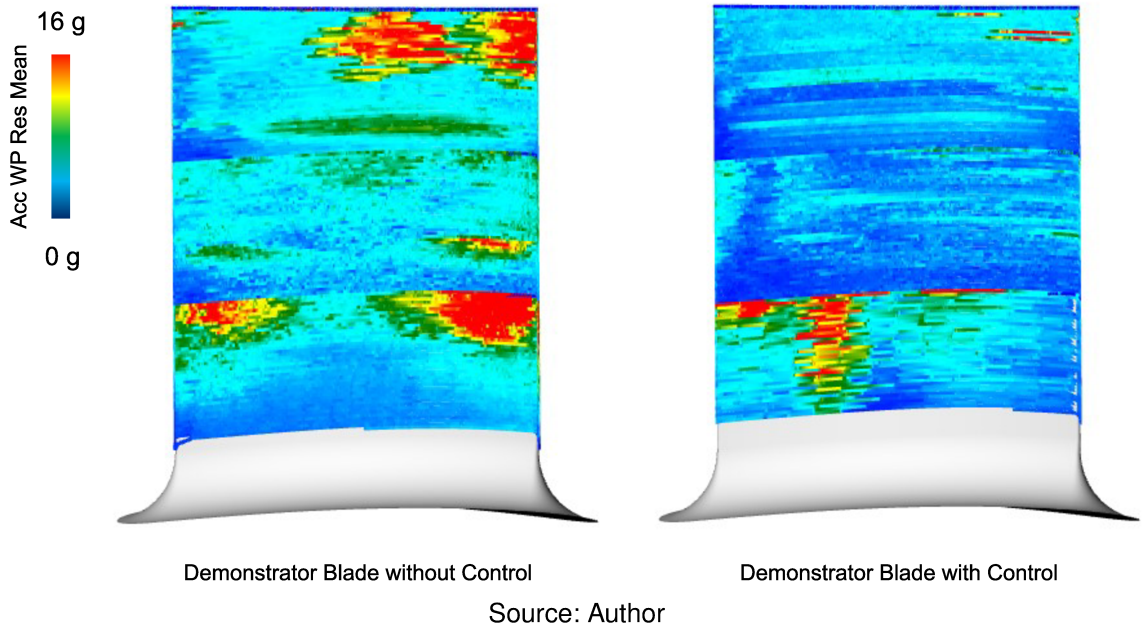

Source: Author

The acceleration highest amplitudes along the finishing operation are displayed in red in Figure 52. In general, the measured acceleration in the workpiece along the process without control was much higher than when the spindle speed adaptation was performed. In fact, analyzing the first block, the average resultant acceleration without control was 7.4 g, while the calculated value for the process with control was 2.08 g. The high amplitude areas seem to be linked with chatter marks in the final geometry of each demonstrator blade. Comparing the digital twin with the real blades in Figure 48, the surface marks defined as *A* and *B* in the blade without control seem to be related with the red areas in the digital twin. The same applies to the mark *1* in the blade with control. Furthermore, the acceleration in the process with control seems more homogeneous, considering finishing of block one.

In summary, the monitoring and control application has shown good results when comparing both final blade surfaces. However, only a single blade was machined for each configuration. Thus, the control performance could be different for a whole blisk and with blades with different geometries. Further analyses of the signals acquired process-parallel and more milling trials with different geometries are required to evaluate the control performance in the resulting surface.

7 SUMMARY AND CONCLUSION

The project described in this document aims to develop a spindle-speed control for reducing vibrations in 5-axis milling of thin-walled turbomachinery components. The evaluation of the monitoring and control functionalities developed was performed by both offline and online tests.

Offline and online applications were developed aiming to monitor and control 5-axis milling processes of thin-walled components. The offline application was used to perform sensitivity analyses of possible parameters to be selected, without processing any workpiece. Additionally, the offline mode was also used to evaluate the monitoring and control logic, which are also implemented in the online application. As the online application was not able to show any graphs, given the required computational resources, these are generated by after process analysis in the offline tool.

The control and monitoring functionalities developed and evaluated in the offline application were integrated within an existing data acquisition system. A second way of communication was added to enable sending data from the PC/IPC to the machine. Therefore, the process-parallel spindle speed control was made possible.

Milling trials were performed with suitable sensory and data acquisition hardware in a 5-axis milling machine. Two demonstrator blades were machined to compare the process with and without the proposed control. The results have shown that the control led to a better final surface quality, which indicates a decrease in vibrations, influenced by spindle speed change. However, further tests should be performed in future works to evaluate the control ability to reduce vibrations in different trials and geometries.

The compensation of the position difference between signal generated and measured should also be revisited and evaluated, to ensure a reliable combination of process and simulation data. Additionally, the number of cutter locations used to implement this functionality could be increased. Although writing only five different cutter locations does not affect the machining performance as using more locations does, the long time required to change this value could impact negatively the control.

Further analysis of the control and monitoring functionalities could be studied such as the dead time, the best place to write, time between calculating the value to be written and then writing it with the synchronized action. The test of how long it takes to calculate OVRA mean and change R parameter could be used to select the correct R parameter reading, and stop using the synchronized action. However, the synchronized action could be necessary to implement a continuous spindle speed change.

Since the computational resources that graphs in the online application developed required were too high to keep, an additional application could be developed. Data from LabVIEW could be streamed to an application that is capable of displaying graphs process-parallel, so more process characteristics could be analyzed.

REFERENCES

1 ROLLS-ROYCE. **Rolls-Royce ships 10,000th blisk from Oberursel**. Last access: 27.01.2022. 2019. Available from: https://www.rolls-royce.com/media/press-releases/2019/11-04-2019-ships-10000-blisk-from-oberursel.aspx.

2 HEXAGON. **Non-Contact Measurement of Blisk Aerofoils and Gas Path Features**. Last access: 27.01.2022. 2022. Available from: https://www.hexagonmi.com/solutions/applications/blisks/non-contact-measurement-of-blisk-aerofoils-and-gas-path-features.

3 DILBA, Denis. **Blisk development: How blade and disk became one**. Last access: 27.01.2022. 2019. Available from: https://aeroreport.de/en/aviation/blisk-development-how-blade-and-disk-became-one.

4 ERICSSON. **A case study on real-time control in manufacturing**. Stockholm, Sweden: Ericsson, 2018.

5 RIENTH, Thorsten. **MTU and Fraunhofer IPT establish blisk prototyping facility: As the ramp-up of the current PW1000G engine generation continues, MTU has already started developing blisk prototypes for the next GTF generation at a dedicated blisk prototyping facility.** Last access: 27.01.2022. 2018. Available from: https://aeroreport.de/en/innovation/mtu-and-fraunhofer-ipt-establish-blisk-prototyping-facility.

6 TETI, R.; JEMIELNIAK, K.; O'DONNELL, G.; DORNFELD, D. Advanced monitoring of machining operations. **CIRP Annals**, v. 59, n. 2, p. 717–739, 2010. ISSN 00078506. DOI: 10.1016/j.cirp.2010.05.010.

7 WIERCIGROCH, Marian; BUDAK, Erhan. Sources of nonlinearities, chatter generation and suppression in metal cutting. **Philosophical Transactions of the Royal Society of London. Series A: Mathematical, Physical and Engineering Sciences**, v. 359, n. 1781, p. 663–693, 2001. ISSN 1364-503X. DOI: 10.1098/rsta.2000.0750.

8 CABRAL, Gustavo Francisco. **Modeling and simulation of tool engagement and prediction of process forces in milling**. 2015. Thesis for PhD in Mechanical Engineering – RWTH Aachen.

9 NEWMAN, S. T.; NASSEHI, A.; XU, X. W., et al. Strategic advantages of interoperability for global manufacturing using CNC technology. **Robotics and Computer-Integrated Manufacturing**, v. 24, n. 6, p. 699–708, 2008. ISSN 07365845. DOI: 10.1016/j.rcim.2008.03.002.

10 YE, Yingxin; HU, Tianliang; ZHANG, Chengrui; LUO, Weichao. Design and development of a CNC machining process knowledge base using cloud technology. **The International Journal of Advanced Manufacturing Technology**, v. 94, n. 9-12, p. 3413–3425, 2018. ISSN 0268-3768. DOI: 10.1007/s00170-016-9338-1.

11 ZHU, Lida; JIANG, Zenghui; SHI, Jiashun; JIN, Chengzhe. An overview of turn-milling technology. **The International Journal of Advanced Manufacturing Technology**, v. 81, n. 1-4, p. 493–505, 2015. ISSN 0268-3768. DOI: 10.1007/s00170-015-7187-y.

12 DEWES, R.C; ASPINWALL, D. K. A review of ultra high speed milling of hardened steels. **Journal of Materials Processing Technology**, v. 69, n. 1-3, p. 1–17, 1997.

13 FAASSEN, R.P.H.; VAN DE WOUW, N.; OOSTERLING, J.A.J.; NIJMEIJER, H. Prediction of regenerative chatter by modelling and analysis of high-speed milling. **International Journal of Machine Tools and Manufacture**, v. 43, n. 14, p. 1437–1446, 2003. ISSN 08906955. DOI: 10.1016/S0890-6955(03)00171-8.

14 ÖZEL, Tuğrul; ALTAN, Taylan. Process simulation using finite element method — prediction of cutting forces, tool stresses and temperatures in high-speed flat end milling. **International Journal of Machine Tools and Manufacture**, v. 40, n. 5, p. 713–738, 2000. ISSN 08906955.

15 GRIGORIEV, Sergej N.; KUTIN, A. A.; PIROGOV, V. V. Advanced Method of NC Programming for 5-Axis Machining. **Procedia CIRP**, v. 1, p. 102–107, 2012. ISSN 22128271. DOI: 10.1016/j.procir.2012.04.016.

16 HOLST, Carsten; KÖNIGS, Michael; GARCIA, Eduardo Maia; GANSER, Philipp; BERGS, Thomas. Spatially Resolved Tool Wear Prediction in Finish Milling. **Procedia CIRP**, v. 104, p. 85–90, 2021. ISSN 22128271. DOI: 10.1016/j.procir.2021.11.015.

17 CUS, F.; ZUPERL, U.; KIKER, E.; MLLFELNER, M. Adaptive controller design for feedrate maximization of machining process. **Journal of Achievements in Materials and Manufacturing Engineering**, v. 17, n. 1-2, p. 237–240, 2006.

18 SCHMITZ, Tony L.; SMITH, Kevin S. **Machining Dynamics**. Boston, MA: Springer US, 2009. ISBN 978-0-387-09644-5. DOI: 10.1007/978-0-387-09645-2.

19 REULEAUX, Franz. **Die praktischen Beziehungen der Kinematik zu Geometrie und Mechanik**. Braunschweig: Friedrich Vieweg und Sohn, 1900.

20 KIENAST, Pascal. **Data-based Investigation of Irregulary Occurring Vibrations in the Milling Process for Series Production of Blisks**. 23/02/2021. Mechanical Engineering Master – RWTH Aachen University, Aachen.

21 DEUTSCHES INSTITUT FÜR NORMUNG. **Bewegungen und Geometrie des Zerspanvorganges**. DIN 6580. Berlin: Deutsches Institut für Normung, 1985.

22 MARKWORTH, Lars. **Fünfachsige Schlichtfräsbearbeitung von Strömungsflächen aus Nickelbasislegierungen**. 2005. PhD - Faculty of Mechanical Engineering – Techn. Hochsch, Aachen.

23 WACINSKI, Manuel. **Keramische Schaftfräswerkzeuge für die Hochgeschwindigkeitsbearbeitung von Nickelbasis-Legierungen**. Stuttgart: Fraunhofer Verlag, 2016.

24 ALTINTAS, Yusuf. **Manufacturing automation: Metal cutting mechanics, machine tool vibrations, and CNC design**. 2nd ed. Cambridge and New York: Cambridge University Press, 2012. ISBN 9781107001480.

25 MUNOA, J.; BEUDAERT, X.; DOMBOVARI, Z.; ALTINTAS, Y.; BUDAK, E.; BRECHER, C.; STEPAN, G. Chatter suppression techniques in metal cutting. **CIRP Annals**, v. 65, n. 2, p. 785–808, 2016. ISSN 00078506. DOI: 10.1016/j.cirp.2016.06.004.

26 TOBIAS, Stephen Albert. **Machine-tool vibration**. [S.l.]: J. Wiley, 1965.

27 INSPERGER, T.; STÉPÁN, G.; BAYLY, P.V; MANN, B.P. Multiple chatter frequencies in milling processes. **Journal of Sound and Vibration**, v. 262, n. 2, p. 333–345, 2003. DOI: 10.1016/S0022-460X(02)01131-8.

28 JASIEWICZ, Marcin; MIĄDLICKI, Karol. Implementation of an Algorithm to Prevent Chatter Vibration in a CNC System. **Materials (Basel, Switzerland)**, v. 12, n. 19, 2019. ISSN 1996-1944. DOI: 10.3390/ma12193193.

29 YUE, Caixu; GAO, Haining; LIU, Xianli; LIANG, Steven Y.; WANG, Lihui. A review of chatter vibration research in milling. **Chinese Journal of Aeronautics**, v. 32, n. 2, p. 215–242, 2019. ISSN 10009361. DOI: 10.1016/j.cja.2018.11.007.

30 QUINTANA, Guillem; CIURANA, Joaquim. Chatter in machining processes: A review. **International Journal of Machine Tools and Manufacture**, v. 51, n. 5, p. 363–376, 2011. ISSN 08906955. DOI: 10.1016/j.ijmachtools.2011.01.001.

31 H. E. MERRITT. Theory of Self-Excited Machine-Tool Chatter Contribution to Machine-Tool Chatter Research -1. **Journal of Manufacturing Science and Engineering, Transactions of the ASME**, v. 87, n. 4, p. 447–454, 1965.

32 KULJANIC, E.; SORTINO, M.; TOTIS, G. Multisensor approaches for chatter detection in milling. **Journal of Sound and Vibration**, v. 312, n. 4-5, p. 672–693, 2008. DOI: 10.1016/j.jsv.2007.11.006.

33 FAASSEN, R.P.H.; VAN DE WOUW, N.; OOSTERLING, J.A.J.; NIJMEIJER, H. Prediction of regenerative chatter by modelling and analysis of high-speed milling. **International Journal of Machine Tools and Manufacture**, v. 43, n. 14, p. 1437–1446, 2003. ISSN 08906955. DOI: 10.1016/S0890-6955(03)00171-8.

34 PARUS, Arkadiusz; PAJOR, Morislaw; HOFFMANN, Marcin. Suppression of self-excited vibration by the spindle speed variation method. **Advances in Manufacturing Science and Technology**, v. 33, n. 4, 2009.

35 PERRELLI, Michele; COSCO, Francesco; GAGLIARDI, Francesco; MUNDO, Domenico. In-Process Chatter Detection Using Signal Analysis in Frequency and Time-Frequency Domain. **Machines**, v. 10, n. 1, p. 24, 2022. DOI: 10.3390/machines10010024.

36 SINUS. **Impulse Hammers**. Last access: 15.02.2022. 2022. Available from: https://sinus-leipzig.de/en/produkte/sensoren/impulshaemmer.

37 KISTLER. **IEPE Triaxial Accelerometer, Miniature, Ceramic Shear, 50 . . . 2000g**. Last access: 15.02.2022. 2022. Available from: https://www.kistler.com/en/product/type-8763b/.

38 DIGI-KEY. **785065-02**. Last access: 15.02.2022. 2022. Available from: https://www.digikey.de/de/products/detail/ni/785065-02/15219155?utm_adgroup=Accessories&utm_source=google&utm_medium=cpc&utm_campaign=Shopping_Product_Test%20and%20Measurement&utm_term=&productid=15219155&gclid=EAIaIQobChMIpZnU7NWk9gIV1ed3Ch1Gwgp3EAQYAiABEgKrX_D_BwE.

39 ZHUO, Yue; HAN, Zhenyu; DUAN, Jiaqi; JIN, Hongyu; FU, Hongya. Estimation of vibration stability in milling of thin-walled parts using operational modal analysis. **The International Journal of Advanced Manufacturing Technology**, v. 115, n. 4, p. 1259–1275, 2021. ISSN 0268-3768. DOI: 10.1007/s00170-021-07051-0.

40 CAMPA, F. J.; LOPEZ DE LACALLE, L. N.; CELAYA, A. Chatter avoidance in the milling of thin floors with bull-nose end mills: Model and stability diagrams. **International Journal of Machine Tools and Manufacture**, v. 51, n. 1, p. 43–53, 2011. ISSN 08906955. DOI: 10.1016/j.ijmachtools.2010.09.008.

41 MASLO, Semir; MENEZES, Bruno; KIENAST, Pascal; GANSER, Philipp; BERGS, Thomas. Improving dynamic process stability in milling of thin-walled workpieces by optimization of spindle speed based on a linear parameter-varying model. **Procedia CIRP**, v. 93, p. 850–855, 2020. ISSN 22128271. DOI: 10.1016/j.procir.2020.03.092.

42 GÜDEN, Davut. **Reduktion werkstückseitiger Schwingungen durch die Optimierung der Anregungsfrequenzen mittels einer modellbasierten Vorhersage der ortsabhän gigen Werkstückdynamik**. 03/07/2019. Master – RWTH Aachen University, Aachen.

43 EDLER, Marius. **Entwicklung einer Methode zur datenbasierten Bewertung der durch Schwingungen beeinflussten Oberflächenqualität beim 5-Achs-Fräsen von Blisks für Flugzeugtrieb- werke**. 2019. Master – RWTH Aachen University, Aachen.

44 BRECHER, Christian; WECK, Manfred. **Werkzeugmaschinen Fertigungssysteme**. Berlin: Springer Vieweg, 2017. ISBN 978-3-662-46567-7.

45 BALACHANDRAN, Balakuma; MAGRAB, Edward B. **Vibrations**. 2. ed. Australia: Cengage Learning, 2009. ISBN 978-0-534-55206-0.

46 JEMIELNIAK, K.; WIDOTA, A. Suppression of self-excited vibration by the spindle speed variation method. **International Journal of Machine Tool Design and Research**, v. 24, n. 3, p. 207–214, 1984.

47 LIU, Chao; XU, Xun. Cyber-physical Machine Tool – The Era of Machine Tool 4.0. **Procedia CIRP**, v. 63, p. 70–75, 2017. ISSN 22128271. DOI: 10.1016/j.procir.2017.03.078.

48 GANSER, P.; VENEK, T.; RUDEL, V.; BERGS, T. DPART - A Digital Twin Framework for the Machining Domain. **MM Science Journal**, v. 2021, n. 5, p. 5134–5141, 2021. ISSN 18031269. DOI: 10.17973/MMSJ.2021_11_2021168.

49 BEDIAGA, I.; MUNOA, J.; HERNÁNDEZ, J.; LÓPEZ DE LACALLE, L. N. An automatic spindle speed selection strategy to obtain stability in high-speed milling. **International Journal of Machine Tools & Manufacture**, v. 49, n. 5, p. 384–394, 2008.

50 ILIYAS AHMAD, Maznah; YUSOF, Yusri; DAUD, Md Elias; LATIFF, Kamran; ABDUL KADIR, Aini Zuhra; SAIF, Yazid. Machine monitoring system: a decade in review. **The International Journal of Advanced Manufacturing Technology**, v. 108, n. 11-12, p. 3645–3659, 2020. ISSN 0268-3768. DOI: 10.1007/s00170-020-05620-3.

51 KRATZ, Stephan. **Position-oriented vibration monitoring of finish milling thin-walled components**. 2011. PhD.

52 VAN DIJK, N. J. M.; DOPPENBERG, E. J. J.; FAASSEN, R.P.H.; VAN DE WOUW, N.; OOSTERLING, J.A.J.; NIJMEIJER, H. Automatic In-Process Chatter Avoidance in the High-Speed Milling Process. **Journal of Dynamic Systems, Measurement, and Control**, v. 132, 2010.

53 NATIONAL INSTRUMENTS. **Understanding FFTs and Windowing**. Last access: 04/01/2022. 2019. Available from: https://download.ni.com/evaluation/pxi/Understanding%20FFTs%20and%20Windowing.pdf.

54 LATHI, B. P. **Sinais e Sistemas Lineares**. 2. ed. Porto Alegre: Bookman, 2007. ISBN 978-85-60031-13-9.

55 KALID AZAD. **An Interactive Guide To The Fourier Transform**. Last access: 04/01/2022. 2013. Available from: https://betterexplained.com/articles/an-interactive-guide-to-the-fourier-transform/.

56 NISAR, Shibli; KHAN, Omar Usman; TARIQ, Muhammad. An Efficient Adaptive Window Size Selection Method for Improving Spectrogram Visualization. **Computational Intelligence and Neuroscience**, v. 2016, p. 1–13, 2016. ISSN 1687-5265. DOI: 10.1155/2016/6172453.

57 MATHWORKS. **From Fourier Analysis to Wavelet Analysis**. Last access: 04/01/2022. 2021. Available from: https://de.mathworks.com/help/wavelet/gs/from-fourier-analysis-to-wavelet-analysis.html.

58 LEE, June-Yule. Variable short-time Fourier transform for vibration signals with transients. **Journal of Vibration and Control**, v. 21, n. 7, p. 1383–1397, 2015. ISSN 1077-5463. DOI: 10.1177/1077546313499389.

59 NATIONAL INSTRUMENTS. **Short-Time Fourier Transform (Advanced Signal Processing Toolkit)**. Last access: 09.01.2022. 2010. Available from: https://zone.ni.com/reference/en-XX/help/371419D-01/lvasptconcepts/aspt_stft/.

60 PARHIZKAR, Reza; BARBOTIN, Yann; VETTERLI, Martin. Sequences with minimal time–frequency uncertainty. **Applied and Computational Harmonic Analysis**, v. 38, n. 3, p. 452–468, 2015. ISSN 10635203. DOI: 10.1016/j.acha.2014.07.001.

61 NATIONAL INSTRUMENTS. **STFT Spectrograms VI**. Last access: 07.01.2022. 2018. Available from: https://zone.ni.com/reference/en-XX/help/371361R-01/lvanls/stft_spectrogram_core/.

62 BRIAN MCFEE. **5.2. The Short-time Fourier Transform (STFT)**. Last access: 04/01/2022. 2020. Available from: https://brianmcfee.net/dstbook-site/content/ch08-stft/STFT.html.

63 ALEXANDRE, Felipe Aparecido; LOPES, Wenderson Nascimento; FERREIRA, Fábio Isaac; DOTTO, Fábio R. L.; AGUIAR, Paulo Roberto de; BIANCHI, Eduardo Carlos. Chatter Vibration Monitoring in the Surface Grinding Process through Digital Signal Processing of Acceleration Signal. **Proceedings**, v. 2, n. 3, p. 126, 2018. DOI: 10.3390/ecsa-4-04927.

64 HUANG, Zhiwen; ZHU, Jianmin; LEI, Jingtao; LI, Xiaoru; TIAN, Fengqing. Tool Wear Monitoring with Vibration Signals Based on Short-Time Fourier Transform and Deep Convolutional Neural Network in Milling. **Mathematical Problems in Engineering**, v. 2021, p. 1–14, 2021. ISSN 1024-123X. DOI: 10.1155/2021/9976939.

65 KRISHNAKUMAR, P.; RAMESHKUMAR, K.; RAMACHANDRAN, K. I. Tool Wear Condition Prediction Using Vibration Signals in High Speed Machining (HSM) of Titanium (Ti-6Al-4V) Alloy. **Procedia Computer Science**, v. 50, p. 270–275, 2015. ISSN 18770509. DOI: 10.1016/j.procs.2015.04.049.

66 ALHARBI, Wael Naji. **Development of a Closed Loop Control System for Vibratory Milling**. 11/2017. Doctor – Liverpool John Moores University, Liverpool.

67 CUS, F.; ZUPERL, U.; BALIC, J. Combined Feedfoward and Feedback Control of End Milling System. **Journal of Achievements in Materials and Manufacturing Engineering**, v. 45, n. 1, p. 1–10, 2011. Last access: 29/11/2021. Available from: https://sites.google.com/site/machinecontroltoolkit/cnc-machine-control-interface.

68 GITTLER, Thomas; GONTARZ, Adam; WEISS, Lukas; WEGENER, Konrad. A fundamental approach for data acquisition on machine tools as enabler for analytical Industrie 4.0 applications. **Procedia CIRP**, v. 79, p. 586–591, 2019. ISSN 22128271. DOI: 10.1016/j.procir.2019.02.088.

69 BLEICHER, Friedrich; SCHÖRGHOFER, Paul; HABERSOHN, Christoph. In-process control with a sensory tool holder to avoid chatter. **Journal of Machine Engineering**, v. 18, n. 3, p. 16–27, 2018. ISSN 1895-7595. DOI: 10.5604/01.3001.0012.4604.

70 SIEMENS. **ARTIS GmbH - CTM tool and process monitoring system**. Last access: 18.03.2022. 2021. Available from: https://mall.industry.siemens.com/mall/en/WW/Catalog/Products/7500289.

71 MARPOSS. **Tool and Process Monitoring System**. Last access: 18.03.2022. 2022. Available from: https://www.marposs.com/eng/product/tool-and-process-monitoring-system.

72 MARPOSS. **Adaptive Control for Monitoring Systems**. Last access: 18.03.2022. 2022. Available from: https://www.marposs.com/eng/product/adaptive-control-for-monitoring-systems.

73 AEROSPACE MANUFACTURING AND DESIGN. **BRINKHAUS ToolScope**. Last access: 20.03.2022. 2014. Available from: https://www.aerospacemanufacturinganddesign.com/product/brinkhaus-toolscope-38448/.

74 KOMET GROUP. **KOMET BRINKHAUS TOOLSCOPE APPS**. Last access: 20.03.2022. 2015. Available from: https://license.kometgroup.com/fileadmin/user_upload/pdf/products/brinkhaus/KOMET-BRINKHAUS-ToolScope-APP_GB.pdf.

75 CALLEJA, A.; GONZÁLEZ, H.; POLVOROSA, R.; GÓMEZ, G.; AYESTA, I.; BARTON, M.; LACALLE, L. LópezN. de. Blisk blades manufacturing technologies analysis. **Procedia Manufacturing**, v. 41, p. 714–722, 2019. ISSN 23519789. DOI: 10.1016/j.promfg.2019.09.062.

76 DELTALOGIC. **Industrial PLC Communication Suite Win32**. 2003. Available from: https://www.sumelco.com/wp-content/uploads/2013/07/ACCON-AGLink_HB_en.pdf.

77 DELTALOGIC. **ACCON-AGLink**. Last access: 5/17/2022. 2022. Available from: https://www.deltalogic.de/products/software/accon-aglink.

78 NATIONAL INSTRUMENTS. **CompactDAQ systems**. Last access: 11.01.2022. 2022. Available from: https://www.ni.com/de-de/shop/compactdaq.html.

79 KISTLER. **Sensor zur Messung der Schallemission (Acoustic Emission) IEPE, bis 900 kHz**. Last access: 15.01.2022. 2022. Available from: https://www.kistler.com/de/produkt/type-8152c/.

80 NATIONAL INSTRUMENTS. **LabVIEW Developer Days Zürich**. Last access: 15.01.2022. 2017. Available from: https://events.ni.com/profile/web/index.cfm?PKWebId=0x137000001.

81 NATIONAL INSTRUMENTS. **CompactRIO-Module**. Last access: 15.01.2022. 2022. Available from: https://www.ni.com/de-de/shop/hardware/compactrio-modules-category.html#.

82 DIRECTINDUSTRY. **BIG KAISER und Kistler präsentieren neues System zur präzisen Zerspankraftmessung**. Last access: 15.01.2022. 2018. Available from: https://trends.directindustry.de/big-kaiser/project-17788-185804.html.

83 AMC. **NI cRIO-9038 Echtzeit Controller im 8 Slot-System**. Last access: 15.01.2022. 2022. Available from: https://www.amc-systeme.de/artikeldetails/cRIO-9038.html.

84 WAGNER, Johannes; BURGEMEISTER, Jan. **Piezoelectric Accelerometers**. 7. ed. Radebeul, Germany: Metra Mess- und Frequenztechnik Radebeul, 2021.

85 WALTER, Patrick L. Selecting Accelerometers for and Assessing Data From Mechanical Shock Measurements. **PCB Piezotronics**, 2007.

86 KISTLER. **IEPE (Integrated Electronics Piezo-Electric)**. Last access: 5/17/2022. 2022. Available from: https://www.kistler.com/en/glossary/term/iepe-integrated-electronics-piezo-electric/.

87 PRO-MICRON. **Spike**. Last access: 5/17/2022. 2022. Available from: https://www.pro-micron.de/spike/?lang=en.

88 PRO-MICRON. **Tolles Lob der Heule Werkzeug AG**. Last access: 5/17/2022. 2019. Available from: https://www.pro-micron.de/heule-werkzeug/.